ADVANCED QUANTUM TECHNOLOGIES
www.advquantumtech.com

Single-Particle Entanglement

*Stefano Azzini, Sonia Mazzucchi, Valter Moretti, Davide Pastorello, and Lorenzo Pavesi**

This review is about single-particle entanglement. Entanglement occurs when the state of a quantum system with at least two degrees of freedom has a particular non-separable form. In the case of single-particle entanglement, this quantum correlation is shared by the same particle being it a photon, a neutron, an ion, or an atom. Here, the basics of quantum entanglement are discussed focusing on the case it is related to the degrees of freedom of a single particle. It is discussed how the violation of peculiar inequalities in this context rules out any realistic non-contextual hidden variable theory alternative to quantum mechanics. Moreover, experiments that demonstrate single-particle entanglement for photons, neutrons, and atoms are discussed. Finally, the applications of single-particle entanglement as a resource for quantum information are discussed and specifically quantum key distribution is detailed, where the use of single-particle entangled photons allows to improve the security of the BB84 protocol.

1. Introduction

Entanglement is one of the most compelling feature of quantum systems. Originally pointed out by Einstein, Podolsky, and Rosen[1] as a clue of the incompleteness of quantum mechanics,[2–4] nowadays it has earned a prominent role in quantum science and technologies as the most important source of non-classical correlations to be used as a resource for quantum information. In fact, several quantum information protocols, such as, for example, teleportation,[5–8] quantum cryptography (QK),[9] quantum key distribution (QKD)[10] and quantum random number generation (QRNG)[11] rely upon the particular features shared by quantum correlations of entangled states.

Remarkably, the analysis of the correlations described in the Einstein–Podolsky–Rosen *Gedankenexperiment* led Bell to his fundamental result: no local realistic hidden-variable theory able to account for the quantum phenomenology of a pair of entangled particles can exist. More precisely, this non-locality issue arises when the quantum system consists of two independent parts, typically a pair of particles, which can take space-like separated locations and the two subsystems have an entangled degree of freedom. It is also possible to consider and exploit different types of entanglement where the non-classical correlations between the two particles involve different degrees of freedom simultaneously.[12,13] This phenomenon is called *hybrid entanglement*.[7] In particular, this variety of possibilities opens up also to the realization of entanglement between different degrees of freedom of a unique particle, such as, for example, the polarization and momentum of a single photon[14,15] or spin and path of a neutron.[16–18] This is the so-called *single particle entanglement* (SPE) or *intraparticle entanglement*, to which this review article is dedicated. Contrary to the case of the *interparticle entanglement*, which involves correlations between two different particles, the intraparticles entangled states are rather easy to produce and possess some robustness properties under decoherence and dephasing.[19] This feature makes intraparticle entangled states particularly exploitable in several quantum information protocols,[7,20,21] even if the non-classical correlation they produce are not shared non-locally by two space-like separated subsystems. This turns in an advantage since it does not require a temporal correlations between the different particles. Moreover, since only single particles are needed, the technique utilizing SPE consumes less resources than those using interparticle entanglement.[7] On the other hand, from a foundational point of view, intraparticle entangled states have been recently used in some experimental tests of non-contextual realistic hidden variables theories alternative to quantum mechanics.[22] These experiments show that intraparticle entanglement demonstrates firmly the *contextual* nature of any realistic hidden-variable reformulation of quantum mechanics.

The review is organized as follows. In Section 2, we introduce the concept of composite systems from a quantum mechanical point of view. Here, we define the important Bell, Clauser, Horne, Shimony, and Holt (BCHSH) inequality whose violation by entangled states proves the non-locality and contextuality of quantum physics. Section 3 defines the single-particle entanglement and poses the theoretical basis of the Kochen–Specker theorem which defines the requirements for non-contextuality. Section 4 is about the experiments which prove SPE with different kinds of particles: photons, neutrons, and atoms. Here, we discuss also

Dr. S. Azzini, Prof. L. Pavesi
Nanoscience Laboratory
Department of Physics
University of Trento
via Sommarive 14, I-38123 Povo, Italy
E-mail: lorenzo.pavesi@unitn.it
Dr. S. Mazzucchi, Prof. V. Moretti
Department of Mathematics
University of Trento, and INFN-TIFPA
via Sommarive 14, I-38123 Povo, Italy
Dr. D. Pastorello
Department of Information Engineering and Computer Science
University of Trento, and INFN-TIFPA
via Sommarive 9, I-38123 Povo, Italy

The ORCID identification number(s) for the author(s) of this article can be found under https://doi.org/10.1002/qute.202000014

DOI: 10.1002/qute.202000014

the analogies between SPE and the properties of classical electromagnetic fields which lead to the debated concept of classical entanglement. Section 5 demonstrates few applications of SPE, especially in quantum key distribution. Finally, Section 6 concludes the review with a comparison between intraparticle and interparticle entanglement.

2. Composite Systems and Entanglement

Entanglement is a particular phenomenon arising in composite quantum systems that has been source of investigations since the very introduction of quantum mechanics.[2] It was originally pointed out in 1935 by Einstein, Podolsky, and Rosen (EPR)[1] as an unsettling consequence of the mathematical formulation of the theory, which according to them suggested its incompleteness. Some months after the EPR paper, Schrödinger described the paradoxical consequences of quantum mechanics when superposition principle and entanglement are extended to macroscopic systems, proposing the example of its notorious cat.[23,24] In 1964, Bell[25] suggested an experimental test able to discriminate between quantum mechanics and alternative local hidden variables theories. Following the Bell's paper, a long series of experiments started, and in 1982, Aspect et al.[26] demonstrated violation of the so-called Bell's inequality. This result refuted local realistic hidden variables theories (up to some loopholes), and the results were in agreement with the quantum predictions. Nowadays, acquaintance has increased with the concept of entanglement, which has lost the role of a mysterious and uncomfortable phenomenon, in favor of becoming an understood practical resource of non-local correlations be exploited as a crucial tool in quantum information.

2.1. Composite Systems

Despite its profound physical implications, from a mathematical point of view the description of entanglement is relatively simple. In particular, this applies when systems associated with finite dimensional Hilbert spaces are considered. The fundamental object leading to the notion of entangled states is the *tensor product* Hilbert space, which arises naturally in the description of compound quantum systems. As first, most familiar, example, let us consider a system composed of two particles. While the pure states of the single particles are described (up to arbitrary phases) in the position representation by wave functions ψ_1 and ψ_2, that is, by vectors ψ in the Hilbert space $L^2(\mathbb{R}^3)$ which are normalized ($\int_{\mathbb{R}^3} |\psi(x)|^2 d^3x = 1$), the pure states of the compound systems (up to arbitrary phases) are functions ψ of two variables $x_1, x_2 \in \mathbb{R}^3$, that is, normalized vectors in the space $L^2(\mathbb{R}^6) = L^2(\mathbb{R}^3) \otimes L^2(\mathbb{R}^3)$, tensor product of the Hilbert spaces associated with the single particles. Actually, this description of composite systems in terms of tensor product is much more general and concerns not only systems which are made of pairs of particles but also any quantum system which is made of two (or many) *independent* subsystems provided some requirements (always true for the quantum systems discussed in this paper) are satisfied. Independence between two subsystems S_1 and S_2 of a quantum system S (with associated Hilbert spaces $\mathcal{H}_1$, $\mathcal{H}_2$, and $\mathcal{H}$, respectively) can be stated in terms of the following three requirements:

a) The observables of each subsystem (selfadjoint operators A_i over $\mathcal{H}_i$, $i = 1, 2$) must be unambiguously identified with observables $\tilde{A}_i$ of the compound system (selfadjoint operators over $\mathcal{H}$).

b) Any pair of observables, one for each independent subsystem, when viewed as observables of S must be made of *compatible* observables (i.e., simultaneously measurable).

c) For any pair of states ρ_1 and ρ_2, one for each independent subsystem, there exists a state ρ of the compound system S such that, for any pair of elementary observables on P_1 and P_2 of S_1 and S_2, respectively, the following holds

$$\mathrm{Tr}[\rho \tilde{P}_1 \tilde{P}_2] = \mathrm{Tr}[\rho_1 P_1]\mathrm{Tr}[\rho_2 P_2] \tag{1}$$

In the formula above, ρ_i are positive trace class operators on $\mathcal{H}_i$ with $\mathrm{Tr}(\rho_i) = 1$, $i = 1, 2$, ρ is a positive trace class operator on $\mathcal{H}$ with $\mathrm{Tr}(\rho) = 1$, and P_1 and P_2 are projection operators on $\mathcal{H}_1$ and $\mathcal{H}_2$, respectively.

For the specific case of a system composed of two particles, conditions a and c mean that observables and states defined for each single particle are still meaningful as observables and states of the compound system, that is, the result of the measurements made on different subsystems are statistically independent. Moreover, according to condition b, any pair of observables, one for each particle, admits a joint measurement.

What is relevant for the general case is that a natural way to implement these three conditions is assuming that the whole system is described by the *tensor product* $\mathcal{H} = \mathcal{H}_1 \otimes \mathcal{H}_2$ of Hilbert spaces. In the case when S_1 and S_2 do not exhaust the total system S and other independent parts S_3, and so forth are needed, further factors are present in the tensor product. If we strict ourself to two independent parts, a is valid simply identifying the selfadjoint operator A_1 over $\mathcal{H}_1$ with the selfadjoint operator $A_1 \otimes I_2$ over the whole Hilbert space and the selfadjoint operator A_2 over $\mathcal{H}_2$ with the selfadjoint operator $I_1 \otimes A_2$ over the whole Hilbert space (I_i denoting the identity operator on $\mathcal{H}_i$). We stress that the map associating A_1 with $A_1 \otimes I_2$ is injective and preserves all relevant properties of the observable, for example, its spectrum corresponding to the experimental values of the outcomes. Furthermore, also b is valid because (assuming A_i everywhere defined)

$$(A_1 \otimes I_2)(I_1 \otimes A_2) = A_1 \otimes A_2 = (I_1 \otimes A_2)(A_1 \otimes I_2) \quad \text{for } i = 1, 2 \tag{2}$$

Eventually condition c is fulfilled by setting $\rho = \rho_1 \otimes \rho_2$. (The mathematically minded reader finds more technically rigorous statements in ref. [27]).

In view of the generalization of the concept of entanglement to a single particle, we must say that in quantum mechanics, there are important examples of systems composed of independent parts which are not a pair of two independent particles. An example is provided by a single elementary particle, such as an electron, which has an *internal structure* and the independent parts correspond to different degrees of freedom. Here, the Hilbert space is the product of two factors $\mathcal{H}_{orb} \otimes \mathcal{H}_{spin}$ with obvious meaning of the terms. A similar decomposition is valid for a photon, for which $\mathcal{H}_{orb} \otimes \mathcal{H}_{pol}$. In both cases $\mathcal{H}_{orb}$ is

infinite-dimensional and can be identified with the space of wavefunctions in position or momentum representation (the position representation of photons is more delicate and has to be treated with a certain care[28]).

Obviously, also the initially mentioned case of a system made of two (or more) particles can be treated similarly. In this case, the space of the system is $\mathcal{H}_1 \otimes \mathcal{H}_2$ where now $\mathcal{H}_i$ is the whole Hilbert space of the considered particle. It is worth stressing that, when the two systems are *indistinguishable* and each of them are described by the Hilbert space $\mathcal{H}$, the overall Hilbert space $\mathcal{H}_1 \otimes \mathcal{H}_2$ must be replaced by $\mathcal{H}_1 \otimes_A \mathcal{H}_2$ or $\mathcal{H}_1 \otimes_S \mathcal{H}_2$, where $\otimes_A$ and $\otimes_S$ denote the antisymmetric or symmetric tensor product depending on the nature of the elementary particles described in $\mathcal{H}$: *fermions* (as electrons) need $\otimes_A$ and *bosons* (like photons) want $\otimes_S$.

2.2. Separable States versus Entangled States

The choice of the tensor product for describing the Hilbert space of composite systems has a paramount consequence when focusing on the states of the system. Let us first consider *pure states*. They are represented by unit vectors $|\psi\rangle \in \mathcal{H}$ up to phases. The product $\mathcal{H} = \mathcal{H}_1 \otimes \mathcal{H}_2$ contains vectors describing *separable states*, that is, vectors factorized as follows

$$|\psi\rangle = |\psi_1\rangle \otimes |\psi_2\rangle \tag{3}$$

as well as all their linear combinations. Pure states which cannot be written as above are said to be *entangled*.

The definition consisting in a negative statement implies that only non-entangled states can be properly defined, and this contributes to make entanglement a difficult concept to pin-down from a physical point of view. The simplest, and most famous, example of a compound quantum system exhibiting the entanglement phenomenology was proposed by Bohm[29] (see also Aharonov and Bohm[30]) in an alternative formulation of the EPR paradox. Let us consider a pair of spin 1/2 particles, so that $\mathcal{H} = \mathcal{H}_{orb} \otimes \mathcal{H}_{1,spin} \otimes \mathcal{H}_{2,spin}$ with $\mathcal{H}_{i,spin} = \mathbb{C}^2$. If we restrict our analysis just to the spin degree of freedom and neglect the orbital part,[31] the Hilbert space of the compound system reduces to $\mathbb{C}^2 \otimes \mathbb{C}^2$. Chosen an orthonormal basis of $\mathbb{C}^2$, for instance the one provided by the two eigenvectors $|z_+\rangle$ and $|z_-\rangle$ of the Pauli matrix σ_z proportional to the z-component of the spin

$$\sigma_z = \begin{pmatrix} 1 & 0 \\ 0 & -1 \end{pmatrix}, \quad |z_+\rangle = \begin{pmatrix} 1 \\ 0 \end{pmatrix}, \; |z_-\rangle = \begin{pmatrix} 0 \\ 1 \end{pmatrix},$$
$$\sigma_z|z_+\rangle = |z_+\rangle, \quad \sigma_z|z_-\rangle = -|z_-\rangle \tag{4}$$

the vectors $\psi \in \mathbb{C}^2 \otimes \mathbb{C}^2$ can be represented as linear combinations of the four orthonormal vectors $|z_+\rangle_1 \otimes |z_+\rangle_2$, $|z_+\rangle_1 \otimes |z_-\rangle_2$, $|z_-\rangle_1 \otimes |z_-\rangle_2$, $|z_-\rangle_1 \otimes |z_+\rangle_2$, where the subscript tags the particle. Particular examples of entangled pure states are the so-called *Bell states*, namely the vectors:

$$|\Phi^+\rangle = \frac{1}{\sqrt{2}}\left(|z_+\rangle_1 \otimes |z_+\rangle_2 + |z_-\rangle_1 \otimes |z_-\rangle_2\right) \tag{5}$$

$$|\Phi^-\rangle = \frac{1}{\sqrt{2}}\left(|z_+\rangle_1 \otimes |z_+\rangle_2 - |z_-\rangle_1 \otimes |z_-\rangle_2\right) \tag{6}$$

$$|\Psi^+\rangle = \frac{1}{\sqrt{2}}\left(|z_+\rangle_1 \otimes |z_-\rangle_2 + |z_-\rangle_1 \otimes |z_+\rangle_2\right) \tag{7}$$

$$|\Psi^-\rangle = \frac{1}{\sqrt{2}}\left(|z_+\rangle_1 \otimes |z_-\rangle_2 - |z_-\rangle_1 \otimes |z_+\rangle_2\right) \tag{8}$$

which actually form an orthonormal basis of $\mathbb{C}^2 \otimes \mathbb{C}^2$.

From a physical point of view, separable vectors in $\mathbb{C}^2 \otimes \mathbb{C}^2$ can be seen as eigenvectors of observables of the form $A_1 \otimes A_2$, with ψ_i being eigenvector of A_i with eigenvalue λ_i, $i = 1, 2$. This means that, at least in principle, for such states there exist observables defined on subsystems which have a definite value, that is, if the observable A_i is measured on the subsystem S_i then the value λ_i will be obtained with probability 1. On the contrary, for each subsystem, there are no observable with a definite value for entangled states. For instance, in the case of the four entangled states (5), (6), (7), and (8) of a compound system of two 1/2-spin particles, there are no directions along which the spin component of a single particle has a definite value. In other words, for any choice of a couple of normalized vectors $\mathbf{n}_1, \mathbf{n}_2 \in \mathbb{R}^3$, the Bell states cannot be eigenvectors of the observable $\mathbf{n}_1 \cdot \sigma \otimes I$ or $I \otimes \mathbf{n}_2 \cdot \sigma$, with I the identity operator and

$$\begin{aligned} \mathbf{n} \cdot \sigma &= n_x\sigma_x + n_y\sigma_y + n_z\sigma_z \\ &= n_x \begin{pmatrix} 0 & 1 \\ 1 & 0 \end{pmatrix} + n_y \begin{pmatrix} 0 & -i \\ i & 0 \end{pmatrix} + n_z \begin{pmatrix} 1 & 0 \\ 0 & -1 \end{pmatrix}, \quad \mathbf{n} = (n_x, n_y, n_z) \end{aligned} \tag{9}$$

Let us now consider mixed states. For general *mixed states*, thus described by *statistical operators* $\rho : \mathcal{H} \to \mathcal{H}$, a *separable mixed state* is by definition a *convex combination* of *products* of mixed states ρ_1, ρ_2 of the subsystems

$$\rho = \sum_i p_i \, \rho_{i1} \otimes \rho_{i2} \quad \text{where } 0 \le p_i \le 1 \text{ and } \textstyle\sum_i p_i = 1. \tag{10}$$

Mixed states which cannot be written as above are said to be *entangled*. It is easy to prove that separable/entangled pure states $|\psi\rangle$ written in terms of statistical operators $|\psi\rangle\langle\psi|$ are a sub-case of separable/entangled mixed states as defined above.

2.3. Entanglement of Two Particles and EPR Phenomenon

As first realized by Einstein, Podolski, and Rosen in a celebrated paper of 1935,[1] entangled states give rise to very peculiar phenomena—often mentioned as the *EPR paradox*—as soon as one assumes the standard *postulate of collapse* of the state after an ideal measurement. Suppose the whole pure state of a bipartite system S made of two subsystems S_1 and S_2 is described by a unit vector of the form

$$\frac{|\psi_a\rangle \otimes |\phi\rangle + |\psi_{a'}\rangle \otimes |\phi'\rangle}{\sqrt{2}} \tag{11}$$

where $|\psi_a\rangle, |\psi_{a'}\rangle \in \mathcal{H}_1$ and $|\phi\rangle \neq |\phi'\rangle \in \mathcal{H}_2$ are of unit norm. We also assume that $A_1|\psi_a\rangle = a|\psi_a\rangle$ and $A_1|\psi_{a'}\rangle = a'|\psi_{a'}\rangle$ for a certain observable A_1 on S_1, with $a \neq a'$. Performing a measurement of A_1 on S_1, due to the collapse of state, we actually act on the whole state, that is, *also* on the part describing S_2. As a matter of fact, if the outcome of the measurement of A_1 is a, then the state of the full system after the measurement will be described by $|\psi_a\rangle \otimes |\phi\rangle$; if the outcome of the measurement of A_1 is a', then the state of the full system after the measurement will be described by $|\psi_{a'}\rangle \otimes |\phi'\rangle$.

For instance, in the particular case of the Bell state (8) of two spin 1/2 particles, for any choice of a unit vector $\mathbf{n} \in \mathbb{R}^3$ the $|\Phi^-\rangle$ state can equivalently be written as

$$|\Phi^-\rangle = \frac{1}{\sqrt{2}}\left(|z_+\rangle_1 \otimes |z_-\rangle_2 - |z_-\rangle_1 \otimes |z_+\rangle_2\right)$$
$$= \frac{1}{\sqrt{2}}\left(|\mathbf{n}_+\rangle_1 \otimes |\mathbf{n}_-\rangle_2 - |\mathbf{n}_-\rangle_1 \otimes |\mathbf{n}_+\rangle_2\right) \quad (12)$$

as one can easily verify by representing the vectors $|z_+\rangle$ and $|z_-\rangle$ as linear combinations of the eigenvectors $|\mathbf{n}_+\rangle$ and $|\mathbf{n}_-\rangle$ of the observable $\mathbf{n}\cdot\sigma$ defined in (9). By the collapse postulate, if we act on S_1 by measuring the spin component along a general direction $\mathbf{n}$, we "instantaneously" produce a change of S_2 which, in principle, can be observed performing measurements on it. This seems to be in explicit contradiction with the *locality* postulate of special relativity (that a maximal speed exists, the one of light, for propagating physical information) in connection with the *realism assumption* that the values of the observables are pre-existent to the measurements and can be changed only through sub-luminal interactions. Indeed, in the particular case where S_1 and S_2 are distinct particles, the measurements of the corresponding observables are allowed to be located in space-like separated regions of space-time. Hence, it is possible to realize a version of the experiment in which we can measure different observables on each side of the system and the choice of these observables (possibly random) and the associated measurement are made in such a short lapse of time that any non-superluminal exchange of information[32] between the two sides is forbidden. If an exchange of information between space like-related events is permitted, the relativity principle implies that an observer evolving along her/his time-like world line can send information to events localized in the her/his past along the same world line, hence potentially giving rise to fantastic temporal paradoxes. This argument also proves that it does not make sense to assume that the "collapse of the state" due to a measurement on S_1 "instantaneously" fixes the values of the relevant observables of S_2, through a superluminal transmission of information, or *vice versa*. A prudent viewpoint here is to adopt a merely statistical interpretation of the quantum state, that is, referred to the statistical properties of many copies of identically-prepared entangled pairs instead of an individual pair, avoiding to relate to the notion of "collapse of the state". An up-to-date discussion on this can be found in ref. [33]. The main aim of EPR was actually to prove that quantum mechanics cannot be a *complete* description of physical reality, paving the way for the so-called *hidden variables theories*.

2.4. BCHSH Inequality from Realism and Locality

For the sake of completeness, we summarize here the Bell's analysis[25] of the version of the EPR phenomenon proposed by Aharonov and Bohm.[30] In this analysis, the physical system is made of a pair of spin 1/2 particles, the whole Hilbert space is given by $\mathcal{H} = \mathcal{H}_{orb} \otimes \mathcal{H}_{1,spin} \otimes \mathcal{H}_{2,spin}$ and the entanglement takes place in the space of spins. In particular, we shall represent the overall state as

$$|\phi\rangle \otimes \frac{|\psi_1\rangle \otimes |\psi_2\rangle + |\psi_1'\rangle \otimes |\psi_2'\rangle}{\sqrt{2}}$$
$$\text{with} \quad |\phi_i\rangle \in \mathcal{H}_{orb}\,, \quad |\psi_i\rangle, |\psi_i'\rangle \in \mathcal{H}_{i,spin} \quad (13)$$

Once created into sharply separated wavepackets described by the two-particle wavefunction ϕ, the pair of particles moves along opposite directions toward the detectors where spin observables are eventually measured. Bell's analysis considers the possibility of explaining entanglement phenomenology, in particular the correlation of the measurement of observables performed on space-like separated subsystems, in terms of a *hidden-variable* theory. Remarkably, he proposes an experiment capable to discriminate between *quantum mechanics* and alternative *hidden-variable theories*.

In these hidden-variable theories, in competition with standard quantum mechanics, it is explicitly assumed that there is an unknown cumulative ("hidden") variable $\lambda \in \Lambda$, belonging to an unspecified set Λ of parameters, which completely fixes the *real* state of the couple of particles into a *realistic way*, according to Einstein's terminology. This means that all observables, of the compound system as a whole as well as of the subsystems, are defined and are function of λ. In particular, in the description of the Bohm's version of the EPR paradox, one has to consider the value $A(\mathbf{a}|\lambda) \in \{\pm 1\}$ of the the spin along the direction $\mathbf{a}$ (a unit vector in the physical 3D space) detected on the particle S_1 and the value $B(\mathbf{b}|\lambda) \in \{\pm 1\}$ of the spin along the direction $\mathbf{b}$ detected on the particle S_2.[34] To make explicit the *experimental context*, that is, the whole set of observables measured on the system S, we denote $A(\mathbf{a}|\lambda, \mathbf{b})$ and $B(\mathbf{b}|\lambda, \mathbf{a})$ the values of the spin components of the two particles along the directions $\mathbf{a}$ and $\mathbf{b}$, respectively. Moreover, the stochastic behavior of measurement outcomes characteristics of quantum mechanics is ascribed to a lack of knowledge of the exact value of the variable λ in a hidden-variable theory. In other words, the quantum state of the system is associated with a probability distribution μ over the space Λ.

To be precise, λ generally indicates a *set* of hidden variables and it is admitted that the state of S_1 may only depend on a subset of these parameters and the state of S_2 depends on another subset. In a complete theory, one could also assume that hidden variables have a deterministic dynamical evolution. We stress also that we are *not* directly assuming that the spin is a *quantum observable*, that is, a selfadjoint operator in a Hilbert space. It is just a quantity that we can measure.

From a physical point of view, the general structure of a hidden-variable theory relies upon the following two assumptions, which are already partially implicit in the used notations.

Realism. $A(\mathbf{a}|\lambda,\mathbf{b})$, $B(\mathbf{b}|\lambda,\mathbf{a})$ *exist at every time and for every choice of the directions* $\mathbf{a},\mathbf{b}$, *independently from their explicit observation, and they are determined by* λ.

Locality. *When measurements are performed on* S_1 *and* S_2 *with devices belonging to causally separate regions of spacetime, the choice of* $\mathbf{a}$ *cannot have any influence on the outcome* $B(\mathbf{b}|\lambda,\mathbf{a})$ *and vice versa, that is* $B(\mathbf{b}|\lambda,\mathbf{a}) = B(\mathbf{b}|\lambda)$ *and* $A(\mathbf{a}|\lambda,\mathbf{b}) = A(\mathbf{a}|\lambda)$.

The realism assumption is completely in contrast with the properties shared by the entangled states. Indeed, for Bell entangled states no spin observables of single particles can have definite values, whatever the direction of the spin component that is measured. Moreover, *if* we assumed that spin observables are quantum, locality would force spin observables measured on the two sides of the system to be mutually compatible quantum observables.

In Bell's original description, realism and locality merge in a single condition. Indeed, in Bell's work,[25] *the hidden variables* λ as well as the realistic description of the spin observables are introduced only when the two subsystems are space-like separated. In a subsequent work,[35] the physical meaning of λ is modified: it loses the mysterious role of a hidden parameter and assumes the meaning of the *common cause* of the results of the measurements of the spin observables. In other words, the symbol λ denotes the events in the common past of S_1 and S_2. That is why a local realistic theory fulfilling Bell's requirements predicts a particular form of the statistical distribution of the measurement results of space-like separated observables, for which the correlations are *predetermined*. However, it is important to point out that Bell's attempt to distance himself from hidden variables can be somehow criticised,[36] since a hidden variable is by definition something additional to the full quantum formalism. Common causes λ do not exist in Hilbert space formulation of quantum mechanics, and, therefore, they deserves the name of hidden variables.

In order to investigate the statistical predictions of a general hidden-variable theory, let us consider $\chi(\mathbf{a},\mathbf{a}',\mathbf{b},\mathbf{b}'|\lambda)$, a measured quantity which depends on four choices of directions $\mathbf{a},\mathbf{a}'$ for S_1 and $\mathbf{b},\mathbf{b}'$ for S_2. We define

$$\chi(\mathbf{a},\mathbf{a}',\mathbf{b},\mathbf{b}'|\lambda) := A(\mathbf{a}|\lambda)B(\mathbf{b}|\lambda) + A(\mathbf{a}'|\lambda)B(\mathbf{b}|\lambda) + A(\mathbf{a}'|\lambda)B(\mathbf{b}'|\lambda) - A(\mathbf{a}|\lambda)B(\mathbf{b}'|\lambda) \tag{14}$$

It holds $\chi(\mathbf{a},\mathbf{a}',\mathbf{b},\mathbf{b}'|\lambda) = A(\mathbf{a}|\lambda)[B(\mathbf{b}|\lambda) - B(\mathbf{b}'|\lambda)] + A(\mathbf{a}'|\lambda)[B(\mathbf{b}|\lambda) + B(\mathbf{b}'|\lambda)]$. Since both $B(\mathbf{b}|\lambda), B(\mathbf{b}'|\lambda) \in \{\pm 1\}$, then only one addend in the right-hand side of the identity above does not vanish. As $A(\mathbf{a}|\lambda), A(\mathbf{a}'|\lambda) \in \{\pm 1\}$, we conclude that it must hold $\chi(\mathbf{a},\mathbf{a}',\mathbf{b},\mathbf{b}'|\lambda) \in \{\pm 2\}$. If we take the expectation value $\mathbb{E}_\mu(\chi)$ of $\chi(\mathbf{a},\mathbf{a}',\mathbf{b},\mathbf{b}'|\lambda)$ when λ varies in Λ according with its probability distribution μ

$$\mathbb{E}_\mu(\chi) := \int_\Lambda \chi(\mathbf{a},\mathbf{a}',\mathbf{b},\mathbf{b}'|\lambda)d\mu(\lambda) \tag{15}$$

we find $-2 \le \mathbb{E}_\mu(\chi) \le 2$ since the measure is positive and the total integral is 1. Defining the expectation value

$$E_\mu(\mathbf{a},\mathbf{b}) := \int_\Lambda A(\mathbf{a}|\lambda)B(\mathbf{b}|\lambda)d\mu(\lambda) \tag{16}$$

for every pair of directions $\mathbf{a},\mathbf{b}$, we obtain the *BCHSH inequality*[37] (after Bell, Clauser, Horne, Shimony, and Holt[38]),

$$-2 \le E_\mu(\mathbf{a},\mathbf{b}) + E_\mu(\mathbf{a}',\mathbf{b}) + E_\mu(\mathbf{a}',\mathbf{b}') - E_\mu(\mathbf{a},\mathbf{b}') \le 2$$

$$\text{for every } \mathbf{a},\mathbf{a}',\mathbf{b},\mathbf{b}'. \tag{17}$$

or, equivalently,

$$0 \le |E_\mu(\mathbf{a},\mathbf{b}) - E_\mu(\mathbf{a},\mathbf{b}')| + |E_\mu(\mathbf{a}',\mathbf{b}) + E_\mu(\mathbf{a}',\mathbf{b}')| \le 2$$

$$\text{for every } \mathbf{a},\mathbf{a}',\mathbf{b},\mathbf{b}'. \tag{18}$$

These inequalities on correlations of measurements of spin components of pair of particles must be satisfied by every realistic local theory. Their violations exclude these theories.

In EPR-type experiments, the BCHSH inequality is typically formulated using the so-called *S*-parameter

$$S_\mu(\mathbf{a},\mathbf{a}',\mathbf{b},\mathbf{b}') = E_\mu(\mathbf{a},\mathbf{b}) + E_\mu(\mathbf{a}',\mathbf{b}) + E_\mu(\mathbf{a}',\mathbf{b}') - E_\mu(\mathbf{a},\mathbf{b}') \tag{19}$$

$$-2 \le S_\mu(\mathbf{a},\mathbf{a}',\mathbf{b},\mathbf{b}') \le 2 \tag{20}$$

The expectation value $E_\mu(\mathbf{a},\mathbf{b})$ is computed on the basis of the experimental count rates in the following convenient way:

$$E_\mu(\mathbf{a},\mathbf{b}) = \frac{N_{++}^{(\mathbf{a},\mathbf{b})} + N_{--}^{(\mathbf{a},\mathbf{b})} - N_{+-}^{(\mathbf{a},\mathbf{b})} - N_{-+}^{(\mathbf{a},\mathbf{b})}}{N_{++}^{(\mathbf{a},\mathbf{b})} + N_{--}^{(\mathbf{a},\mathbf{b})} + N_{+-}^{(\mathbf{a},\mathbf{b})} + N_{-+}^{(\mathbf{a},\mathbf{b})}} \tag{21}$$

where $N_{ij}^{(\mathbf{a},\mathbf{b})}$ identifies the count rate corresponding to the measurement values i and j of the two observables tested along the directions $\mathbf{a}$ and $\mathbf{b}$, respectively, with $i = A(\mathbf{a}|\lambda) \in \{\pm 1\}$ and $j = B(\mathbf{b}|\lambda) \in \{\pm 1\}$. The ratio $N_{ij}^{(\mathbf{a},\mathbf{b})} / \sum_{i,j} N_{ij}^{(\mathbf{a},\mathbf{b})}$ gives an estimate of the joint detection probability of the observables of the quantum state under measurements along $\mathbf{a}$ and $\mathbf{b}$. The expectation values corresponding to the other measurement directions, that is, $E_\mu(\mathbf{a}',\mathbf{b})$, $E_\mu(\mathbf{a}',\mathbf{b}')$ and $E_\mu(\mathbf{a},\mathbf{b}')$, are calculated in a same manner.

2.5. Quantum Violation of the BCHSH Inequality

What is the quantum prevision instead? First of all, the *spin observable along* $\mathbf{a}$ must be properly viewed as the selfadjoint operator $\mathbf{a}\cdot\sigma := \sum_{k=x,y,z} a_k\sigma_k$ in $\mathbb{C}^2$. In this context, we have to interpret $E_\mu(\mathbf{a},\mathbf{b})$ as an expectation value with respect to a (generally mixed) quantum state ρ (neglecting the orbital part of the state which does not play a role here)

$$E_\rho(\mathbf{a},\mathbf{b}) = tr\left[\rho(\mathbf{a}\cdot\sigma \otimes \mathbf{b}\cdot\sigma)\right] \tag{22}$$

We restrict the choice of the state to *entangled* pure Bell states $\Phi^+,\Phi^-,\Psi^+,\Psi^-$ defined in (5), (6), (7), (8). In this case, one can easily verify that the BCHSH inequality (17) is violated for suitable choices of vectors $\mathbf{a},\mathbf{a}',\mathbf{b},\mathbf{b}'$. Indeed, by setting $\rho_+ = |\Phi^+\rangle\langle\Phi^+|$ and $\rho_- = |\Psi^-\rangle\langle\Psi^-|$ and choosing

$$\mathbf{a} = \mathbf{e}_x\,, \quad \mathbf{a}' = \mathbf{e}_z\,, \quad \mathbf{b} = \frac{\mathbf{e}_x + \mathbf{e}_z}{\sqrt{2}}\,, \quad \mathbf{b}' = \frac{\mathbf{e}_z - \mathbf{e}_x}{\sqrt{2}} \tag{23}$$

(where $\mathbf{e}_x, \mathbf{e}_y, \mathbf{e}_z$ are the unit vectors along three orthogonal axes of the physical rest space of the laboratory), the following holds:

$$E_{\rho_\pm}(\mathbf{a},\mathbf{b}) + E_{\rho_\pm}(\mathbf{a}',\mathbf{b}) + E_{\rho_\pm}(\mathbf{a}',\mathbf{b}') - E_{\rho_\pm}(\mathbf{a},\mathbf{b}') = \pm 2\sqrt{2} \tag{24}$$

The same result can be obtained by setting $\rho_+ = |\Psi^+\rangle\langle\Psi^+|$ and $\rho_- = |\Phi^-\rangle\langle\Phi^-|$ and

$$\mathbf{a} = \mathbf{e}_x\,, \quad \mathbf{a}' = -\mathbf{e}_z\,, \quad \mathbf{b} = \frac{\mathbf{e}_x + \mathbf{e}_z}{\sqrt{2}}\,, \quad \mathbf{b}' = \frac{\mathbf{e}_z - \mathbf{e}_x}{\sqrt{2}} \tag{25}$$

This discussion can be recast for photons as well. Here observables $\mathbf{a}\cdot\sigma$ are interpreted as polarization observables. $\mathbf{e}_z\cdot\sigma$ is the HV-polarization observable (HV are the horizontal and vertical directions in some reference frame), $\mathbf{e}_y\cdot\sigma$ the RL-polarization observable (RL are the right and left circular polarization directions in the same reference frame) and $\mathbf{e}_x\cdot\sigma$ refers to polarization axes inclined of $\pi/4$ with respect to HV. In this case, the Bell states of a pair of photons can be written as

$$\begin{aligned}
|\Phi^+\rangle &= \frac{|V\rangle\otimes|V\rangle + |H\rangle\otimes|H\rangle}{\sqrt{2}},\\
|\Phi^-\rangle &= \frac{|V\rangle\otimes|V\rangle - |H\rangle\otimes|H\rangle}{\sqrt{2}},\\
|\Psi^+\rangle &= \frac{|V\rangle\otimes|H\rangle + |H\rangle\otimes|V\rangle}{\sqrt{2}},\\
|\Psi^-\rangle &= \frac{|V\rangle\otimes|H\rangle - |H\rangle\otimes|V\rangle}{\sqrt{2}},
\end{aligned} \tag{26}$$

where $|V\rangle$ and $|H\rangle$ denote the state with vertical and horizontal linear polarization, respectively. For instance, in the case of the state $|\Phi^+\rangle$, the maximal violation of Bell's inequalities can be obtained in the case where the orientation angles $\mathbf{a}, \mathbf{b}, \mathbf{a}', \mathbf{b}'$ of the polarization analyzers satisfy the equalities

$$\mathbf{a}\cdot\mathbf{b} = \mathbf{b}\cdot\mathbf{a}' = \mathbf{a}'\cdot\mathbf{b}' = \theta, \quad \mathbf{a}\cdot\mathbf{b}' = 3\theta \tag{27}$$

with $\theta = \pi/8$, yielding the maximum value

$$E_{\Phi^+}(\mathbf{a},\mathbf{b}) + E_{\Phi^+}(\mathbf{a}',\mathbf{b}) + E_{\Phi^+}(\mathbf{a}',\mathbf{b}') - E_{\Phi^+}(\mathbf{a},\mathbf{b}') = 2\sqrt{2} \tag{28}$$

Since $2\sqrt{2} > 2$, we conclude that *the result predicted by Quantum Theory, with the said choices of directions and entangled states, is incompatible with realism and locality*. The number $2\sqrt{2}$ is the maximum violation of the BCHSH inequality attainable for a quantum state ρ and is called the *Tsirelson's bound*.[39]

It follows that the *local realism* is rejected by experimental data accumulated along the years in several very delicate experiments performed to test BCHSH inequalities on couples of particles in entangled states. See ref. [28] for a review on the various experiments and ref. [40] for a recent important experimental achievement on the subject. The non-locality of quantum mechanics—with the above specific meaning due to Bell[33]—is nowadays widely accepted as a real and fundamental feature of Nature.[2,3,41] A more sophisticated discussion on entanglement, realism, and relativistic *local-causality* was presented by Bell in ref. [35], (see also refs. [42] and [4] and Chapter 5 of ref. [43]). This analysis will not be discussed here. We stress, without entering into detail, that the quantum violation of locality together with the stochastic nature of outcomes of measurements do not permit superluminal propagation of physical information.[2,35]

It is interesting to point out that entanglement is a necessary condition for the violation of the Bell inequality. Indeed, if the state ρ of the compound system is factorised, that is, of the form

$$\rho = \sum_i p_i \rho_{i1}\otimes\rho_{i2} \tag{29}$$

(with $0 \le p_i \le 1$ and $\sum_i p_i = 1$ and ρ_{i1} and ρ_{i2} states of the subsystems) then the quantum correlation satisfies the BCHSH inequality. Indeed, each addend $\rho_{i1}\otimes\rho_{i2}$ can be rearranged in the form

$$\rho_{i1}\otimes\rho_{i2} = \sum_j q_j |\psi_{j1}\rangle\otimes|\psi_{j2}\rangle\langle\psi_{j1}|\otimes\langle\psi_{j2}| \tag{30}$$

with $0 \le q_j \le 1$, $\sum_j q_j = 1$ and the vectors $|\psi_{j1}\rangle\otimes|\psi_{j2}\rangle$ form a Hilbert basis of $\mathcal{H}_1\otimes\mathcal{H}_2$. Let us start from the elementary case $\rho = |\psi_1\rangle\otimes|\psi_2\rangle\langle\psi_1|\otimes\langle\psi_2|$ and use the well-known technical fact that the function $f(x_1,x_2,x_3,x_4) = x_1x_3 + x_2x_3 + x_2x_4 - x_1x_4$, satisfies the following inequality (see, e.g., refs. [28,43])

$$|f(x_1,x_2,x_3,x_4)| \le 2 \quad \text{if} \quad x_1,x_2,x_3,x_4 \in [-1,1] \tag{31}$$

Next, a trivial computation proves that

$$\begin{aligned}
&E_\rho(\mathbf{a},\mathbf{b}) + E_\rho(\mathbf{a}',\mathbf{b}) + E_\rho(\mathbf{a}',\mathbf{b}') - E_\rho(\mathbf{a},\mathbf{b}')\\
&= \langle\psi_1|\mathbf{a}\cdot\sigma\psi_1\rangle\langle\psi_2|\mathbf{b}\cdot\sigma\psi_2\rangle + \langle\psi_1|\mathbf{a}'\cdot\sigma\psi_1\rangle\langle\psi_2|\mathbf{b}\cdot\sigma\psi_2\rangle\\
&\quad + \langle\psi_1|\mathbf{a}'\cdot\sigma\psi_1\rangle\langle\psi_2|\mathbf{b}'\cdot\sigma\psi_2\rangle - \langle\psi_1|\mathbf{a}\cdot\sigma\psi_1\rangle\langle\psi_2|\mathbf{b}'\cdot\sigma\psi_2\rangle
\end{aligned} \tag{32}$$

Since

$$\langle\psi_1|\mathbf{a}\cdot\sigma\psi_1\rangle, \langle\psi_1|\mathbf{a}'\cdot\sigma\psi_1\rangle, \langle\psi_2|\mathbf{b}\cdot\sigma\psi_2\rangle, \langle\psi_2|\mathbf{b}'\cdot\sigma\psi_2\rangle \in [-1,1] \tag{33}$$

by applying (31), we can easily see that the absolute value of the right-hand side of (33) is bounded by 2. This proves that a factorized pure state satisfies the BCHSH inequality:

$$\begin{aligned}
&-2 \le E_\rho(\mathbf{a},\mathbf{b}) + E_\rho(\mathbf{a}',\mathbf{b}) + E_\rho(\mathbf{a}',\mathbf{b}') - E_\rho(\mathbf{a},\mathbf{b}') \le 2\\
&\text{for every } \mathbf{a},\mathbf{a}',\mathbf{b},\mathbf{b}'
\end{aligned} \tag{34}$$

By linearity of the trace (22), an incoherent superposition of factorized pure states—as in (30) or as in (29)—gives rise to the same result. Hence, *factorized states do not violate BCHSH inequality and, in principle, admit an hidden-variable description*. In a sense, they are more classical than entangled states. This shows how, at least for a bipartite system, entanglement is the fundamental feature of quantum states giving rise to non-classical correlations.

The natural question arising from this result with factorized states is whether or not pure *entangled* states exist satisfying the BCHSH inequality. In fact, they exist, and there also exist

pure entangled states which violate BCHSH inequality without reaching the maximal value $2\sqrt{2}$.[28,33] In fact, in the case of bipartite systems it can be proved that, for any entangled pure state ρ, there exist measurement directions $\mathbf{a}, \mathbf{b}, \mathbf{a}', \mathbf{b}'$ such that the BCHSH inequality is violated.[44] This is not true for all entangled mixed states. Indeed, Werner provided examples of entangled mixed states satisfying all Bell-type inequalities and admitting a local hidden variables model describing the results of projective measurements.[45]

As a byproduct of this discussion, the violation of BCHSH inequality can be used as an *entanglement witness*, paying attention to the fact that it only gives sufficient but not necessary condition for entanglement. Indeed, by introducing the operator $O_{(\mathbf{a},\mathbf{b})}$ on $\mathcal{H} = \mathcal{H}_1 \otimes \mathcal{H}_2$ defined by

$$O_{(\mathbf{a},\mathbf{b})} = 2I_1 \otimes I_2 - \mathbf{a}\cdot\sigma \otimes (\mathbf{b}-\mathbf{b}')\cdot\sigma - \mathbf{a}'\cdot\sigma \otimes (\mathbf{b}+\mathbf{b}')\cdot\sigma \quad (35)$$

the inequality (35) can be written as $\mathrm{Tr}[\rho O_{(\mathbf{a},\mathbf{b})}] \geq 0$ for all separable states ρ, while for the Bell state $\rho_+ = |\Phi^+\rangle\langle\Phi^+|$ we obtain $\mathrm{Tr}[\rho_+ O_{(\mathbf{a},\mathbf{b})}] < 0$ for suitable choices of the vectors $\mathbf{a}, \mathbf{b}$. It is interesting to investigate selfadjoint (Hermitian) operators O on $\mathcal{H} = \mathcal{H}_1 \otimes \mathcal{H}_2$ which are able to distinguish between separable and entangled states as the operator O in (36). In fact, it is possible to prove that any entangled state ρ_{ent} admits an entanglement witness, that is, and selfadjoint operator O such that $\mathrm{Tr}[\rho_{ent} O] < 0$, while $\mathrm{Tr}[\rho O] \geq 0$ for all separable states.[46–48]

3. Single-Particle Entanglement and Non-Contextuality

If the compound quantum system described by a tensor product Hilbert space $\mathcal{H} = \mathcal{H}_1 \otimes \mathcal{H}_2$ does not consist of a pair of spatially distant particles, but it is a single particle with an internal structure, the non-separable states of the system are called *intraparticle* or *single-particle entangled states* (SPE). In this case, the system is not composed of two space-like separated subsystems and the EPR phenomenology does no longer give rise to the non-locality issues discussed in the previous sections in relation with Bell-type inequalities. However, intraparticle entangled states still provide the tool to test the conflict between quantum mechanics and other features expected by the classical description of physics, in particular its *non-contextuality*.

Examples of such a system is a single spin-1/2 massive particle, for which the degrees of freedom of momentum and spin are used to form SPE states, or a single photon, where, for example, the degrees of freedom of polarization and momentum are exploited. For these single particles, the Hilbert space is the Hilbert tensor product $L^2(\mathbb{R}^3, d^3k) \otimes \mathbb{C}^2$ (momentum picture). However, the analysis can be simplified if we can restrict the possibilities in the momentum space $L^2(\mathbb{R}^3, d^3k)$ to a 2D subspace. Indeed, let us consider the single particle case where, through a suitable filter apparatus, only the linear combinations of two state vectors labeled by two momenta $k_1, k_2 \in \mathbb{R}^3$ are accessible to the system. These two pure states, defined by a pair of unit-norm vectors $|\psi_{k_1}\rangle$ and $|\psi_{k_2}\rangle$, are wavefunctions strictly concentrated around k_1 and k_2, respectively. Since $k_1 \neq k_2$, it is reasonable to assume $\langle\psi_{k_1}|\psi_{k_2}\rangle = 0$. This way, the span of this pair of vectors is isomorphic to $\mathbb{C}^2$ and the effective Hilbert space of the system reduces to $\mathcal{H} = \mathbb{C}^2_{momentum} \otimes \mathbb{C}^2_{polarization/spin}$. Furthermore, observables corresponding to real linear combinations of $\sigma_1, \sigma_2, \sigma_3$ can be introduced also in the first factor. From an experimental point of view for single photons, all these observables are associated with linear optical devices as *beam-splitters*, *mirrors*, *polarization analyzers* and so on. Not only polarization but also orbital angular momentum degrees of freedom can be exploited to generate SPE states with single photons.[49,50]

In this setting, an intraparticle entangled Bell state $|\Phi^+\rangle$ for a photon[14,15] is, for example,

$$|\Phi^+\rangle = \frac{1}{\sqrt{2}}\left(|\psi_{k_1}\rangle \otimes |H\rangle + |\psi_{k_2}\rangle \otimes |V\rangle\right) \quad (36)$$

and the analogous state for a spin 1/2 particle is [22]

$$|\Phi^+\rangle = \frac{1}{\sqrt{2}}\left(|\psi_{k_1}\rangle \otimes |z_+\rangle + |\psi_{k_2}\rangle \otimes |z_-\rangle\right) \quad (37)$$

Even if the EPR phenomenology, that is, the (apparently) paradoxical consequences of entanglement in space-like separated systems, does not play any role here, the states above still present the peculiar features of entanglement. For instance, in the case of the Bell state (38), there are no direction $\mathbf{n}$ for which the component of the spin of the particle is well defined since the state $|\Phi^+\rangle$ cannot be an eigenvector of observables of the form $I \otimes \mathbf{n}\cdot\sigma$. Furthermore, it is interesting to investigate the meaning of Bell inequalities violations in this context. Indeed, dealing with SPE, the role of locality is negligible whereas that of non-contextuality is crucial.

3.1. Non-Contextual Hidden Variables Theories and Bell Inequalities

Within the context of *hidden-variable theory* to explain *quantum mechanics*, a quantum system S is actually supposed to be partially classic and the observed randomness of measurement outcomes is due to a non-complete knowledge of the system, making quantum randomness merely epistemic. As already discussed in Section 2.2, there are *hidden variables*, cumulatively denoted by $\lambda \in \Lambda$, which completely fix a classical-like state of the system and the values of every observable that is *always defined* according to the *realism* hypothesis. If we knew λ, we would also know the precise value $v_\lambda(O) \in \sigma(O)$ every observable O has.

In this framework, Bell's analysis refers to a *local* hidden-variable theory, that assumes that the results of measurements in a region of space-time are not influenced by measurements which are performed in a region which is space-like separated. More precisely, the mathematical formalism implicitly assumes *non-contextuality*, that is, *for any choice of the hidden parameter $\lambda \in \Lambda$, the values $v_\lambda(O_1)$ and $v_\lambda(O_2)$ of two observables which are measured in two space-like separated regions do not depend on the whole set of observables which are simultaneously measured*. That is why we write $v_\lambda(O_1)$ and $v_\lambda(O_2)$ instead of $v_\lambda(O_1|O_2)$ and $v_\lambda(O_2|O_1)$. We stress that this requirement is here a consequence of locality: the choice of O_2 is made in a spacetime region which is space-like separated from the region where O_1 is measured. As a matter of fact, a local hidden-variable theory is a particular case of

a *non-contextual hidden variables theory*. This class of classical-like description of quantum phenomenology relaxes the locality requirement present in local hidden-variable theory and relies upon the following assumptions:

Realism. *All observables O always attain precise values $v_\lambda(O) \in \mathbb{R}$ determined by $\lambda \in \Lambda$, independently from our measurements.*

Non-Contextuality. *The value $v_\lambda(O)$ cannot depend on the choice of other observables which are simultaneously measured with O.*

The realism hypothesis implicitly assumes that for any quantum observable O, fixed $\lambda \in \Lambda$ the values $v_\lambda(O)$ belong to the spectrum of O. The non-contextuality assumption deals with *simultaneous measurements* of observables. These, by a quantum mechanical point of view, must be *compatible*, hence described by commuting operators. Examples of couples of compatible observables can be simply provided in the case where the Hilbert space of the system is a tensor product since, as remarked in Section 2, observables referred to different factors commute. Hence, one simple system to test a non-contextual hidden-variable theory is the two-qubit system (37), where the Hilbert space $\mathcal{H} = \mathbb{C}^2_{momentum} \otimes \mathbb{C}^2_{polarization}$ is associated with the states of a photon whose propagation direction is restricted to two possible vectors k_1, k_2. In this setting, for any choice of $\mathbf{a}, \mathbf{b} \in \mathbb{R}^3$ we can construct the couple of quantum compatible observables $O(\mathbf{a}) = \mathbf{a} \cdot \sigma \otimes I$ and $O(\mathbf{b}) = I \otimes \mathbf{b} \cdot \sigma$. In fact, the spectrum of both (spin-like) observables contains just the two values ± 1. Furthermore, given a quantum state ρ, according to non-contextual hidden-variable theories this state corresponds to a probability measure μ over the space Λ of hidden variables $\lambda \in \Lambda$ representing our partial knowledge of the "real" state of the system.

Within this setup, the already introduced BCHSH inequality can be used to distinguish between hidden-variable descriptions which assume or do *not* assume realism and non-contextuality. Similarly to the discussion of Section 2.2, *entangled states* play a crucial role, even if locality does not enter the game. As in the Bell's analysis of entangled particles, it is now convenient to introduce the quantity

$$\chi(\mathbf{a}, \mathbf{a}', \mathbf{b}, \mathbf{b}'|\lambda) = v_\lambda(O(\mathbf{a}))v_\lambda(O(\mathbf{b})) + v_\lambda(O(\mathbf{a}'))v_\lambda(O(\mathbf{b})) + v_\lambda(O(\mathbf{a}'))v_\lambda(O(\mathbf{b}')) - v_\lambda(O(\mathbf{a}))v_\lambda(O(\mathbf{b}')) \quad (38)$$

We define the expectation value $\mathbb{E}_\mu(\chi)$ of $\chi(\mathbf{a}, \mathbf{a}', \mathbf{b}, \mathbf{b}'|\lambda)$ as in (5). When λ varies in Λ with a probability distribution μ, with the same reasoning as in Section 2.2, we find again $-2 \leq \mathbb{E}_\mu(\chi) \leq 2$. Indeed, defining

$$E_\mu(\mathbf{a}, \mathbf{b}) := \int_\Lambda v_\lambda(O(\mathbf{a}))v_\lambda(O(\mathbf{b}))d\mu(\lambda) \quad \text{for every unit vector } \mathbf{a}, \mathbf{b} \quad (39)$$

we obtain again the *BCHSH inequality*,

$$-2 \leq E_\mu(\mathbf{a}, \mathbf{b}) + E_\mu(\mathbf{a}, \mathbf{b}') + E_\mu(\mathbf{a}', \mathbf{b}') - E_\mu(\mathbf{a}, \mathbf{b}') \leq 2 \quad \text{for every } \mathbf{a}, \mathbf{a}', \mathbf{b}, \mathbf{b}' \quad (40)$$

These inequalities regarding correlations of measurements of the spin-like components of a bipartite system must be satisfied by every realistic non-contextual theory.

In contrast, the quantum result violates these inequalities. Indeed, if we restrict the choice of the state to *entangled* pure *Bell's state* $\rho = |\Phi^+\rangle\langle\Phi^+|$ given by (37) and we fix the axes $\mathbf{a}, \mathbf{a}', \mathbf{b}, \mathbf{b}'$ as in (23), we find (24). Since $2\sqrt{2} > 2$, we conclude that *the result predicted by Quantum Theory, with the said choices of observables and Bell's intraparticle-entangled states, is incompatible with a realistic non-contextual hidden-variable theory.*

In view of the discussion of SPE experiments in Section 4, we remind that the same remarks made at the end of Section 2.2 about the use of BCHSH inequality in EPR-type experiments, hold here for the use of (41) in SPE experiments. In particular, relations (19), (20) and (21) can be extended here to the couple of observables associated with the two internal degrees of freedom of the same particle. Moreover, it is interesting to point out that the collection of the count rates $N_{ij}^{(\mathbf{a},\mathbf{b})}$ appearing in (21) is, from an experimental point of view, less demanding in the case of SPE. Indeed, in the case of interparticle entanglement, the empirical frequencies $N_{ij}^{(\mathbf{a},\mathbf{b})} / \sum_{i,j} N_{ij}^{(\mathbf{a},\mathbf{b})}$ are referred to outcomes of joint measurements of two observables performed on two different particles *belonging to the same entangled pair*. Hence, the experimental setting as well as the source of entangled pairs are required to allow the precise identification of the single particles in the entangled pairs. In particular, a strict control of times of arrival plays an important role in this context. On the contrary, for SPE this difficulty is no longer present since the count rates $N_{ij}^{(\mathbf{a},\mathbf{b})}$ refer to measurements of compatible observables performed *on the same particle*. Since no identification of entangled pairs is required, a strict control of arrival times is not mandatory.

3.2. The Kochen–Specker Theorem

The problem of contextuality in the form described above was explicitly addressed by S. Kochen and E. Specker in 1967.[51] They proved a "no-go" theorem which shows the impossibility of translating the mathematical formalism of quantum mechanics into a realistic non-contextual hidden-variable theory. Bell proved the same statement in 1966[52] before proving his inequalities, that is, most probably in 1963. Recently, a series of experiments probing different form of contextuality based on test of Kochen–Specker's theorem have been proposed.[14,22,53,54]

The Kochen–Specker theorem does not deal with the statistical predictions, namely the outcomes of experiments, as the BCHSH inequalities. It considers the consequences of assigning to every quantum observable, that is, every self-adjoint operator A on a complex Hilbert space, a definite value $v(A) \in \mathbb{R}$. In the hidden-variable theory interpretation, $v(A)$ are the (unknown) values of the observables A simultaneously fixed by the choice of the hidden variable $\lambda \in \Lambda$. Explicitly, $v_\lambda(A)$, that is, every observable assumes a value fixed by λ independently from the measurements as the realism postulate dictates. Natural requirements are

1. $v(A) \in \mathbb{R}$
2. $v(A + A') = v(A) + v(A')$ and $v(AA') = v(A)v(A')$ if A and A' commute[55,56]

It is not even necessary to assume that the values $v(A)$ belong to the spectrum of A to produce the no-go result of Kochen and Specker. In fact, the Kochen–Specker theorem proves that, *if* $2 < \dim(\mathcal{H}) < \infty$, *there is no map associating each observable A over $\mathcal{H}$*

with a value $v(A) \in \mathbb{R}$ such that conditions 1 and 2 are fulfilled, at exclusion of the trivial map $v(A) = 0$ for all A.[57]

There are many proofs of the Kochen–Specker theorem, the first one was provided by Bell in ref. [52] relying on the fundamental *Gleason's theorem* (see refs. [27,43] for a modern proof according to Bell's approach). For this reason the result should be named the *Bell–Kochen–Specker theorem*. The finite-dimensionality hypothesis can be omitted requiring suitable continuity properties of v[43] (see ref. [41] for a critical and historical discussion on the subject).

If one wants to insist on a hidden-variable formulation, the simplest way out from the no-go result by Kocken and Specker is just to reject the *realism* assumption, admitting that *not all observables are defined even if we fix the hidden state λ*. Another possibility assumes that all observables are always and simultaneously defined and relies on the idea of *contextuality* (already proposed in ref. [52] in a more general context). In this view, the value $v_\lambda(A)$ fixed by the hidden state λ also depends on the set $\mathcal{A} \ni A$ of pairwise compatible observables which are measured simultaneously with A. A more precise notation for the value taken by A when λ is given is therefore $v_\lambda(A|\mathcal{A})$. Notice that we are not saying that the value of A depends on the *values* of the observables in $\mathcal{A}$, but only on the *choice* of $\mathcal{A}$. We also stress that all those values $v_\lambda(A|\mathcal{A})$ of a given observable A are assumed to *co-exist* and are not fixed by the measurement procedure of A and $\mathcal{A}$. Conversely, in quantum mechanics, the *realism* postulate is rejected and the value of A is fixed by its measurement and does not depend on any choice of $\mathcal{A}$.

Since commutativity is not a transitive relation, there are many sets of pairwise compatible observables $\mathcal{A}$, $\mathcal{A}'$ including A such that they contains pairs of observables $B \in \mathcal{A}$, $B' \in \mathcal{A}'$ with $BB' - B'B \neq 0$. In addition, there must be choices of $\mathcal{A}$ and $\mathcal{A}'$ giving rise to $v_\lambda(A|\mathcal{A}) \neq v_\lambda(A|\mathcal{A}')$ just in view of the Kochen–Specker theorem. A hidden-variable theory with these peculiarities on the value of observables is said to be *contextual*: $\mathcal{A} \ni A$ is the *context* of A. From this regard, the Kochen–Specker theorem rules out *realistic non-contextual* hidden-variable theories but still permits *realistic contextual* hidden-variable theories.[58]

An alternative version of the Kochen–Specker theorem, more suitable for experimental verification on bipartite systems described by $\mathbb{C}^2 \otimes \mathbb{C}^2$ not necessarily entangled, deals with *tests* on the quantum system, namely observables whose values are only 0 (NO) and 1 (YES). Tests are mathematically represented by *orthogonal projectors* P in $\mathcal{H}$. A map assigning values $p(P) \in \{0, 1\}$ to tests P can be also viewed as a *sharp probability distribution*, taking only values 0 or 1. As before, in the context of a hidden-variable theory, the physical interpretation is that $p(A)$ depends on some hidden variable λ and we can write $p_\lambda(P)$. This alternate version of the Kochen–Specker theorem establishes that *for $2 < \dim(\mathcal{H}) < \infty$, there is a set $\mathcal{P}$ of tests such that no assignment map $p : \mathcal{P} \to \{0, 1\}$ exists satisfying the following pair of natural requirements.*

1. *if $P, P' \in \mathcal{P}$ are compatible and mutually exclusive, at most one of $p(P)$, $p(P')$ does not vanish.*
2. *if $P_1, P_2, \ldots, P_N \in \mathcal{P}$ are compatible, mutually exclusive, and $P_1 + \cdots + P_N = I$ then exactly one of the values $p(P_1), \ldots, p(P_N)$ does not vanish.*

The two versions of the Kochen–Specker theorem are equivalent as soon as one assumes the standard foundations of the quantum theory (an equivalence proof can be found in ref. [43]). To prove their theorem for $\dim(\mathcal{H}) = 3$, Kochen and Specker wrote down a set $\mathcal{P}$ of 117 tests (projecting onto 1D subspaces) showing that $\mathcal{P}$ satisfies the second version of the Kochen–Specker theorem with an elaborate proof.[51]

There are some interesting experiments (or experiment proposals) toward falsification of non-contextual hidden variable theories which use *single photons* with the Hilbert space of momenta constrained to be a 2D space as previously discussed. In ref. [54] a direct state-independent experimental evidence of the thesis of the Kochen–Specker theorem, in the test version, is produced. Here, a single photon and the decomposition of its (constrained) Hilbert space $\mathcal{H} = \mathbb{C}^2_{\text{angular momentum}} \otimes \mathbb{C}^2_{\text{polarization}}$ yield a set of 18 tests. Another experiment discussed in the same paper uses again a single photon but the (constrained) Hilbert space is decomposed as $\mathcal{H} = \mathbb{C}^2_{\text{momentum}} \otimes \mathbb{C}^2_{\text{polarization}}$. In both cases, the experiment is performed preparing the photon in a number of initial states of different types, including pure and mixed states, factorized or intraparticle entangled. Agreement is found with the Kochen–Specker no-go result encoded in a state-independent violation of an inequality constructed out of the results of the tests. A different experiment refers to the first version of the Kochen–Specker theorem.[14] Here, the system is a single photon whose Hilbert space is $\mathcal{H} = \mathbb{C}^2_{\text{momentum}} \otimes \mathbb{C}^2_{\text{polarization}}$. The experimental setup requires to prepare the system in a SPE state and non-contextuality violation is certificated by the violation of the BCHSH inequality. A similar experiment is proposed by ref. [59], where a single spin-1/2 particle is constrained to have a space of states of the form $\mathcal{H} = \mathbb{C}^2_{\text{momentum}} \otimes \mathbb{C}^2_{\text{spin}}$ and SPE is explicitly exploited.

4. Experimental Implementations of Single-Particle Entanglement

The concepts of entanglement and of non-locality are associated in the EPR gedanken experiment. This has led to consider them equivalent. However, single-particle entanglement precludes any classical description and is local. In this case, its quantum signature is contextuality and not non-locality, as discussed in Section 3.

Remark. It is worth stressing that, though it is common to speak about *quantum contextuality*, this notion is actually an oxymoron if literally interpreted: after the Kochen–Speker theorem, contextuality is a necessary property of every realistic hidden-variable theory (if any) that is assumed to be capable to explain the experimental phenomenology of quantum systems. Quantum mechanics is a logically consistent theory as it stands, in particular it is not realistic in the precise sense used in the Kochen–Speker theorem, just due to the existence of incompatible observables. Instead, contextuality just arises when forcing a description of the phenomenology of quantum mechanics to be realistic. Therefore, when a paper (as the present work) refers to tests on quantum contextuality it actually means tests about the impossibility to span the same quantum phenomenology within a *realistic* non-contextual classical theory involving some hidden variable. In particular to be forced to assume contextuality we have to

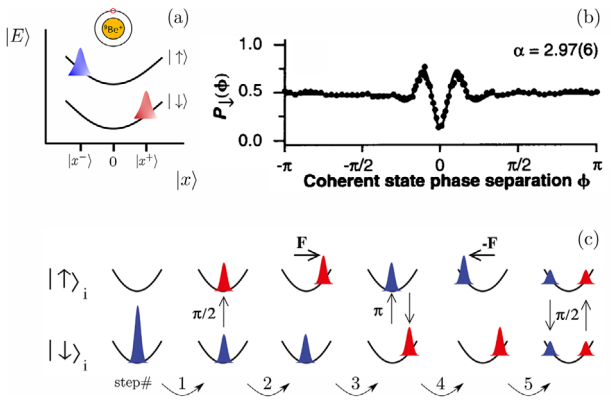

Figure 1. a) Schematic representation of a SPE where the position and the electronic states of a single Beryllium ion—laser-cooled in a potential trap—are entangled. The wave packets show the probability of finding the ion in the given electronic state. b) Measured (dots) and fit (line) interference signals $P_{|\downarrow\rangle}$ as a function of the phase difference ϕ between the two coherent wave packets, for a given value of the coherent states amplitude α. Reproduced with permission.[60] Copyright 2020, American Association for the Advancement of Science. c) Sketch of the harmonic oscillator potential and the wave packets for each component of the ion's internal states $|\uparrow\rangle$,$|\downarrow\rangle$. Each of the six images represents a time snapshot of the ion state between two successive steps of the measurement protocol. Adapted with permission.[61] Copyright 2020, The Nobel Foundation.

always assume to deal with realistic theories alternative to quantum mechanics.

The first experimental example of such a locally entangled state can be considered the mesoscopic Schrödinger cat-like state of cold atoms realized with trapped Be ions by the group of Wineland, in 1996.[60] By applying a specific sequence of laser pulses (see **Figure 1**c) to a laser-cooled single $^9Be^+$ ion trapped in a harmonic potential, they were able to entangle the local spatial position of the atom wave packet inside the trap with its hyperfine ground state, namely they entangled an external (motional) state with an internal (electronic) quantum state, respectively. The result is pictured in Figure 1a and can be written as

$$|\psi\rangle = \frac{1}{\sqrt{2}}\left(|x^-\rangle \otimes |\uparrow\rangle + |x^+\rangle \otimes |\downarrow\rangle\right) \tag{41}$$

where $|x^{\mp}\rangle$ are two localized ($\approx 7\,nm$) coherent atomic wave packets with an average of ca. 9 vibrational quanta and separated by more than $80\,nm$, while $|\uparrow\rangle$ and $|\downarrow\rangle$ are two internal electronic quantum states of distinct energies.[60] Even if these kets refer to different degrees of freedom of the same particle, the state of equation (42) can be seen as entangled since it cannot be separated into a product of individual states each one defined in a different Hilbert space. Because of the efficient coupling implemented between the ion's hyperfine ($|\uparrow\rangle$,$|\downarrow\rangle$) and motional ($|x^-\rangle$,$|x^+\rangle$) states, the state (42) can be seen as the superposition of two spatially separated coherent harmonic oscillator states (the wave packets in Figure 1a). Their coherence can be verified via the observation of an interference pattern appearing when the two wave packets are combined (situation after step 5 in Figure1c). Experimentally, this happens when measuring the probability $P_{|\downarrow\rangle}$ that the ion is in the $|\downarrow\rangle$ internal state for a given value of the relative coherent state motional phase separation ϕ (the relative phase ϕ is dictated by the phases of the control laser beams[60]). The experimental results are reported in Figure 1b. The state (42) is repeatedly generated and measured while sweeping the phase ϕ. The observation of interference fringes in $P_{|\downarrow\rangle}$ as a function of ϕ directly proves the quantum superposition, and thus the entanglement.[60] A key component in the experiment is the laser that allows measuring the internal quantum state $|\downarrow\rangle$ of the single ion independently of its state of motion. In other words, the quantum correlation generated between the internal and external states of the ion imprints the superposition of the hyperfine ground states (situation after step 1 in Figure1c) in a superposition of the motional states (situation after step 4 in Figure 1c). The latter is monitored by measuring the former. Let us note that these measurements refer to the quantum coherence of this particular single-particle entangled state and do not represent a measurement of intraparticle entanglement as the ones described in the following. Interestingly, the 1 to 5 sequence in Figure 1c can be considered as a Mach–Zehnder interferometer where the state splits at the beginning and recombines at the end, in full analogy with the typical scheme employed for SPE demonstration. However, proving SPE was not the aim of ref. [60] which leaves room for future SPE-oriented investigations with atomic ions.

4.1. Generalities about Single-Particle Experiments

The Kochen–Specker theorem (Section 3.2) states the contextual character of any realistic hidden variable theory that should explain quantum mechanics, and it is applied to any quantum state, including separable ones. Let us consider a bipartite system made of two independent sub-systems not space-like separated, analogous to what depicted in Figure 1. When the level of correlation between the measurements of the two observables corresponding to the two sub-systems violates the BCHSH inequality, Local HV theory must be contextual in order to agree with quantum physics. Therefore, the violation of the BCHSH inequality for measurements performed on different degrees of freedom of a single particle is a demonstration of intraparticle entanglement and of contextual behavior of any realistic hidden variable theory able to explain the same phenomenology at the same time. This idea was initially introduced in 1984 by Home and colleagues,[62] who, first in 1999,[63] suggested an interferometric arrangement for testing this single-particle inequality using neutrons, a work then published in 2001.[64] Practically at the same time, the first experiment with single photons was performed by Żukowski and colleagues, and published in 2000.[14]

We note that few experimental tests of quantum contextuality have been reported for which entanglement and, even, quantum states are not necessary.[22,53,54,65–67] These experiments prove certain versions of the Kochen–Specker theorem, which do not need entangled state, and, as a consequence, these tests are particularly promising for quantum information applications. In particular, recent results[68] indicate that a violation of the Kochen–Specker non-contextuality can be converted into a violation—by the same degree—of a generalized Bell inequality without the requirement of preparing and measuring entangled states. However, in this review we deal with intraparticle entanglement and we refer the reader to the cited papers for a discussion of quantum contextuality tests.

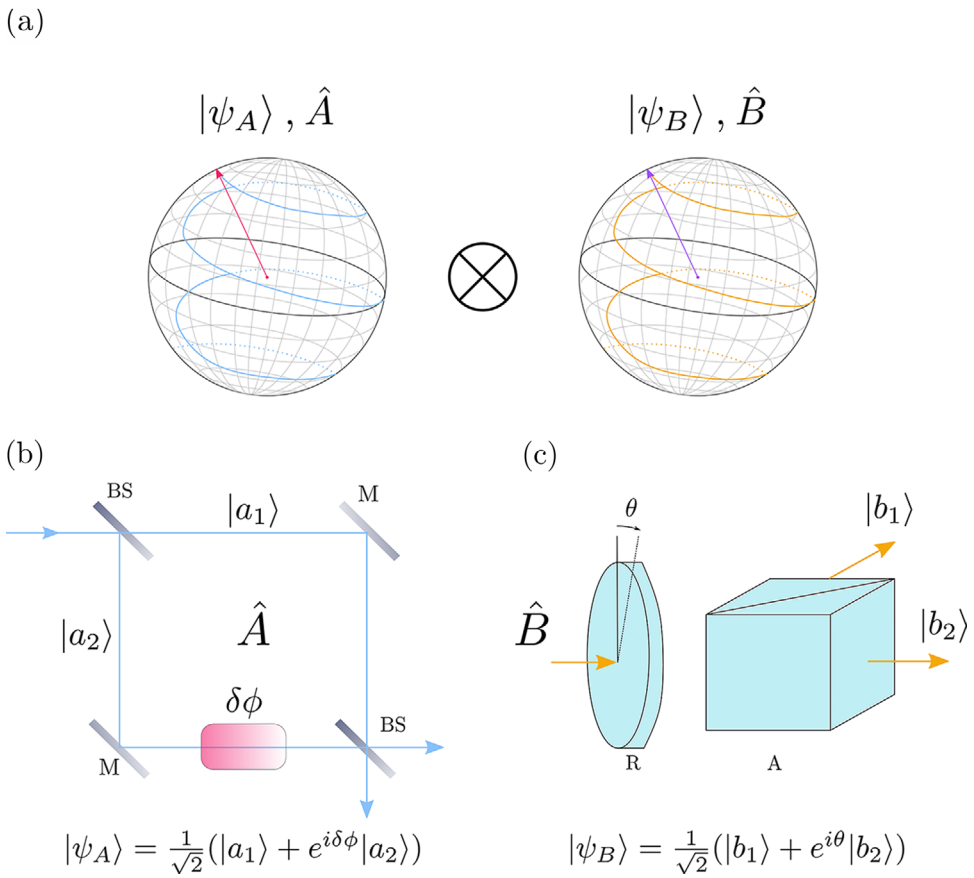

Figure 2. a) Pictorial view of the entanglement of two qubits, $|\psi_a\rangle$ and $|\psi_b\rangle$, of a same particle ($\hat{A}$ and $\hat{B}$ being the operators associated with the observables). b) Scheme of a Mach–Zehnder interferometer, the experimental setup used for performing rotations on the Bloch sphere of $\hat{A}$, when $\hat{A}$ represents the momentum of the single particle. c) Sketch of the device used to perform rotations on the Bloch sphere of $\hat{B}$, when $\hat{B}$ represents the spin of a single particle. Here, the device is a sequence of a rotator (R) and an analyzer (A).

Violation of BCHSH inequalities by SPE states have been reported for a few types of particles, namely single photons,[14,15,69,70] single neutrons[16–18,71] and single atoms.[72,73] Entanglement has been shown between different degrees of freedom of the single particles: spin-momentum and spin-orbital momentum for photons; spin-momentum and spin-energy for neutrons; spin-momentum for atoms. Despite being different in nature, all these experiments share the same fundamental idea, a pictorial view of which is sketched in **Figure 2**. The time evolution of two qubit observables of a same particle, for example, $|\psi_A\rangle$ and $|\psi_B\rangle$, can be mapped to a trajectory onto a Bloch sphere, since each one of them can be parametrized by Bloch vectors. The single particle can thus be prepared in a state in which the two qubits, each one associated with a different observable (e.g., $\hat{A}$ and $\hat{B}$), are entangled (see Figure 2a). Therefore, measuring the intraparticle entanglement corresponds to seek for those pairs of Bloch vectors featuring strong correlations. If $\hat{A}$ is, for example, the momentum of the particle, a Mach–Zehnder interferometer can be used, specific to the nature of the particle. If $\hat{B}$ is, for example, the spin of the particle, a combination of a spin rotator and a spin analyzer can be used, whose experimental implementation depends on the single particle studied (see Figure 2b). In the following, we describe in details some experiments which are relevant to prove the fundamental quantum aspects of nature, and, by doing this, they pave the way to quantum information applications (see more in the next section).

4.2. Single-Photon Entanglement

Historically, experiments involving photon pairs featuring strong correlations in polarization have been the first ones to provide proofs toward the falsification of local realistic hidden-variable theory, namely to show that nature is indeed non-realistic and/or non-local.[26,74] As a matter of fact, local realistic hidden-variable theories are a particular case of non-contextual realistic hidden-variable theories (discussed in Section 3.2), for which the locality requirement has been relaxed. Non-contextual realistic hidden-variable theories assume that the predetermined result of a particular measurement of an observable does not depend on the choice of another observable commuting with the first one and simultaneously measured. These observables, in general, do not need to be space-like separated. In 1967, the Kochen–Specker theorem ruled out such a form of local realism from a mathematical point of view. However, only about 20 years ago, the

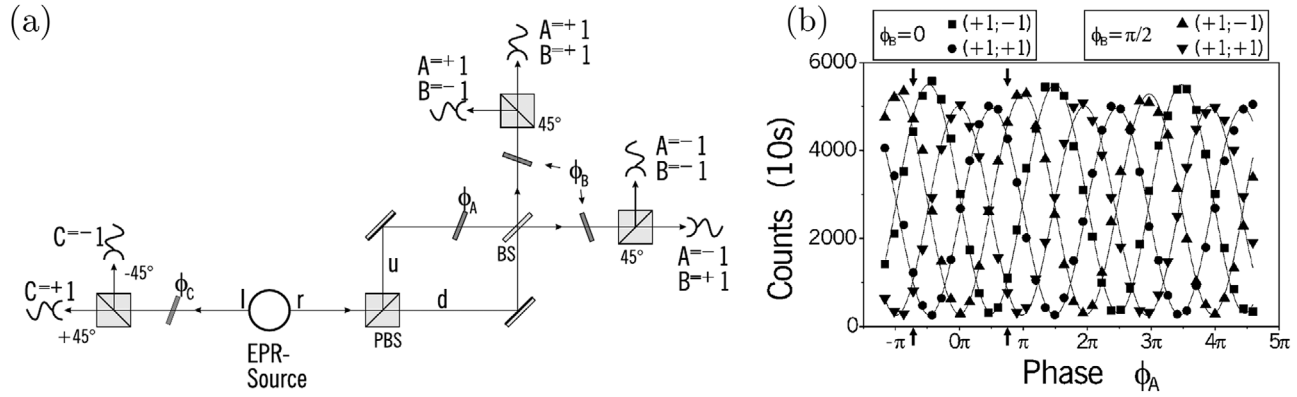

Figure 3. a) Experimental setup used to test non-contextual HV theories on spin and momentum degrees of freedom of a single heralded photon. b) Single photons counts as a function of ϕ_A for the two values of ϕ_B indicated. The arrows indicate the values of ϕ_A for which a maximum violation of the BCHSH inequality is reported. Adapted with permission.[14] Copyright 2000, The American Physical Society.

first issues were raised about the usefulness of the Kochen–Specker theorem, because of the impossibility to experimentally test it with finite time and precision measurements.[75,76] In 1999, Żukowski et al. pointed out that all experiments testing local realistic hidden-variable theories with photon pairs are affected by possible loopholes (e.g., detection loophole) and, thus, cannot ensure the non-locality. They proposed, therefore, an experiment on a single photon, heralded from a photon pair, where two distinct commuting observables are measured, that is, the polarization (the photon spin angular momentum) and the propagation direction (the photon linear momentum or path). In this way, they showed a possible implementation of the varying context needed to test and falsify non-contextual hidden-variable theories, and paving the way to SPE experiments with photons.

4.2.1. Single-Photon Spin-Momentum Entanglement

The first experimental test of a BCHSH inequality violation for joint measurements of commuting observables on a single particle was carried out on heralded single-photons where the spin-path degrees of freedom are entangled.[14] In this case, the entangled state is described by a tensor product Hilbert space $\mathcal{H} = \mathcal{H}_1 \otimes \mathcal{H}_2$, where $\mathcal{H}_1$ and $\mathcal{H}_2$ are disjoint Hilbert spaces in which the spinor and spatial wave functions describing the internal structure of the photon are defined. Thus, the Hilbert space of the system can be explicitly written to be $\mathcal{H} = \mathbb{C}^2_{spin} \otimes \mathbb{C}^2_{momentum}$. The experimental setup used for this first measurement is reported in **Figure 3**a. Polarization entangled photon pairs at the wavelength of 702 nm are produced via a type-II spontaneous parametric down conversion (SPDC) in the state $|\psi_{initial}\rangle = \frac{1}{\sqrt{2}}(|H_1\rangle \otimes |V_2\rangle + |V_1\rangle \otimes |H_2\rangle)|r\rangle_1|l\rangle_2$, where $|H\rangle$ and $|V\rangle$ are the horizontal and vertical polarization states, respectively, that is, the basis of the Hilbert space $\mathbb{C}^2_{spin}$, while $|r\rangle_1$ is the right-going photon 1, $|l\rangle_2$ the left-going photon 2. The latter is the heralder of single photons to the right side, where a polarizing beam splitter is used to prepare the intra-photon entangled state $|\psi\rangle = \frac{1}{\sqrt{2}}(|H\rangle \otimes |d\rangle + |V\rangle \otimes |u\rangle)$, where $|d\rangle$ and $|u\rangle$ are the down and up paths, respectively, forming the basis of the momentum space $\mathbb{C}^2_{momentum}$. It has to be noted that, because of the type-II phase matching condition, each heralded single-photon is already a polarization qubit. Therefore, the single-photon entanglement is generated just after the polarizing beam splitter on the right side of the source, which indeed entangles the polarization and propagation directions of the single photons. The phase shifter ϕ_A allows to implement rotations in the spatial basis, while the beam splitter BS operates the projections onto the paths $|u\rangle$ and $|d\rangle$. For each one of these, the birefringent phase plate ϕ_B (fast axis vertical) followed by a polarizing beam splitter (PBS) oriented at 45° perform, respectively, rotation and projection in the polarization basis. The authors of this experiment used only four detectors (single-photon avalanche photodiodes), namely they did not register the outputs of the polarization measurements on the $|d\rangle$ path at the right side of BS.

The experimental evidence of spin-momentum single-photon entanglement is given by the observation of interference fringes with a visibility larger than $1/\sqrt{2} \simeq 0.71$ obtained from successive single photon detection events as a function of the phase shift ϕ_A, for the polarization phase ϕ_B set to 0 and $\pi/2$. These are values of ϕ_B for which a maximum violation of the BCHSH inequality (20) is expected. The expectation values needed in the calculation of the S-parameter are determined on the basis of the experimental count rates following the formulation (21). The results are shown in Figure 3b. The arrows indicate the values of the phase shift ϕ_A where the count rates are taken, for each value of ϕ_B, in order to evaluate the correlation coefficients and compute the S-parameter. A maximum violation is expected, for example, for the values $\phi_A = -0.72\pi$ and $\phi_B = 0.75\pi$ where one obtains $S = 2.595 \pm 0.015$. This S-value represents a large violation of non-contextuality, and, therefore, a proof of single-photon entanglement.

The violation of two distinct Bell inequalities with single photons entangled in momentum and polarization has also been reported in another similar experiment.[15] The scheme of this experimental setup is shown in **Figure 4**a. Photon pairs are here produced via a type-I collinear SPDC nonlinear process at a wavelength of 915.8 nm. The photon pairs are split by a non-polarizing beam splitter, such that the reflected photons, detected by a photon counter, herald single photons in the transmission path. A Glan–Thompson polarizer set to vertical direction

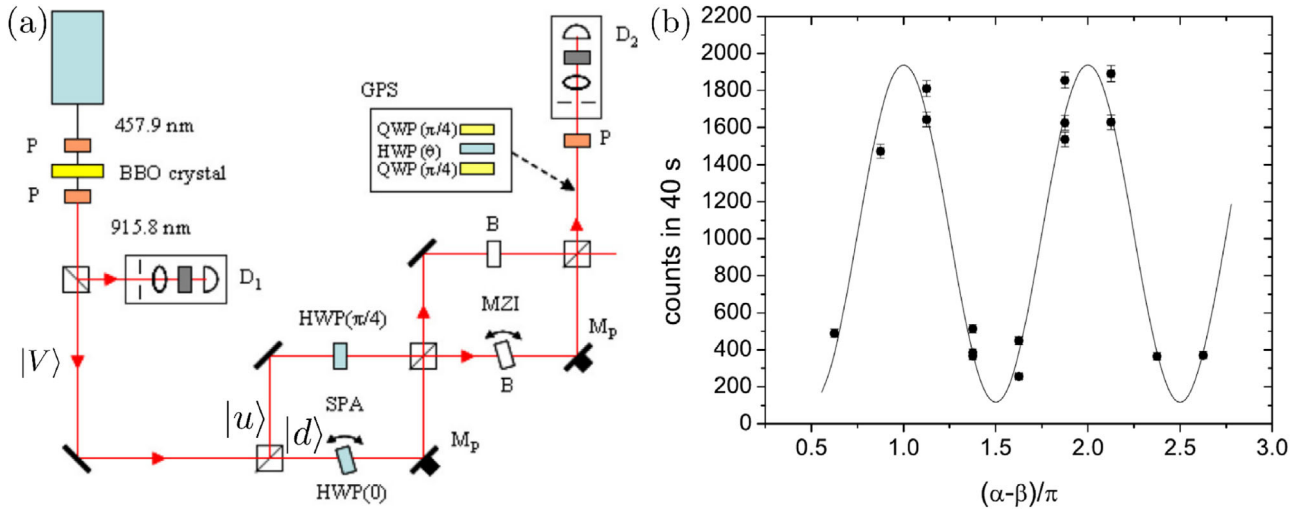

Figure 4. a) Experimental setup used to generate and test SPE between polarization and momentum of heralded single photons produced in a type-I SPDC process. HWP, half-wave-plate; SPA, state preparation arrangement. b) Counts of single photons events, as a function of the momentum–spin phase difference $\alpha - \beta$ (π units), used to compute the *S*-parameter reporting a violation of the BCHSH inequality (see main text). Adapted with permission.[15] Copyright 2009, IOP Publishing.

is placed just after the down-conversion crystal to ensure a high rejection of the horizontally polarized pump laser. Indeed, because of the type-I phase matching condition, in which the generated pair shares the same linear polarization state (i.e., vertical, orthogonal to the pump), the resulting heralded single photons do not constitute a polarization qubit as in the previously discussed experiment (namely, their polarization state is simply vertical). For this reason, a state preparation arrangement (indicated by SPA in Figure 4a) is needed to generate the intraparticle entanglement. This stage is implemented by a non-polarizing beam splitter which puts the vertically polarized heralded single photons into a superposition of two paths. In the top one, the polarization state of the photon is turned to horizontal via a half-wave plate set at 45° with respect to the vertical direction (HWP($\pi/4$) in Figure 4a). While in the other arm, an identical half-wave plate at 0° (in Figure 4a HWP(0), fast axis oriented vertically) is used for equalizing the two optical paths and for finely tuning the phase difference δ. At the output beam splitter of the state preparation arrangement stage, single photons are found in the entangled state $|\psi\rangle = \frac{1}{\sqrt{2}}(|H\rangle \otimes |u\rangle + \exp(i\delta)|V\rangle \otimes |d\rangle)$, with obvious meaning of the symbols in reference to Figure 4a.

The state preparation arrangement stage is followed by an analyzer stage, namely a Mach–Zehnder interferometer functioning as a spatial basis rotator and projector. Indeed, a Mach–Zehnder interferometer acts as a unitary gate which rotates the momentum-space qubit by a total phase difference α. The output of the Mach–Zehnder interferometer is sent to the combination of a half-wave plate and a polarizing beam splitter, respectively. These are used to perform a rotation of an angle β and to project the polarization state on a linear basis just before the single photon detector (D_2). The experimental results of the single photon detection events as a function of the relative phases difference $\alpha - \beta$ are reported in Figure 4b for one type of test. A violation of the BCHSH inequality is observed for $\alpha = -\pi/4$, $\alpha' = -\pi/2$, $\beta = -3\pi/8$ and $\beta' = 3\pi/8$ where $S = 2.47 \pm 0.06 > 2$.

4.2.2. Single-Photon Spin-Orbit Entanglement

The total angular momentum of a photon is the sum of its spin angular momentum (SAM) and orbital angular momentum (OAM).[77,78] While the first one has been known since the pioneering works of Poynting (theory, 1909) and Beth (experiment, 1936), only much later, in 1992, an experiment was proposed by Allen et al.[79] to measure the OAM of light. They realized that Laguerre–Gauss laser beams with an azimuthal phase dependence of the type $\exp(-il\phi)$, with ϕ being the azimuthal angle, are characterized by an amount of OAM equal to $l\hbar$, with l taking any integer positive or negative integer values. OAM is a particularly interesting resource for quantum information since l is an unbounded integer value. Therefore, the discrete Hilbert space of OAM can be infinitely dimensional, opening the possibility to implement high dimensional quantum states.[49] Moreover, OAM can be coupled to SAM in inhomogeneous anisotropic media—normally referred to as *q* plate[80]—via the so-called Pancharatnam–Berry geometrical phases,[81] for which the input polarization (spin) can affect the output wavefront (orbit), that is, optical spin-orbit interaction. In these experimental conditions, a complete conversion of the optical angular momentum from its spin form to its orbital form can take place. This unexpected effect remains true at the quantum level, so that *q* plates are actually exploited for both generating SPE states in polarization and transverse spatial structure (wavefront), and for transferring quantum information from the SAM to the OAM degrees of freedom, and vice-versa.[82] The Hilbert space of the SPE can be written as the tensor product of the Hilbert spaces corresponding to SAM and to OAM, namely $\mathcal{H} = \mathbb{C}^2_{SAM} \otimes \mathbb{C}^2_{OAM}$. The most natural way to implement the coupling of these degrees of freedom is to use the spin-to-orbital angular momentum conversion mechanism available in a *q* plate, for example, the one corresponding to $q = 1$ illustrated in **Figure 5**a.

Two main experimental reports about spin-orbit entangled states of single photons have been published.[69,70] The first

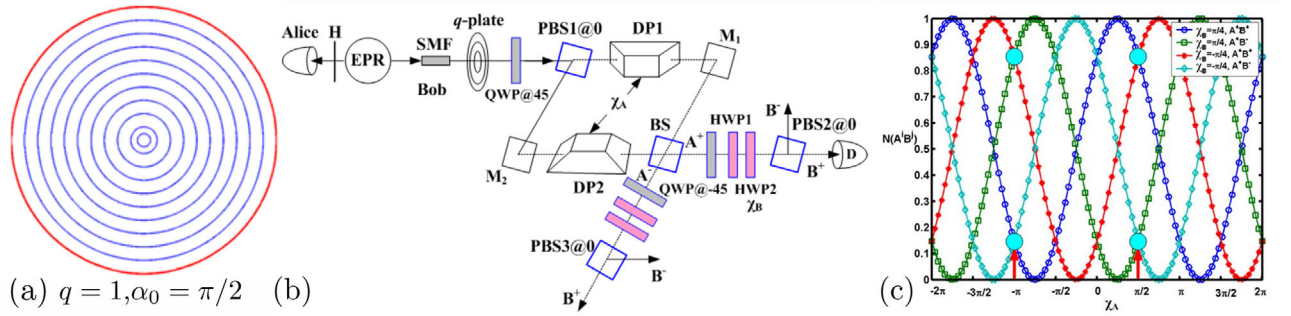

Figure 5. a) Drawing of a rotational invariant q plate; b) scheme of the experiment first proposed in ref. [69] for the implementation and measurement of single photon spin-momentum entanglement (see ref. [69] for details); c) theoretically predicted single-photon counts as a function of the phase χ_A with χ_B fixed. Adapted with permission.[69] Copyright 2010, The Optical Society.

one[69] is inspired by the set-up of Figure 3a: an experimental scheme is presented (see Figure 5b) which allows to prepare and manipulate single photon spin-orbit Bell states expected to produce a maximum violation of Bell-like inequalities. Polarization entangled photon pairs are produced by type-I SPDC. Since B(ob) photons are coupled to a single mode fiber supporting only $l = 0$ OAM mode, OAM entanglement is ruled out,[49] and the SAM-entangled state of the pair is the following: $|\psi_{SAM}\rangle = \frac{1}{\sqrt{2}}(|H_A\rangle \otimes |H_B\rangle + |V_A\rangle \otimes |V_B\rangle) = \frac{1}{\sqrt{2}}(|L_A\rangle \otimes |R_B\rangle + |R_A\rangle \otimes |L_B\rangle)$, where $|L\rangle$ and $|R\rangle$ are the circular left- and right-handed input eigenmodes of any q plate, obtained after the substitutions: $|H\rangle = (|L\rangle + |R\rangle)/\sqrt{2}$ and $|V\rangle = (|L\rangle - |R\rangle)/i\sqrt{2}$. From the quantum operator describing the $q = 1$ plate,[69] the state of the pair passed through it has the formal structure of a Greenberger-Horne-Zeilinger GHZ state: $|\psi_{GHZ}\rangle = \frac{1}{\sqrt{2}}[|L\rangle_A(|L\rangle \otimes |l = -2\rangle)_B + |R\rangle_A(|R\rangle \otimes |l = +2\rangle)_B]$. The detection of the A photon by Alice results in the heralding of a spin-orbit entangled single-photon to Bob: $|\psi\rangle = \frac{1}{\sqrt{2}}(|L\rangle \otimes |l = -2\rangle)_B + |R\rangle \otimes |l = +2\rangle)_B$. To prove this, joint measurements of the two qubits have to be performed for different measurement directions of the observables SAM and OAM. The Bloch spheres of SAM and OAM are spanned by adjusting a phase parameter, respectively, $\frac{1}{\sqrt{2}}(|H\rangle \pm \exp(i\chi_B)|V\rangle)$ for spin and $\frac{1}{\sqrt{2}}(|l = -2\rangle \pm \exp(i\chi_A)|l = +2\rangle)$ for orbit state (with χ_B and χ_A as reported in Figure 5b). The rotation of the OAM states is performed by means of a Mach–Zehnder interferometer employing Dove prisms in each arm (DP1 and DP2 in Figure 5b). A relative rotation angle of α between the Dove prisms imparts to the two input linear polarization components $|H\rangle$ and $|V\rangle$ a phase difference $\chi_A = 2l\alpha$, while leaving the polarization states undisturbed. Note that, for the Mach–Zehnder interferometer gate with Dove prisms to correctly behave, a quarter-wave plate (QWP@45 in Figure 5b) has to be placed before the input polarizing beam splitter (PBS1@0 in Figure 5b) to transform circular polarizations into linear ones. The non-polarizing beam splitter BS at the output of the Mach–Zehnder interferometer performs the projection operation onto the two possible OAM states. In each output port, a quarter-wave plate (QWP@-45 in Figure 5b) allows to restore the circular polarizations, before the single photons traverse two half-wave plates providing the phase difference $\chi_B = 2\beta$, between $|L\rangle$ and $|R\rangle$. In this way, the SAM states are rotated. Finally, two polarizing beam splitters (PBS2@0 and PBS3@0 in Figure 5b), one in each output arm, project the single photon onto the two orthogonal states of the circular basis. From the count rates of the single-photon detection events at the detectors (ports A^+ and A^-) as a function of the values of the phases χ_A and χ_B, interference fringes with high visibility are expected, from which the correlation coefficients $E(\chi_A, \chi_B)$ can be calculated using (21), and subsequently the S-parameter computed as $S = E(\chi_A, \chi_B) - E(\chi_A, \chi_B^{'}) + E(\chi_A^{'}, \chi_B) + E(\chi_A^{'}, \chi_B^{'})$. By choosing $\chi_A = \pi/2$ ($\alpha = 22.5°$), $\chi_A^{'} = -\pi$ ($\alpha = -45°$), $\chi_B = \pi/4$ ($\beta = 22.5°$) and $\chi_B^{'} = -\pi/4$ ($\beta = -22.5°$), as indicated by the arrows in Figure 5c, an S-parameter as high as $2\sqrt{2}$ (the Tsirelson's bound) is theoretically predicted. This would represent a relevant violation of non-contextual hidden-variable theories at the limit of the quantum prediction, that would prove the quantum nature of the spin-orbit photon entanglement.

A modified version of this experiment is reported by Karimi et al.[70] (see **Figure 6**a), and single-photon spin-orbit entanglement is here actually demonstrated. The spin-orbit entanglement is again generated by means of a q plate, acting on a photon belonging to a pair produced via SPDC. In this case, while the SAM state is measured as in ref. [69] (SAM phase here is θ), the gate performing rotation of the OAM state and its relative projection is implemented by means of a computer-controlled spatial light modulator. In the spatial light modulator, a four-sector hologram pattern is defined, which can be rotated at a variable angle χ. To demonstrate entanglement, the CHSH inequality is used, with the S-parameter computed as $S = E(\theta, \chi) - E(\theta, \chi^{'}) + E(\theta^{'}, \chi) + E(\theta^{'}, \chi^{'})$. The interference fringes obtained from successive single-photon detection events as a function of the hologram angle χ for 4 different fixed values of the half-wave plate angle θ are displayed in Figure 6b (black dots represent $\theta = 0$, dark gray dots $\theta = \pi/4$, gray dots $\theta = \pi/2$, and light gray $\theta = 3\pi/4$). The high-visibilities indicate that SPE is realized, and the authors report indeed a violation of the CHSH inequality by 17 standard deviations at $\chi = \pi/16$ (with the following choice of variables: $\theta = 0$, $\theta^{'} = \pi/4$, and $\chi^{'} = \chi + \pi/8$).

For the sake of completeness, we must remind to the reader a couple more experiments reporting on spin-orbit SPE with photons.[83,84] In ref. [83], the violation of the CHSH inequality is observed with an experimental setup similar to the ones described above but allowing for the generation of a SPE tunable

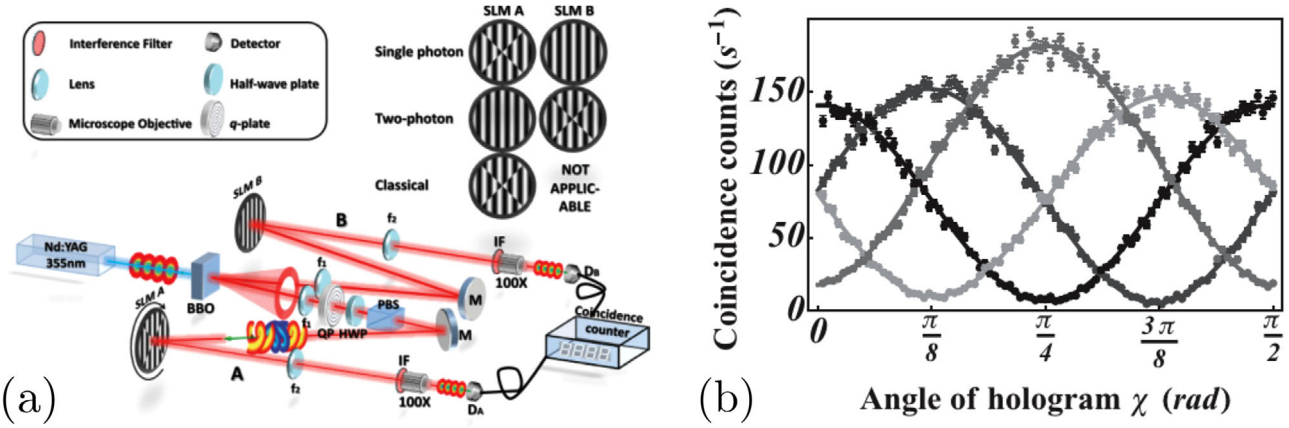

Figure 6. a) Sketch of the experimental setup used to test spin-orbit entanglement of single photons in ref. [70]; b) experimental A(lice)-B(ob) photon coincidence counts as a function of the orientation angle of the four-sector hologram for different values of the polarization direction (see main text for details). Adapted with permission.[70] Copyright 2010, The American Physical Society.

via the control of the degree of coherence of the superposition of the two qubits. In a more recent work,[84] a dielectric metasurface is shown to entangle the spin and the orbit of single photons.

4.2.3. Single-Photon Entanglement versus Classical Entanglement

The peculiar correlations between different degrees of freedom of the same particle resulting from SPE have an interesting analogue in classical light beams. This analogy, controversially called *classical entanglement*, was first pointed out by Spreeuw[85] and refers to correlations between different degrees of freedom of a physical system that admits a mathematical description in terms of tensor product Hilbert spaces.[86] A specific example is provided by a vector beam of light displaying a non-uniform polarization pattern, as in refs. [87,88], where the classical entanglement is between transverse spatial modes and polarization. In fact, the electric field of a paraxial beam can be written as

$$\mathbf{E}(\rho, z) = \mathbf{e}_1 f_1(\rho, z) + \mathbf{e}_2 f_2(\rho, z) \tag{42}$$

where the unit vectors $\mathbf{e}_1, \mathbf{e}_2$ are associated with the polarization, while the scalar functions f_1, f_2 describe the wavefront. The coordinate z is taken along the propagation direction and $\rho = x\mathbf{e}_1 + y\mathbf{e}_2$ denotes the transverse position vector.

The field (43) can be described as a vector in the tensor product Hilbert space $\mathcal{H}_1 \otimes \mathcal{H}_2$, where $\mathcal{H}_1$ and $\mathcal{H}_2$ refer to the polarization and spatial degrees of freedom, respectively. By Schmidt decomposition, the vector (43) can be re-arranged to

$$\mathbf{E}(\rho, z) = \sqrt{\lambda_1}\mathbf{u}_1 g_1(\rho, z) + \sqrt{\lambda_2}\mathbf{u}_2 g_2(\rho, z) \tag{43}$$

where $\lambda_1, \lambda_2 \in [0, 1]$ and $\mathbf{u}_1, \mathbf{u}_2$ and g_1, g_2 are orthonormal vectors in $\mathcal{H}_1$ and $\mathcal{H}_2$, respectively, and

$$\langle g_1, g_2 \rangle_{\mathcal{H}_2} = \int_{\mathbb{R}^2} \bar{g}_1(\rho, z) g_1(\rho, z) d\rho = 0 \tag{44}$$

If $\lambda_1 \lambda_2 = 0$ then the field (44) is *separable*, otherwise it is called *classically entangled*. In particular, if $\lambda_1 = \lambda_2 = 1/2$, then the field (44) is mathematically equivalent to the maximally entangled Bell state of two qubits. The orthogonality condition (45) can be fulfilled if the functions g_1, g_2 have non-overlapping supports. In this case, one obtains a classical version of the polarization-path entanglement discussed in Section 4.2.1. Another possibility is to exploit first-order spatial modes of the electromagnetic field.[89,90] In this case, (45) still holds even if the supports of g_1 and g_2 do actually overlap. This particular form of polarization-mode classical entanglement can be experimentally produced similarly to its quantum analogue described in Section 4.2.2. From an experimental point of view, the fundamental difference is the replacement of count rates with measurement of light intensities. This means using photodetectors, which give a photocurrent proportional to the input light intensities, instead of single photon detectors such as the single-photon avalanche photodiodes, which give a current pulse each time a photon is absorbed. To move from the classical framework to the quantum one, the intensity measurements translate to photocounts associated with the detection probabilities in each output port of the measurement device.[89]

The classical-quantum mathematical analogy can be developed further. In particular, a Bell test allows to certify the non-separability of the vector field (44). The procedure is completely similar to its quantum analogue. Given a couple of unit vectors $\mathbf{a}, \mathbf{b}$ associated with the joint measurement of the two degrees of freedom involved, the correlation coefficient $E(\mathbf{a}, \mathbf{b})$ (see Equation (21)) is in this case evaluated as

$$E(\mathbf{a}, \mathbf{b}) = \frac{I_{++}^{(\mathbf{a},\mathbf{b})} + I_{--}^{(\mathbf{a},\mathbf{b})} - I_{+-}^{(\mathbf{a},\mathbf{b})} - I_{-+}^{(\mathbf{a},\mathbf{b})}}{I_{++}^{(\mathbf{a},\mathbf{b})} + I_{--}^{(\mathbf{a},\mathbf{b})} + I_{+-}^{(\mathbf{a},\mathbf{b})} + I_{-+}^{(\mathbf{a},\mathbf{b})}} \tag{45}$$

where $I_{\pm\pm}^{(\mathbf{a},\mathbf{b})}$ are light intensites. The S-parameter is still given by Equation (19).

It is worth stressing that the intensities are completely classical notions, so that this notion of "classical entanglement" and its properties can be completely discussed in the classical framework.[91] For instance, the violation of the Bell inequality in terms of intensities may be completely consistent with locality and non-contextuality, here referred to classical wavepackets of light. In addition, it is worthwhile to point out the detailed

analysis presented in ref. [92], where the authors show how the non-contextual bound for Bell-like inequalities increases when multi-photon counts or intensity measurements are considered. Indeed, when more than one indistinguishable photons arrive at the detector, a realistic non-contextual description has to be properly formulated. It yields alternative Bell-like inequalities presenting higher classical bounds that depend explicitly on the number of detectable photons. The case of a classical light beam where photon counts are replaced by intensity measurements is handled by a limiting procedure which, again, produces a non-contextual bound greater than what can be experimentally achieved. In other words, classical systems are always non-contextual and can never violate any properly derived Bell inequality. The known fundamental problems instead arise when the experiments are able to highlight the particle nature of the light, that is, when experimental data regard single photon counts rather than intensities. In that case, the violation of Bell's inequality must be ascribed to properties of the particles the light is made of, whose quantum state must be quantum entangled (entangled state of pairs of particles or intraparticle entangled state of single photons). Only here, the well known problems with locality or non-contextuality arise with the photons of the considered light beam.[92,93] As a matter of fact, a complete classical description of the Bell inequality in this classical context is presented in,[94] where the violation of the CHSH inequality is ascribed to particular coherence properties of the light beam. It is important to remark that in this case the S parameter is a figure of merit which describes collective properties of the light beam, instead of the particular form of the state vector of the single photons.

The particular intra-system correlations and non-separability properties present in classically entangled systems have been recently exploited, for example, in high-speed kinematic sensing.[87] Indeed, a classically entangled beam of the form (44) displays a non-uniform polarization pattern. Polarization and spatial degrees of freedom are so strongly correlated that, by altering the spatial profile of the beam, the polarization changes accordingly. We refer the interested reader to the many papers dealing with this subject (see e.g., refs. [88,91–93]).

4.3. Single-Neutron Entanglement

Neutrons are fermions, which experience the four fundamental forces and interfere. These facts represent a fertile experimental ground for quantum precision measurements. The first observation of interference phenomena of neutron matter waves having a wavelength of a few Ångstroms but macroscopic coherence lengths (≈100 μm) was reported in 1974 by Rauth et al.[95] A silicon crystal interferometer, similar to the one sketched in **Figure 7**b and still used nowadays, was employed. The idea of sending polarized neutrons in a Mach–Zehnder interferometer (Figure 7a) for creating spin-momentum (or spin-path) entangled states at the single particle level appeared for the first time in 2001.[64] Due to the negligible absorption of neutron beam splitters made of silicon and to the very high neutron detector efficiency, single neutrons were suggested as ideal candidates for probing experimentally that, for a single particle, Bell's inequality is a consequence of non-contextuality, so that it can be violated independently of the locality condition.

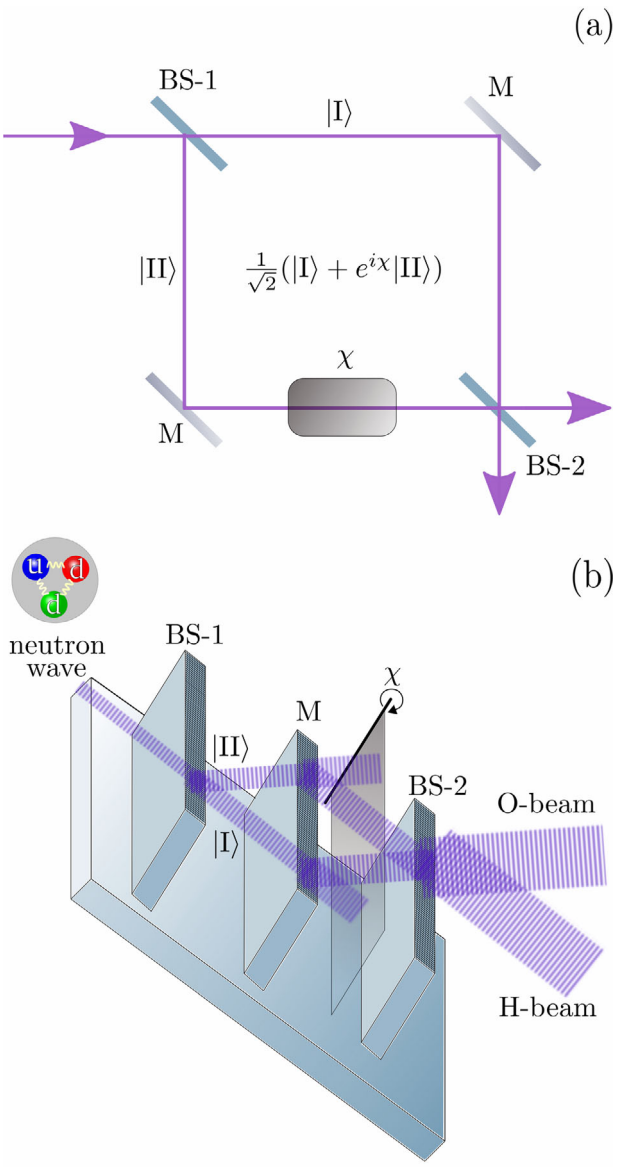

Figure 7. a) A Mach–Zehnder interferometer to create a single neutron superposition state of momenta I and II, with relative phase χ. b) Sketch of a silicon perfect-crystal neutron interferometer in Laue geometry using a sided aluminum plate as phase shifter.

4.3.1. Single-Neutron Interferometry

The geometry of a neutron interferometer is presented in Figure 7b. It comprises three parallel plates (≃3 ÷ 5 mm-thick) at which neutron diffraction in Laue geometry happens due to the comparable values of the lattice parameter and the wavelength of the thermal neutrons (≃2 Å). This is the so-called triple Laue configuration. The interferometer is used for both the preparation and the manipulation of the spatial degrees of freedom of neutrons (see Figure 7a): first, each neutron is set in a superposition state of two paths $\frac{1}{\sqrt{2}}(|\mathrm{I}\rangle + |\mathrm{II}\rangle)$, the spatial sub-system defined by $\mathbb{C}^2_{momentum}$; second, the Bloch sphere of the corresponding qubit (the neutron's path degree of freedom)

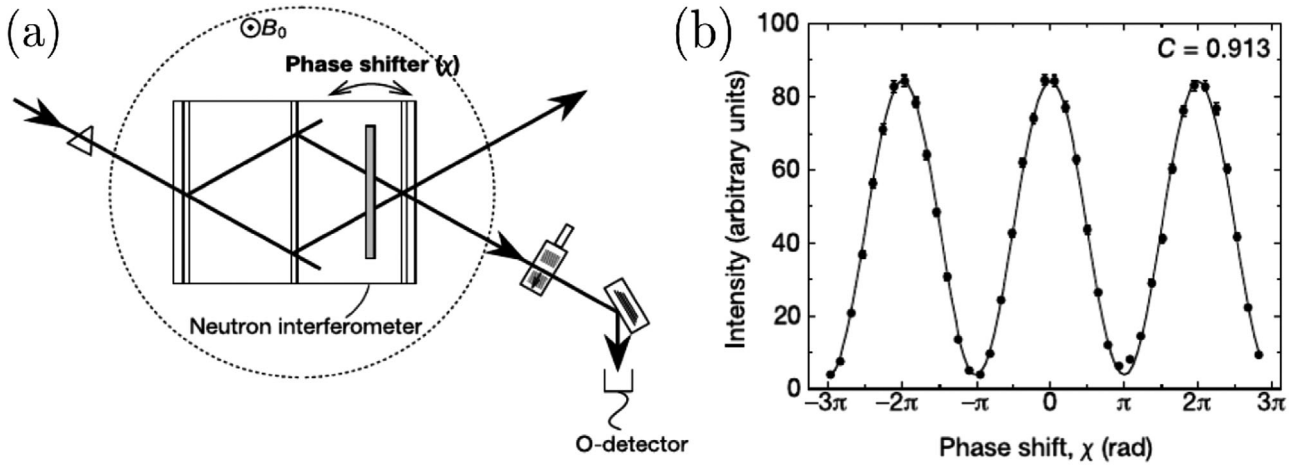

Figure 8. a) Schematic view of the experimental setup employed for implementing rotations on the Bloch sphere of the momentum of the single neutron. b) Visibility (C) of the interference fringes as a function of the phase shift between the two orthogonal single neutron momenta. Adapted with permission.[16] Copyright 2003, Springer Nature.

is spanned by varying the relative phase difference between the paths $\left(\frac{1}{\sqrt{2}}(|\mathrm{I}\rangle + e^{i\chi}|\mathrm{II}\rangle)\right)$, thus preparing the state for the measurement. Finally, the resulting interference fringes can be monitored at one or both the output ports (so-called O-beam and H-beam of a neutron interferometer, see Figure 7b), where a neutron detector can count the neutrons.

Specifically, a narrow window of wavelengths and angles of the incoming neutrons wave amplitude ψ_0 splits at the first interferometer plate into two coherent sub-beams, thus defining two interferometric paths, namely the orthogonal basis of $\mathbb{C}^2_{momentum}$. The sub-beam of path I is transmitted at the first plate, reflected at the second one and reflected again at the third one, before being detected in the so-called O-beam. The sequence seen by the sub-beam of path II is reflection, reflection, transmission, before recombining coherently in the O-beam as well. A phase shifter is inserted in order to vary the relative phase between the two sub-beams and consequently observe interference. The total intensity in the O-beam is given by $I_O = |trr\psi_0 + rrt\psi_0 e^{i\chi}|^2$, which can be written as $I_O = A(1 + \cos\chi)$, where r and t are the reflection and the transmission amplitude coefficients of each plate, respectively, $A = |\psi_0|^2|r|^4|t|^2$ and χ is the relative phase difference between the two paths. The phase shifter is an aluminum plate (≃1-cm-thick) having one of its edges as rotation axis, and rotated across both beam paths, so that the optical paths seen by the two sub-beams are different by geometry (**Figure 8**a). The observation of interference oscillations with high visibility in the, for example, O-beam intensity measured with a neutron detector is a proof of the capability of the setup to prepare and manipulate the spatial sub-system of a single neutron (Figure 8b).

4.3.2. Single-Neutron Spin-Path Entanglement

To implement a spin-path entangled state with a single neutron, the preparation and manipulation of the spinor degree of freedom of the particle has to be addressed too.

Two different set-ups have been reported by Hasegawa and coworkers in **Figure 9**a,b. In both cases, a polarized beam of neutrons with spin $|\uparrow\rangle$ is prepared by a magnetic prism and sent in the interferometer. A magnetic guide field, directed along z-axis in Figure 9, is employed to maintain the polarization of the neutron beam across the interferometer. In the first set-up, Figure 9a, the spin of the two split sub-beams $|\mathrm{I}\rangle$ and $|\mathrm{II}\rangle$ is turned by $+\pi/2$ for path $|\mathrm{I}\rangle$ and $-\pi/2$ for path $|\mathrm{II}\rangle$, by means of a Mu-metal sheet in the form of a 0.5 mm-thick oval ring magnetized by 2 DC coils. This creates a superposition state of the two spins, namely $\frac{1}{\sqrt{2}}(|\leftarrow\rangle + |\rightarrow\rangle)$, and results in the preparation of the entangled Bell state $|\psi\rangle = \frac{1}{\sqrt{2}}(|\leftarrow\rangle \otimes |\mathrm{I}\rangle + |\rightarrow\rangle \otimes |\mathrm{II}\rangle)$. In the second improved set-up, Figure 9b, a $\pi/2$-spin turner is placed between the magnetic prisms and the interferometer, so that the two sub-beams just after the first splitter plate are both in the same spin state $|\leftarrow\rangle$. The creation of the spin qubit with the relative preparation of the spin-path entangled state is performed by implementing a Larmor-accelerator in the form of a Mu-metal tube that, by reducing the strength of the magnetic guide field, produces a $\pi/2$-spin flip in one of the two paths because of the different Larmor precessions.

In both set-ups, the manipulation of the neutron's spin degree of freedom is realized after the interferometer with a spin rotator that allows adjusting the angle α to select neutrons with a given polarization direction (**Figure 10**a), namely the state $\frac{1}{\sqrt{2}}(|\leftarrow\rangle + e^{i\alpha}|\rightarrow\rangle)$. With the phase shifter fixed, the observation of interference fringes with sufficiently high contrast, as a function of the spin rotation α, confirms the manipulation of the spin subsystem as well (Figure 10b).

The experimental proof of the spin-path entanglement is given by the measurement of interference fringes in the O-beam intensity with visibility larger than $1/\sqrt{2} \simeq 0.71$. The fringes are statistically obtained from successive discrete count rates of single-neutron events as a function of the phase difference χ between the two paths for the spinor rotation angle α set to 0, $\pi/2$, π and $3\pi/2$. These are the values of α for which a maximum violation

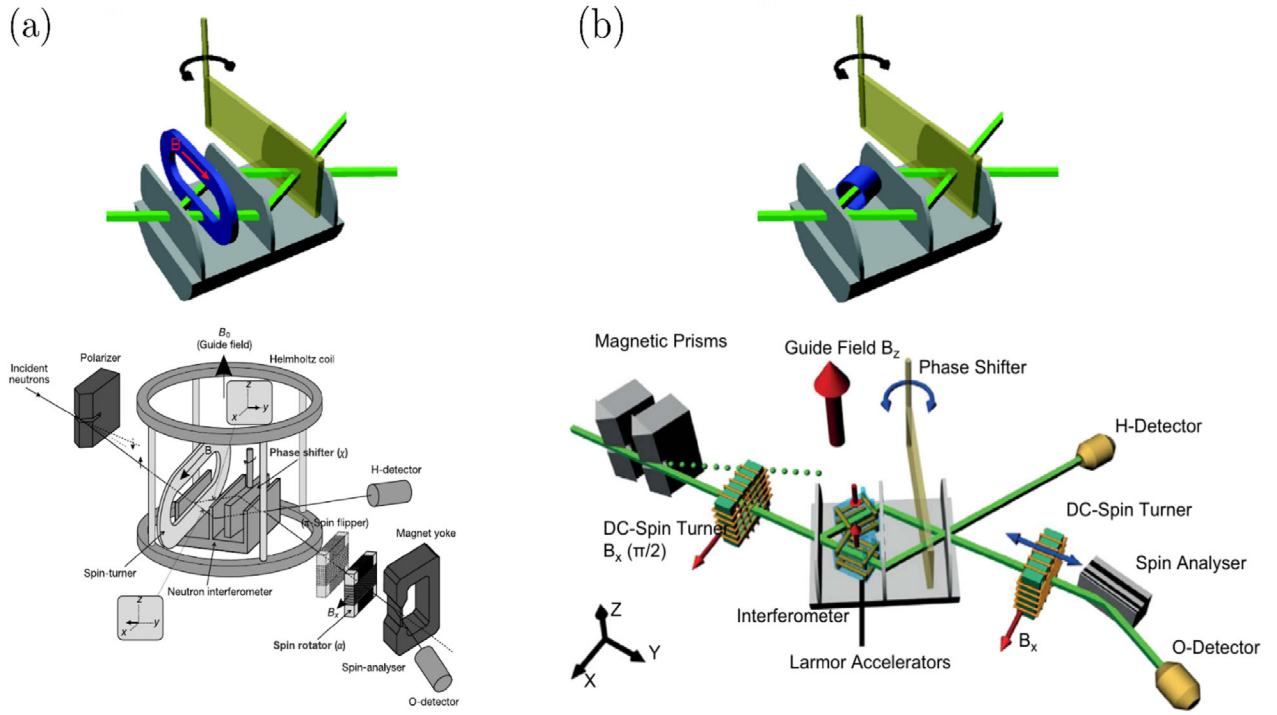

Figure 9. Schemes of experimental setups for creating and manipulating spin-path entangled single neutrons (see main text for a description). a) Adapted with permission.[16] Copyright 2003, Springer Nature. b) Adapted under the terms of a Creative Commons CC-BY license.[17] Copyright 2014, The Authors, published by Elsevier.

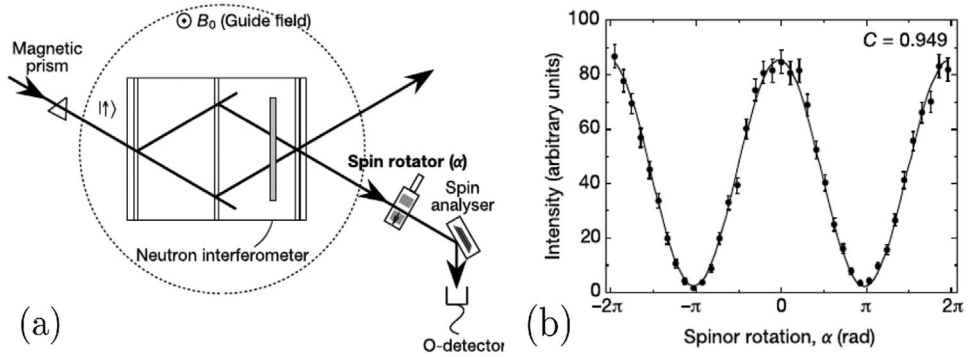

Figure 10. a) Scheme of the experimental setup realizing rotations on the Bloch sphere of the spin of the single neutron. b) Visibility (C) of the intensity interference fringes as a function of the spin rotation angle. Adapted with permission.[16] Copyright 2003, Springer Nature.

is expected for the BCHSH inequality $-2 \leq S' \leq 2$, with

$$S' \equiv E(\alpha_1, \chi_1) + E(\alpha_1, \chi_2) - E(\alpha_2, \chi_1) + E(\alpha_2, \chi_2) \tag{46}$$

The expectation values $E(\alpha, \chi)$ are determined by (21):

$$E(\alpha, \chi) = \frac{N(\alpha, \chi) + N(\alpha + \pi, \chi + \pi) - N(\alpha, \chi + \pi) - N(\alpha + \pi, \chi)}{N(\alpha, \chi) + N(\alpha + \pi, \chi + \pi) + N(\alpha, \chi + \pi) + N(\alpha + \pi, \chi)} \tag{47}$$

The measurement results are reported in **Figure 11** for the first (left) and second (right) set-ups. Highlighted with vertical dashed lines are the values of the phase shift χ at which the count rates are taken for each value of α in order to evaluate the correlation coefficients $E(\alpha, \chi)$ from (48) and compute the S'-parameter from (47). A maximum violation is expected, for example, for the set $\alpha_1 = 0$, $\alpha_2 = \pi/2$, $\chi_1 = \pi/4$ and $\chi_2 = -\pi/4$, giving for the first set-up $S' = 2.051 \pm 0.019$ and for the second set-up $S' = 2.365 \pm 0.013$. This last is a violation by 28σ of the expectation of the classical non-contextual model. Finally, for this spin-path entanglement of single neutrons, the influence of the geometric phase acquired during the time-dependent interaction with the radio-frequency field on the violation of the BCHSH inequality has also been experimentally investigated and observed.[96] Because of the time dependent magnetic field, only the spin qubit of the entangled state acquires the geometric phase appearing as a pure phase factor tied to it.

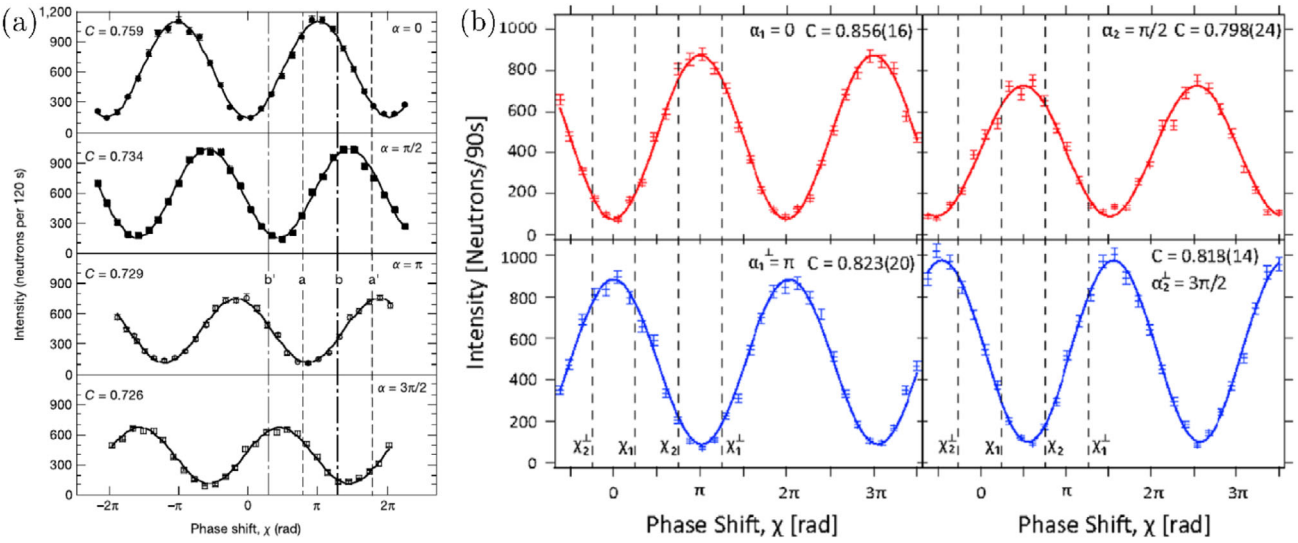

Figure 11. Interference fringes proving single-neutron spin-path entanglement: a) First set-up. Adapted with permission.[16] Copyright 2020, Springer Nature. b) Second improved set-up. Adapted under the terms of a Creative Commons CC-BY license.[17] Copyright 2014, The Authors, published by Elsevier.

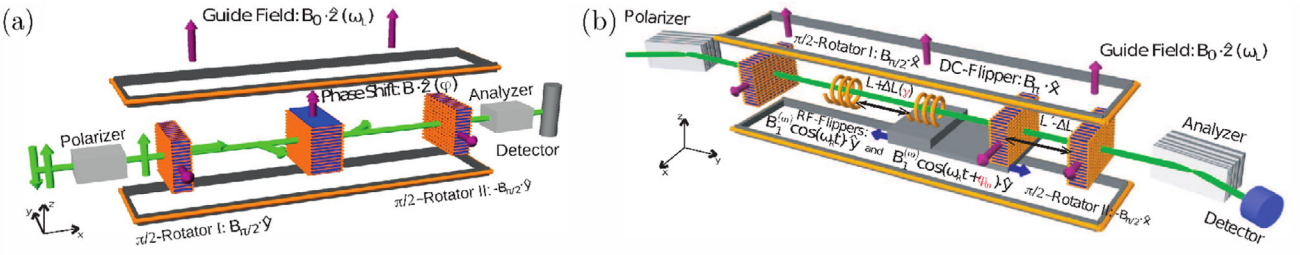

Figure 12. a) Sketch of a neutron polarimeter: analogously to an interferometer, it allows performing rotations of the neutrons spin qubit. b) Setup of a modified neutron polarimeter for realizing spin-energy entanglement of neutrons. Figures kindly provided by Stephan Sponar.[97]

4.3.3. Neutron Polarimetry for Spin-Energy Entanglement

Neutron polarimeters are experimental apparatuses less sensitive to ambient mechanical and thermal conditions than the neutron interferometers.[97] Moreover, they are brighter than diffraction-based interferometers which propagate neutrons only within millidegrees angles. The scheme of a neutron polarimeter is shown in **Figure 12**a. It can be reduced to that of a Mach-Zehnder-type interferometer. The first $\pi/2$-spin rotator R_1 acts like a beam splitter, creating a coherent superposition of spin $|\uparrow\rangle$ and spin $|\downarrow\rangle$, by transforming the incoming polarized state $|\psi_i\rangle = |\uparrow\rangle$ to $|\psi_1\rangle = \frac{1}{\sqrt{2}}(|\uparrow\rangle + |\downarrow\rangle)$. Then a static magnetic field $B \cdot \hat{z}$ is responsible of a phase shift ϕ which allows to perform rotations onto the neutron's spin qubit Bloch sphere: $|\psi_2\rangle = \frac{1}{\sqrt{2}}(|\uparrow\rangle + e^{i\phi}|\downarrow\rangle)$. After a second $\pi/2$-spin rotator R_2, the single neutrons are found in the final state $|\psi_f\rangle = \frac{1}{2}((1-e^{i\phi})|\uparrow\rangle + (1+e^{i\phi})|\downarrow\rangle)$. Similarly to the result for the output beam of the interferometer, the probability of finding the system in state $|\uparrow\rangle, |\downarrow\rangle$ is given by $P_{|\uparrow\rangle,|\downarrow\rangle} = \frac{1}{2}(1 \mp \cos\phi)$.

Here, an entanglement between the spinor and energy degrees of freedom is created via the interaction of a polarized neutron with a time-dependent magnetic field $B(t) = B_1^{\omega}\cos(\omega t)\cdot\hat{y}$ of a radio frequency (RF) flipper resonant with the guide field (see Figure 12b), that is, $\omega = 2|\mu|B_0/\hbar$, with μ the neutron magnetic moment.[71] The amplitude of the RF field is tuned to $B_1^{\omega} = \pi\hbar/(2\tau|\mu|)$ to initiate the spin-flip process over the time τ the neutron takes to traverse the magnetic coil. In such an interaction, the total energy of the neutron is no longer conserved due to absorption and emission of an RF-photon, depending on its spin state. This results in the preparation of the SPE state $|\psi\rangle = \frac{1}{\sqrt{2}}(|E_0+\hbar\omega\rangle \otimes |\uparrow\rangle + |E_0-\hbar\omega\rangle \otimes |\downarrow\rangle)$, where E_0 is the initial total energy of the neutron. The second RF-flipper, ϕ_ω-phase shifted with respect to the first one, and a DC-flipper $B_\pi \cdot \hat{y}$ are placed on a translation stage at a variable distance $L + \Delta L$, allowing to vary the phase γ of the neutron's energy subspace, yielding the final state $|\psi_f\rangle = \frac{1}{\sqrt{2}}(e^{-i\phi_\omega}|\uparrow\rangle + e^{i\gamma}e^{i\phi_\omega}|\downarrow\rangle) \otimes E_0$. The experimental proof of the spin-energy entanglement is carried out in a similar way to as in the interferometry experiments: single-neutron detections are counted as a function of the phase γ for values of the spinor phase ϕ that yields maximum violation of the BCHSH inequality (in (47) α is replaced by ϕ, and χ by γ to describe this experiment). The measured interference fringes are shown in **Figure 13**, where α stands for γ in the text. From these, it is possible to calculate a $S' = 2.333 \pm 0.002$.[98]

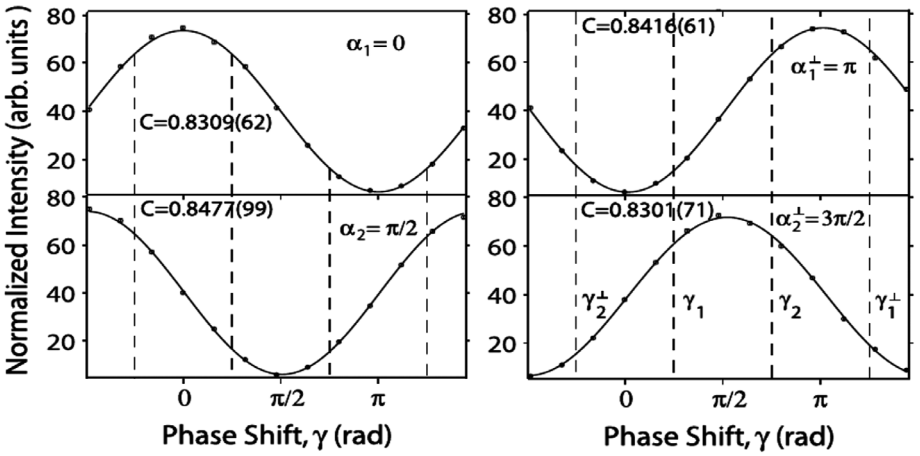

Figure 13. Intensity fringes proving single-neutron spin-energy entanglement. Adapted with permission.[71] Copyright 2010, Elsevier.

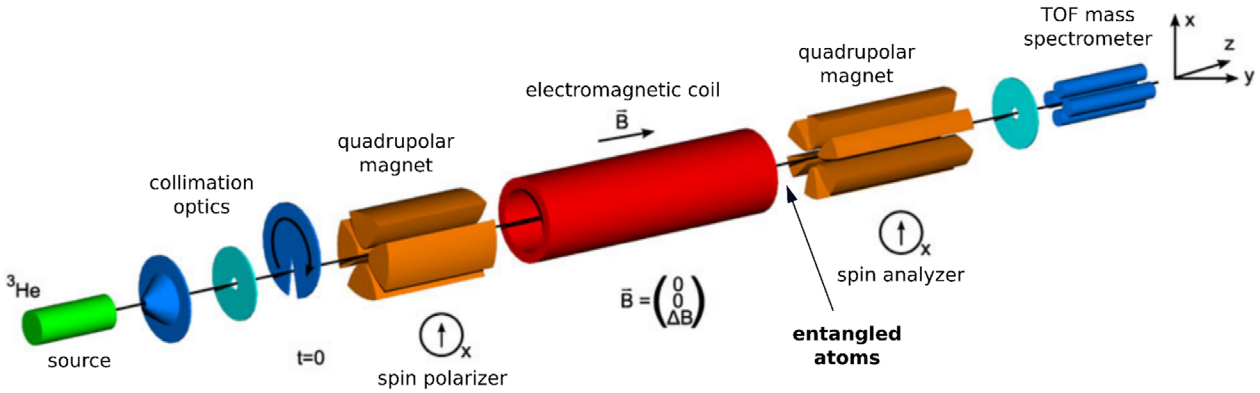

Figure 14. Scheme of the experimental setup used to produce and detect spin-momentum entanglement of ^{3}He atoms. Adapted with permission.[72] Copyright 2011, Springer Nature.

4.4. Single-Atom Entanglement: The Non-Classical Spin–Momentum Correlations of ^{3}He

Contrary to neutron experiments which exploit the wave-nature of neutrons, single atom experiments have been reported in 2011 by the group of DeKieviet[72] based on the massive property of ^{3}He atomic beams. Here, SPE is based on quantum correlations between two commuting variables: one discrete - the nuclear spin - and the other one continuous - the linear momentum. The resulting non-factorizable state is defined in the Hilbert space $\mathcal{H} = \mathbb{C}^2_{spin} \otimes \mathbb{C}^2_{momentum}$. A longitudinal Stern-Gerlach arrangement, where the nuclear spin and the linear momentum of single ^{3}He atoms are entangled, allows demonstrating SPE. The experiment is based on the theoretical analysis of the entanglement between the translational and the spin degrees of freedom in a standard Stern-Gerlach apparatus, originally carried out by Plastino and co-workers,[99] who also considered a measure of contextuality previously given by de la Torre.[100] However, the work of Jeske et al.[72] is focused on the entanglement between spin and longitudinal momentum of the single atoms, thanks to the combination of, respectively, spin rotation and arrival time measurements of each ^{3}He particle in the same experiment. In this respect, this type of single-atom entanglement follows more closely the discussion reported by Harshman,[101] concerning the different types of entanglement at play in a general scenario of non-relativistic particles scattering. Despite being based on the particle instead on the wave nature of a quantum object, the implementation of the intraparticle entanglement described in this section looks particularly similar to the neutron spin-path entanglement described in Section 4.3.2.

The experiment is schematized in **Figure 14**. It is a simplified version of the home-built atomic beam spin echo apparatus originally introduced in ref. [102]. The setup consists in four main parts:

i. a spin polarizer, realized by means of a quadrupole Stern–Gerlach magnet. x-polarized ^{3}He atoms are prepared such that the only spin-up components $|\uparrow_x\rangle$ are left in the beam.
ii. A spin rotator. The prepared wave packet is put in a coherent superposition of the $|\uparrow_z\rangle$ and $|\downarrow_z\rangle$ wave packets by means of a coil generating a weak magnetic field ΔB along the z-direction, thus becoming the new quantization axis of motion. This makes $|\uparrow_x\rangle = \frac{1}{\sqrt{2}}(|\uparrow_z\rangle + |\downarrow_z\rangle)$. The uniform magnetic field is responsible for an anomalous Zeeman effect resulting in two new energy levels in the hyperfine structure of ^{3}He atoms, related to their nuclear magnetic moment

and identified by two opposite values of the nuclear magnetic quantum number, one corresponding to $|\uparrow_z\rangle$ and the other one to $|\downarrow_z\rangle$ eigenstates. Because the two opposite spin states have different energies inside the magnetic field region, at the exit of the coil they will acquire slightly different momenta, say $|p^+\rangle$ and $|p^-\rangle$, which result to be intimately linked to their spins. At this point, the beam is composed by atoms whose state is no longer separable in a product of spin and momentum states, that is, they are entangled in their two degrees of freedom: $|\psi\rangle = \frac{1}{\sqrt{2}}(|\uparrow_z\rangle \otimes |p^+\rangle + |\downarrow_z\rangle \otimes |p^-\rangle)$. As a result, the initial wave packet $|\uparrow_x\rangle$ is split in a coherent superposition of two (opposite) spin wave packets with different central momenta, thus featuring a relative phase depending on the value of ΔB (Zeeman splitting). The single-particle entangled state can be seen as built from an atomic nuclear spin qubit, $\frac{1}{\sqrt{2}}(|\uparrow_z\rangle \pm e^{i\alpha}|\downarrow_z\rangle)$, and an atomic momentum qubit, $\frac{1}{\sqrt{2}}(|p^+\rangle \pm e^{i\nu}|p^-\rangle)$, where the phases α and ν depend on the amplitude of the magnetic field and the time spent within the coil, respectively. Finally, two aspects should be noted: first, the initial spin polarization is necessary to determine the spin direction afterward (unpolarized atomic beams do not react to an applied magnetic field); second, maximum entanglement occurs for minimum overlap between the two wave packets,[101] namely if the state has a spin component expectation value $\langle \hat{S}_z \rangle = 0$, a condition automatically satisfied by the design of the experiment.[72]

iii. A spin analyzer. Another Stern–Gerlach magnet is used as a spin analyzer, always oriented along the x-direction. This projection operation eliminates the $|\downarrow_x\rangle$ components and allows detecting the acquired phase difference as a Larmor precession of the spin about the beam axis, namely the spin rotation, for any value of ΔB, practically fixing α.

iv. A time-of-flight mass spectrometer used as a detector. The dependence of the phase difference on the momentum of the atom is resolved by means of an efficient time-of-flight mass spectrometer,[103] capable of detecting single ^{3}He atoms at their time of arrival. This is directly proportional to their de Broglie wavelength (momentum), and, therefore, this allows determining ν. The detector measures the count rates $N(\alpha,\nu)$ of single-atom events in the transmitted atomic spin-up beam projected along the x-direction.

The experimental data for combined spin rotation and time of flight measurement can be shown in a 2D plot of the count rates as a function of the magnetic field along ,for example, the horizontal axis, and the de Broglie wavelength along, for example, the vertical axis.[72] As a function of the magnetic field, the plot shows the oscillatory behavior expected for the Larmor precession of a spin in an external field,[104] with regions of high intensity corresponding to spin-up and regions of low intensity corresponding to spin-down. Horizontal cross-cuts of such a contour plot are shown in **Figure 15** for the four different values of ν selected by the authors: in each one of them, the values of α used by the authors for computing the expectation values according to (21) are highlighted as well. A first experimental hint of single-atom spin-momentum entanglement can be found in the large visibility of the interference fringes. However, a measure of the S-parameter is needed to fully certify the achievement of SPE. A further analysis of the data[72] or eventually other experiments will be of help in this direction.

5. Single-Particle Entanglement for Quantum Information Applications

In this section, we focus on SPE as a resource for Quantum Information. The most remarkable application is in Quantum Key Distribution (QKD) protocols. Since the availability of optical fibers for communication and the easy of manipulation of photons, here we concentrate on photon-based protocols. Entanglement was proposed as a resource for QKD in a 1991 paper[10] where quantum correlations are used to share a private key between two clients and the violation of BCHSH inequality is tested to check the presence of an eavesdropper. Since then, several protocols based on bipartite and multipartite entanglement have been proposed.[105–107] The enormous advantages of *inter*particle entanglement in QKD are given by the application of non-local correlations to distribute the secret key and the possibility to prove the security protocol within a *device-independent* scenario. However, *intra*particle entanglement is a non-negligible resource for QKD even if the clients cannot share a quantum state of a qubit pair. The fact of being able to transmit an entangled state by means of a single particle can be used as a resource to improve existing protocols like the BB84.[108] In particular, we consider SPE among polarization and momentum of a single photon. Assuming the photon is confined in an interferometer where the momentum space can be restricted to $\mathbb{C}^2$ as explained in Section 4.2, we can identify the two possible values of the momentum with the corresponding paths in the interferometer.

5.1. Single-Particle Entanglement for Quantum Key Distribution

5.1.1. Two Qubits Carried by One Particle

Let us consider a single photon with a definite value of the momentum (for example, it travels along a given path defined by a waveguide) and suppose it is polarized along the vertical direction: it is described in the 4D Hilbert space $\mathcal{H} = \mathcal{H}_m \otimes \mathcal{H}_p$ and its quantum state is given by

$$\mathcal{H} \ni |\Psi\rangle = |0\rangle \otimes |V\rangle \equiv |0V\rangle \tag{48}$$

where $|0\rangle \in \mathcal{H}_m$ is the momentum state and $|V\rangle \in \mathcal{H}_p$ is the polarization state. Assume that there is another possible path for the photon (e.g., a second arm in an interferometer) and $|1\rangle$ is the momentum state of the photon traveling there, so $\{|0\rangle, |1\rangle\}$ is a basis of $\mathcal{H}_m$. On the other hand, let $|H\rangle$ be the state of horizontal polarization so $\{|V\rangle, |H\rangle\}$ is the basis of $\mathcal{H}_p$. Considering two degrees of freedom of the photon we obtain a qubit pair realized by means of a single particle. We can define the orthonormal basis $\mathcal{B} = \{|\Psi_i\rangle\}_{i=0,1,2,3}$ of the overall Hilbert space of the photon by

$$|\Psi_0\rangle := |0V\rangle\ ,\ |\Psi_1\rangle := |0H\rangle\ ,\ |\Psi_2\rangle := |1V\rangle\ ,\ |\Psi_3\rangle := |1H\rangle \tag{49}$$

Let us introduce some quantum gates that can be physically implemented by optical elements. Suppose that the photon in the

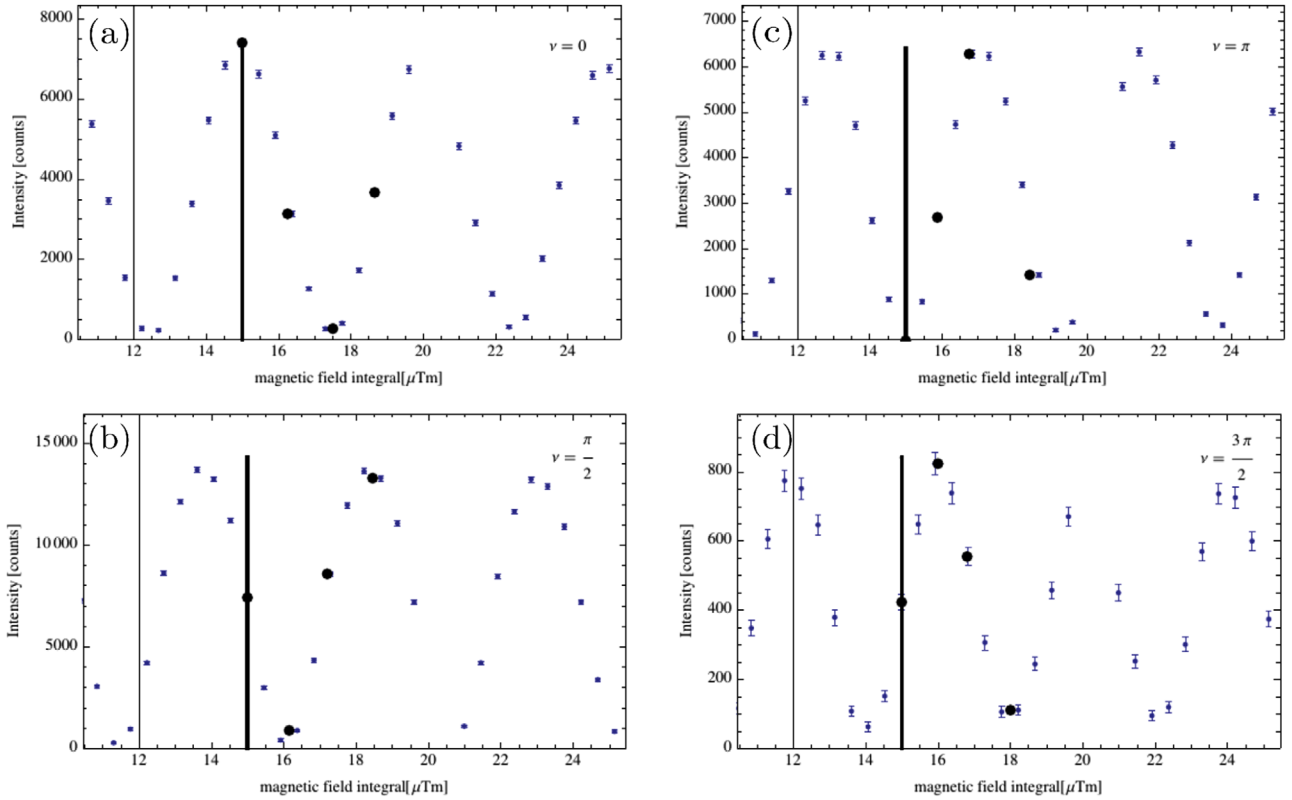

Figure 15. Spin rotation curves: atom detection events as a function of the applied magnetic field, for four fixed values of the phase of the momentum qubit ($\nu = 0, \frac{\pi}{2}, \pi, \frac{3\pi}{2}$). The vertical thick black bars indicate the origin of the value of the phase shift of the spin qubit ($\alpha = 0$), while the black dots indicate the remaining values ($\alpha = \frac{\pi}{2}, \pi, \frac{3\pi}{2}$). Adapted with permission.[72] Copyright 2007, Springer Nature.

state (49) is confined in an interferometer where it is traveling in the path called *arm-0* and crosses a *50:50 beam splitter* that is represented by the unitary operator U_{BS} defined by

$$U_{BS}|0\rangle := \frac{1}{\sqrt{2}}(|0\rangle + i|1\rangle) \tag{50}$$

$$U_{BS}|1\rangle := \frac{1}{\sqrt{2}}(|0\rangle - i|1\rangle) \tag{51}$$

That is, the photon is put in a coherent superposition of a transmitted photon in the arm-0 and a reflected photon in the arm-1 with a relative phase $\frac{\pi}{2}$. The beam splitter leaves the polarization unaffected so the transformation acting on the state (49) is $\mathbb{I} \otimes U_{BS}$.

In this section, we adopt the formalism of quantum gates to describe the quantum operations performed on the two degrees of freedom of the single particle. In particular, we give a compact description of the preparation of the SPE states as two-qubit quantum gates, as well as we describe the QKD protocols as simple quantum circuits. Let us recall that a *n-qubit gate* is nothing but a unitary operator acting on the Hilbert space $(\mathbb{C}^2)^{\otimes n}$ of n qubits. Quantum gates have a well-known graphical representation borrowed by classical logical gates. In the following, we describe the presence of an optical element in one of the arms of the interferometer in terms of controlled quantum gates. A controlled quantum gate CU is a two-qubit gate represented by

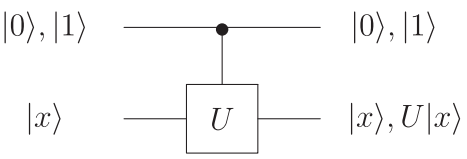

(52)

that applies operation U on the second qubit when the first qubit is in $|1\rangle$, it acts as the identity when the first qubit is in $|0\rangle$ and its action extends by linearity.

We denote the action of the operator U_{BS} as the 1-qubit gate:

(53)

Another 1-qubit gate acting on the momentum degree of freedom is the phase gate defined by $P_\phi(\alpha|0\rangle + \beta|1\rangle) := \alpha|0\rangle + e^{i\phi}\beta|1\rangle$ introducing a relative phase. It can be physically realized by a *phase shifter* installed in the arm-1 of the interferometer. We denote it by

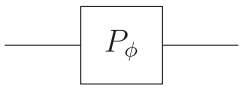

(53)

We can construct the Hadamard gate on the first qubit by

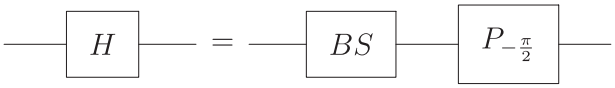

(54)

as a direct consequence of definition (51).

Let us consider two 1-qubit gates R_1 and R_2 acting on the polarization degree of freedom that can be physically realized by means of *polarization rotators* like waveplates:

$$R_1|V\rangle := |H\rangle \qquad R_1|H\rangle := |V\rangle \tag{55}$$

$$R_2|V\rangle := \frac{|V\rangle + |H\rangle}{\sqrt{2}} \qquad R_2|H\rangle := \frac{|V\rangle - |H\rangle}{\sqrt{2}} \tag{56}$$

In order to describe the application of a polarization rotator in one of the two arms of the interferometer we need to consider a controlled gate where the control qubit is given by the momentum degree of freedom. If the rotator R_i ($i = 1, 2$) is installed in the arm-1 then its action is represented by the following 2-qubit gate:

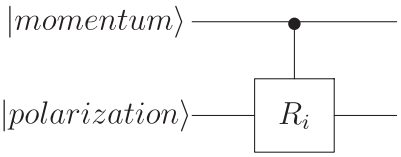

(57)

On the other hand if the rotator described by R_i is installed in the arm-0 of the interferometer then its action is represented by the following gate:

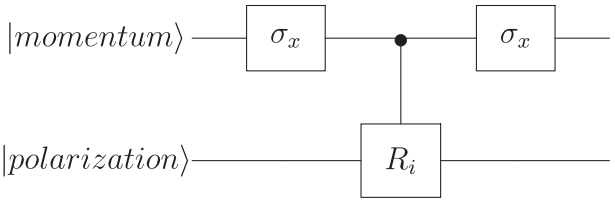

(58)

where the Pauli matrix σ_x acts as a NOT-gate on the basis $\{|0\rangle, |1\rangle\}$.

If we need to produce an intraparticle maximally entangled state $|\Phi\rangle = \frac{1}{\sqrt{2}}(|0V\rangle + |1H\rangle)$ from the initial state (49), we apply the following Bell-type gate:

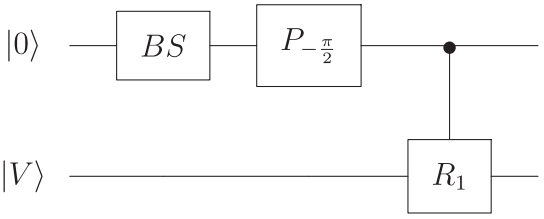

(59)

physically realized by putting a phase shifter and a polarization $\frac{\pi}{2}$-rotator in the arm-1 (i.e., the path of the reflected photon) to implement the Hadamard gate.

5.1.2. The First Proposal of QKD with SPE States

The first QKD protocol based on SPE was proposed in ref. [109] in terms of single photons processed by an interferometer. Here, Alice randomly emits a photon triggering either a single-particle source S_0 or another single-photon source S_1, where S_0 emits a photon in the momentum state $|0\rangle$ and S_1 emits a photon in $|1\rangle$. The polarization state of the emitted photon is randomly chosen from either the rectilinear basis $\{|H\rangle, |V\rangle\}$ or the diagonal basis $\{|D_+\rangle, |D_-\rangle\}$, with $|D_\pm\rangle = (|H\rangle \pm |V\rangle)/\sqrt{2}$. By means of a beam-splitter and a phase shifter the Hadamard gate is applied to the momentum state. Then a polarization rotator placed in one arm of the interferometer realizes a controlled gate $\mathsf{C}R_1$. In other words, Alice acts with a Bell gate on the state $|x\rangle \otimes |y\rangle$, where $x = 0, 1$ and $y = V, H, D_\pm$, creating a maximally entangled momentum-polarization state. This state is transmitted to Bob. Bob, in turn, operates inversely to project the particle into the initial state chosen by Alice. The following scheme summarizes the protocol:

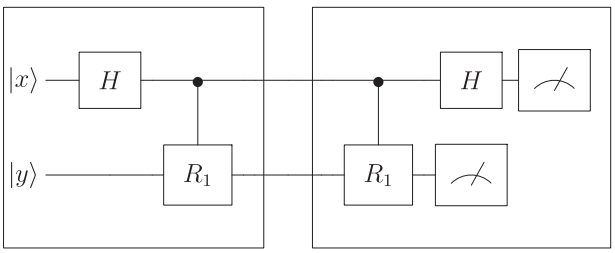

$x = 0, 1; y = V, H, D_\pm$ *Alice* | *Bob*

Under the assumptions that the detectors can measure the polarization of a detected particle (Bob uses a polarizing beam-splitter and two conventional detectors) and that the right basis for the polarization measurement is selected, Bob recovers the state sent by Alice. After the quantum transmission, Alice and Bob publicly announce their choices of basis storing the matching outcomes. Finally, they compare portions of the sifted key to check the channel security.

In the present protocol, both Alice and Bob apply suitable time delay loops in the interferometer arms so that the two pulses of the same particle cannot be simultaneously accessed in the public quantum channel. Therefore, an eavesdropper (Eve) cannot gain the path information of Alice's initial state using the same apparatus as Bob's without disturbing the transmitting time. On the other hand, Eve is able to eavesdrop the transmission entangling the polarization degree of freedom of the transmitted particle with an ancillary qubit in her hands. Let us describe the Eve's operation by a unitary operator U_E on the enlarged Hilbert space $\mathcal{H}_p \otimes \mathcal{H}_E$, where $\mathcal{H}_E$ is the Hilbert space of the Eve's ancilla:

$$U_E|H\rangle \otimes |\phi\rangle = \frac{1}{\sqrt{2}}(|H\rangle \otimes |\psi_0\rangle + |V\rangle \otimes |\psi_1\rangle) \tag{60}$$

$$U_E|V\rangle \otimes |\phi\rangle = \frac{1}{\sqrt{2}}(|H\rangle \otimes |\varphi_0\rangle + |V\rangle \otimes |\varphi_1\rangle) \tag{61}$$

Here, $|\phi\rangle$ is the initial state of the Eve's ancilla and $\langle\psi_0|\psi_1\rangle = \langle\varphi_0|\varphi_1\rangle = 0$. Suppose Alice initializes the state $|0H\rangle$, so the particle is transmitted in the state:

$$|\Psi\rangle = \frac{1}{\sqrt{2}}(|0H\rangle + |1V\rangle) \tag{62}$$

under the eavesdropping interaction, the system *particle-Eve's ancilla* evolves in:

$$\begin{aligned}|\Psi'\rangle = &\frac{1}{2}|0\rangle \otimes (|H\rangle \otimes |\psi_0\rangle + |V\rangle \otimes |\psi_1\rangle) \\ &+ \frac{1}{2}|1\rangle \otimes (|H\rangle \otimes |\varphi_0\rangle + |V\rangle \otimes |\varphi_1\rangle)\end{aligned} \tag{63}$$

Once applied the Bob's operations, the final state is

$$\begin{aligned}|\Psi''\rangle = &\frac{1}{2\sqrt{2}}[|0H\rangle \otimes (|\psi_0\rangle + |\varphi_0\rangle) + |1V\rangle \otimes (|\psi_0\rangle - |\varphi_0\rangle) \\ &+|0V\rangle \otimes (|\psi_1\rangle + |\varphi_1\rangle) + |1V\rangle \otimes (|\psi_1\rangle - |\varphi_1\rangle)]\end{aligned} \tag{64}$$

The goal of Eve is gaining information about Bob's outcomes measuring her ancilla. We can calculate the final state $|\Psi''\rangle$ for the other seven possibile Alice's initializations and calculate the reduced density operator ρ_E of Eve's ancilla. Assuming Alice selects one of the eight initializations with equal probability, we obtain the completely mixed state:

$$\rho_E = \frac{1}{2}(|\psi_0\rangle\langle\psi_0| + |\psi_1\rangle\langle\psi_1| + |\varphi_0\rangle\langle\varphi_0| + |\varphi_1\rangle\langle\varphi_1|) = \mathbb{I} \tag{65}$$

Therefore, Eve gains no information about Alice's initialized states and Bob's outcomes measuring her ancilla.

Now let us consider an intercept-and-resend attack. Eavesdropping on momentum qubits and polarization qubits introduce errors with probability 0.5 and 0.25, respectively. Denoting the error rates estimated from momentum bits and polarization bits by e_m and e_p, respectively, we have $2e_m = 4e_p = \gamma$, where γ is the fraction of intercepted particles. Alice and Bob can estimate γ taking $\max\{2e_m, 4e_p\}$ obtaining the secret key rate:

$$r_{key} = 1 - \frac{1}{2}\mathsf{H}(\max\{e_m, 2e_p\}) - \mathsf{H}\left(\frac{1}{2}\max\{e_m, 2e_p\}\right) \tag{66}$$

where H is the binary entropy function.

5.1.3. Improvement of BB84

Production of SPE states of photons is a resource to improve the standard BB84 protocol as shown in ref. [20]. Let us consider the orthonormal basis $\mathcal{B}$ of the overall Hilbert space of the particle defined in (50), we can construct another orthonormal basis acting on $|\Psi_{0,1,2,3}\rangle$ with the following circuit:

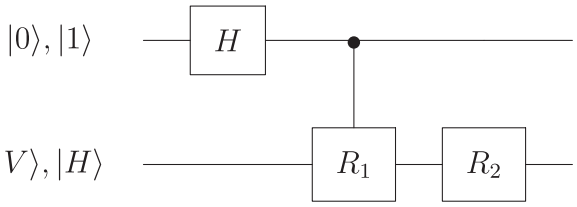

(67)

From the physical viewpoint we have that the photon passes through a beam-splitter with a phase shifter $P_{-\frac{\pi}{2}}$ (to realize the Hadamard gate) and a polarization rotator R_1 in the path of the reflected wavepacket (arm-1) and a rotator R_2 on both arms. The resulting basis, denoted by $\mathcal{C}$, is made by the entangled states:

$$|\Phi_0\rangle = \frac{1}{\sqrt{2}}\left(|0\rangle \otimes \frac{|V\rangle + |H\rangle}{\sqrt{2}} + |1\rangle \otimes \frac{|V\rangle - |H\rangle}{\sqrt{2}}\right) \tag{68}$$

$$|\Phi_1\rangle = \frac{1}{\sqrt{2}}\left(|0\rangle \otimes \frac{|V\rangle - |H\rangle}{\sqrt{2}} + |1\rangle \otimes \frac{|V\rangle + |H\rangle}{\sqrt{2}}\right) \tag{69}$$

$$|\Phi_2\rangle = \frac{1}{\sqrt{2}}\left(|0\rangle \otimes \frac{|V\rangle + |H\rangle}{\sqrt{2}} - |1\rangle \otimes \frac{|V\rangle - |H\rangle}{\sqrt{2}}\right) \tag{70}$$

$$|\Phi_3\rangle = \frac{1}{\sqrt{2}}\left(|0\rangle \otimes \frac{|V\rangle - |H\rangle}{\sqrt{2}} - |1\rangle \otimes \frac{|V\rangle + |H\rangle}{\sqrt{2}}\right) \tag{71}$$

The bases $\mathcal{B}$ and $\mathcal{C}$ are mutually unbiased, that is, any element of a basis is given by an equal superposition of the elements of the other one.

Suppose two communicating parties, namely Alice and Bob, agree the basis $\mathcal{B}$ and $\mathcal{C}$, so a BB84-like QKD protocol can be defined as follows:

Step 1. Alice prepares a particle in a state selected from $\mathcal{B}$ or $\mathcal{C}$ and sends it to Bob.

Step 2. Bob performs a measurement on the received particle w.r.t. $\mathcal{B}$ or $\mathcal{C}$.

Step 3. The procedure is repeated many times. Alice declares on a public classical channel the selected basis for any preparation and Bob declares which measurements he performed. When the basis choices correspond they store a bit pair of the sifted key.

Step 4. Alice and Bob estimate the error rate.

Alice and Bob select their respective bases for preparations and measurements acting with beam-splitters, rotators, and phase shifters. The scheme of the QKD protocol is given by the following circuit:

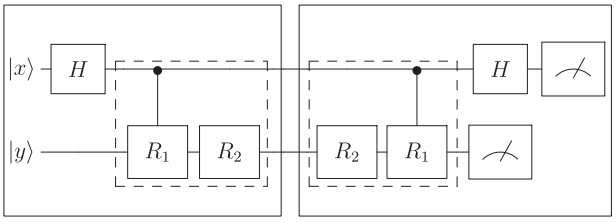

$x = 0, 1; y = V, H$ *Alice* | *Bob*

The solid boxes denote Alice and Bob's apparatuses, the dashed boxes represent the operations that Alice (Bob) applies to prepare (measure) the state w.r.t. the basis $\mathcal{C}$. On the other hand, if Alice (Bob) does not apply that operations she prepares (he measures) the state w.r.t. $\mathcal{B}$. For example, the process where Alice selects the basis $\mathcal{B}$ and Bob selects the basis $\mathcal{C}$ is represented by

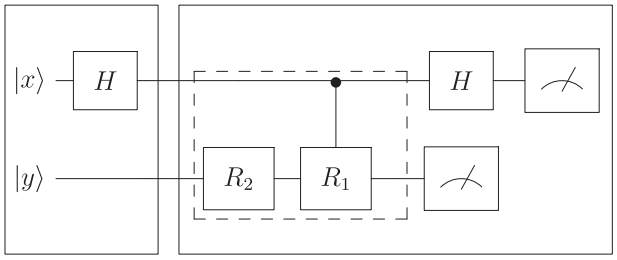

$x = 0, 1; y = V, H$

Alice | Bob

A joint measurement of polarization and momentum can be performed by means of two polarizing beam-splitters and four detectors. In particular, the value of the momentum is measured detecting the photon in the corresponding path.

The illustrated QKD scheme not only increases the secret key rate transmitting two qubits via one particle but it is robust also under *side-channel attacks* based on faulty devices.[20] Before analyzing a standard intercept-and-resend attack, we briefly illustrate that this protocol is immune to one-sided attacks when the standard BB84 is completely vulnerable. Assume Eve is the manufacturer of the devices used by Alice and she has installed a *trojan horse* in the polarization rotator R_2 that is placed in both arms of the interferometer: When the rotator is activated (i.e., Alice applies her dashed box) the amount of angolar momentum acquired rotating the polarization of the photon can be transmitted to Eve by means of another photon in a mode coupled with the device. Let us represent this attack by a linear map $\mathcal{E} : \mathcal{H}_m^{(A)} \otimes \mathcal{H}_p^{(A)} \otimes \mathsf{F}_E \to \mathcal{H}_m^{(A)} \otimes \mathcal{H}_p^{(A)} \otimes \mathsf{F}_E$ where $\mathcal{H}_m^{(A)} \otimes \mathcal{H}_p^{(A)}$ is the Hilbert space of the photon processed by Alice and F_E is the Fock space of the photons produced by Alice's device rigged by Eve. The action of $\mathcal{E}$ on product states is defined by

$$\mathcal{E} : |m\rangle \otimes |V\rangle \otimes |\omega\rangle_E \mapsto |m\rangle \otimes \frac{1}{\sqrt{2}}(|V\rangle + |H\rangle) \otimes |\Omega\rangle_E$$

$$m = 0, 1 \tag{72}$$

$$\mathcal{E} : |m\rangle \otimes |H\rangle \otimes |\omega\rangle_E \mapsto |m\rangle \otimes \frac{1}{\sqrt{2}}(|V\rangle - |H\rangle) \otimes |\Omega'\rangle_E,$$

$$m = 0, 1 \tag{73}$$

where $|\omega\rangle_E \in \mathsf{F}_E$ is the vacuum state. The above transformation describes the action of the Alice's operation R_2 under the side-attack by Eve, so a photon in either $|\Omega\rangle_E \in \mathsf{F}_E$ or $|\Omega'\rangle_E \in \mathsf{F}_E$, with $\langle\Omega|\Omega'\rangle_E = 0$, is created according to the recoil of the polarization rotator. Without entanglement (i.e., considering product states as in (81)), Eve obtains the Alice's choice of basis and the outcome information measuring the *probe* photon, without the need of intercepting the transmitted photon. Thus, in the standard 1-qubit BB84 Eve can completely gain the key without revealing her presence. On the other hand intraparticle entanglement employed in this protocol prevents a perfectly hidden eavesdropping. Assume Alice wants to prepare the state $|\Phi_0\rangle$, then the action of the rigged rotator R_2 is described by the following transformation:

$$\mathcal{E} : \frac{1}{\sqrt{2}}(|0V\rangle + |1H\rangle) \otimes |\omega\rangle_E \mapsto$$

$$\mapsto \frac{1}{\sqrt{2}}\left(\frac{1}{\sqrt{2}}(|0V\rangle + |1H\rangle) \otimes |\Omega\rangle + \frac{1}{\sqrt{2}}(|0V\rangle - |1H\rangle) \otimes |\Omega'\rangle\right) \tag{74}$$

As a consequence of the attack and the relative production of entanglement with Eve's system, Alice does not send the entangled state $|\Phi_0\rangle$ but the separable mixed state $\rho = \frac{1}{2}(|\varphi^+\rangle\langle\varphi^+| + |\varphi^-\rangle\langle\varphi^-|)$ where $|\varphi^\pm\rangle = \frac{1}{\sqrt{2}}(|0V\rangle \pm |1H\rangle)$. Thus, Eve's attack turns out to be an error source that can be detected estimating the error rate. Otherwise, a Bell test can be performed on a sample of the prepared entangled states to check whether a side-channel attack has suppressed the entanglement. Let us assume that Eve riggs the rotator R_1 (placed only in one arm) instead of R_2, when she detects its activation then she performs a measurement of the momentum destroying the coherent superposition. In this case, Alice does not produce the desired entangled state and the side-attack cannot be hidden from an error estimation or a Bell test.

Now let us consider a standard intercept-and-resend-attack: Assuming an eavesdropper (Eve) knows the bases $\mathcal{B}$ and $\mathcal{C}$, she can move an attack intercepting the transmitted particle on the quantum channel, performing one of the two possible measurements and sending the measured particle to Bob. By the eavesdropping of the announcements on the classical channel, Eve can discover when she has selected the right basis gaining information about the secret key.

Since Eve's mesurements w.r.t. the wrong basis are an error source, the presence of an eavesdropping can be detected by the estimation of the error rate by the clients: Alice and Bob compare a portion of the sifted key. Following the analysis of ref. [20], one can calculate the threshold for a tollerable error rate. Assuming that Eve intercepts and measures a fraction $\gamma \in [0, 1]$ of the transmitted particles, the probability that she introduces an error for any particle (the *error rate*) is

$$e = \frac{\gamma}{2} \cdot \frac{3}{4} \tag{75}$$

given by the product of the probability that Eve selects the wrong basis ($=\frac{\gamma}{2}$) and the probability that Bob obtains a bit pair different from that sent by Alice ($=\frac{3}{4}$). The information $\mathcal{I}_E$ gained by Eve after knowing the bases announcements is γ bits/particle. In terms of error rate we have

$$\mathcal{I}_E = \frac{8}{3}e \tag{76}$$

Suppose that Alice and Bob select the same basis: If Alice sends the bit pair $\hat{b}$ then Bob's outcome b is randomized according to

the probability distribution:

$$\mathbb{P}(b) = \begin{cases} 1-e & b = \hat{b} \\ \frac{e}{3} & b \neq \hat{b} \end{cases} \tag{77}$$

thus the Shannon entropy of the random variable b is

$$\mathsf{H}(b) = -(1-e)\log_2(1-e) - 3\frac{e}{3}\log_2\left(\frac{e}{3}\right) \tag{78}$$

which is the information loss in terms of bits/particle due to the errors introduced by Eve. The mutual information between Alice and Bob (i.e., the correlation of their raw keys) is given by

$$\mathcal{I}(A;B) = 2 - \mathsf{H}(b) \tag{79}$$

The *secret key rate r* can be calculated as the difference between the information shared by the clients and the information gained by the eavesdropper:

$$r = \mathcal{I}(A;B) - \mathcal{I}_E \tag{80}$$

In order to have a positive secret key rate, Alice and Bob must check that the error rate is less than 0.36. The estimation of the error rate can be found comparing portions of the sifted key.

5.1.4. Momentum-Measurement Protocol

Let us consider a general QKD protocol (based on a scheme proposed in ref. [110]) where a secret key can be distributed by means of the measurements of the momentum of the transmitted particle without observing the polarization. Also this scheme can be considered an improvement of BB84 but the fact of performing only one measurement allows a more simple physical implementation w.r.t. the protocol describe above.

Assume that Alice prepares one of the following momentum-polarization states:

$$\begin{aligned} |\Psi_0\rangle &= \frac{1}{\sqrt{2}}(|0\rangle + |1\rangle) \otimes |V\rangle, \quad |\Psi_1\rangle = \frac{1}{\sqrt{2}}(|0\rangle - |1\rangle) \otimes |V\rangle \\ |\Phi_0\rangle &= \frac{1}{\sqrt{2}}(|0V\rangle + |1H\rangle), \quad |\Phi_1\rangle = \frac{1}{\sqrt{2}}(|0V\rangle - |1H\rangle) \end{aligned} \tag{81}$$

$|\Psi_0\rangle, |\Psi_1\rangle$ are separable states and $|\Phi_0\rangle, |\Phi_1\rangle$ are entangled states. Let us represent Alice's preparation in terms of gates:

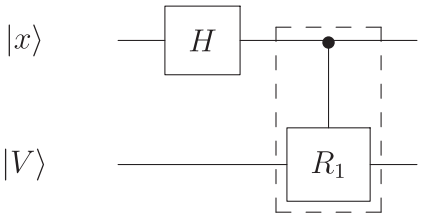

(82)

where she chooses the *input state* $|x\rangle$ ($x = 0, 1$) and whether to apply the polarization rotator (the controlled gate $\mathsf{C}R_1$ in the dashed box). For example, if Alice selects the input state $|0\rangle$ and she applies $\mathsf{C}R_1$ then she sends the state $|\Phi_0\rangle$.

Table 1. Bob's knowledge about transmitted states. × denotes a lack of information.

Bob's $\mathsf{C}R_1$ gate	Bob's outcome	Alice's input state	Transmitted state	Symbols
No	1	$\|0\rangle$	$\|\Phi_0\rangle$	*Symbol*1
No	1	$\|1\rangle$	×	
No	0	$\|0\rangle$	×	
No	0	$\|1\rangle$	$\|\Phi_1\rangle$	*Symbol*1
Yes	1	$\|0\rangle$	$\|\Psi_0\rangle$	*Symbol*2
Yes	1	$\|1\rangle$	×	
Yes	0	$\|0\rangle$	×	
Yes	0	$\|1\rangle$	$\|\Psi_1\rangle$	*Symbol*2

Bob's apparatus is symmetric w.r.t. Alice's one with a polarization rotator ($\mathsf{C}R_1$) and a Hadamard gate (BS + phase shifter):

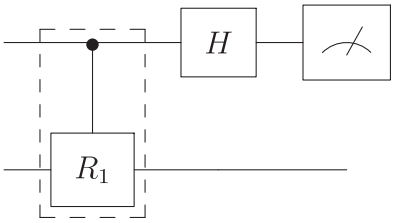

(83)

Suppose that Alice sends the separable state Ψ_0 (Ψ_1) and Bob does not apply $\mathsf{C}R_1$ then he measures the value 0 (1) with probability 1. If instead Bob applies $\mathsf{C}R_1$, then he obtains a randomized outcome. On the other hand, suppose that Alice sends the entangled state Φ_0 (Φ_1) and Bob applies $\mathsf{C}R_1$, then he measures the value 0 (1) with probability 1. If instead Bob does not apply $\mathsf{C}R_1$, then he obtains a randomized outcome.

Let us assume that Bob does not apply $\mathsf{C}R_1$ and measures the value 1, if Alice announces that her input state is $|0\rangle$, then Bob knows that the transmitted state is $|\Phi_0\rangle$. On the other hand, if Alice announces that her input state is $|1\rangle$ then Bob is not able to decide if the transmitted state is $|\Psi_1\rangle$ or $|\Phi_1\rangle$ (all cases are reported in **Table 1**).

With the following correspondence:

Transmission of an entangled state: *Symbol*1

Transmission of a separable state: *Symbol*2 (84)

Alice and Bob can share a binary secret key.

The QKD protocol can be summarized by these instructions:

Step 1. Alice prepares one of the four state (91) and sends it to Bob.

Step 2. Bob applies the gate $\mathsf{C}R_1$ with probability $\frac{1}{2}$ and measures the momentum of the particle.

Step 3. After many repetitions of Step 1 and Step 2, Alice announces whether her input state is $|0\rangle$ or $|1\rangle$ for any transmitted particle.

Step 4. Bob announces his measurement outcomes (according to Table 1, Alice and Bob obtain their sifted key).

Step 5. Alice and Bob compare a sample of the sifted key to estimate the error rate.

Eve can move an intercept-and-resend attack by means of an apparatus that is identical to Bob's and randomly choosing to either apply gate CR_1 or not. Assume that Eve intercepts the photon without applying CR_1 and measures the value 0 then she infers that the state sent by Alice is either $|\Phi_1\rangle$, $|\Phi_0\rangle$ or $|\Psi_0\rangle$ (see Table 1 replacing Bob with Eve). Since the other separable state $|\Psi_1\rangle$ is ruled out, if Eve re-sends the state $|\Psi_0\rangle$, then she transmits the correct state to Bob with probability $\frac{1}{2}$. Assuming Eve intercepts every transmitted particle, she introduces the error rate $e = \frac{1}{3}$ in the sifted key[110] that is greater than the error rate of $\frac{1}{4}$ for BB84 under a standard intercept-and-resend attack. Moreover, the protocol turns out to be robust under a *detector-blinding attack*[110] where Eve is able to blind Bob's measurement device.

5.2. Applications of Single-Particle Entanglement beyond QKD

In the previous section we have reviewed three strategies to distribute a secret key. However, SPE is a resource for quantum information processing that is not limited to QKD. For instance, a procedure for transferring momentum(path)-polarization SPE to interparticle entanglement between spatially separated photons (or spin-1/2 particles) is presented in ref. [111]. Here, information encoded in the entanglement between two different degrees of freedom of the same particle is transmitted across a distance by creating an interparticle entangled spin state. Moreover, few quantum teleportation schemes based on SPE have been proposed.[7,21,112] In a standard quantum teleportation scheme, a target quantum state is not directly transmitted from a sender to a receiver but it is reconstructed by the receiver exploiting the initial sharing of a maximally interparticle entangled state. Using SPE states a non-standard version of teleportation can be performed by the transmission of a single quantum particle. In the following, we review these further applications of SPE to quantum information transmission and processing.

5.2.1. Entanglement Swapping

The capability of transferring single-particle entanglement to entanglement among two spatially separated particles is crucial to develop several quantum information applications with SPE states. Let us outline a scheme proposed in ref. [111] to perform entanglement swapping from intraparticle entanglement to interparticle entanglement. Assume that Alice prepares the SPE state $|\psi\rangle = \alpha|0H\rangle + \beta|1V\rangle$ of a photon by means of the Bell-type gate (61) realized with optical elements as described above. Next, Alice prepares an ancillary qubit (realized by another physical particle) in $|H\rangle_a$ and performs a CNOT on $|H\rangle_a$ controlled by the polarization qubit in $|\psi\rangle$. In the rectilinear polarization basis, the CNOT acts as follows: $\mathrm{CNOT}|HH\rangle = |HH\rangle$, $\mathrm{CNOT}|HV\rangle = |HV\rangle$, $\mathrm{CNOT}|VH\rangle = |VV\rangle$, $\mathrm{CNOT}|VV\rangle = |VH\rangle$. The resulting state of the two-particle system is

$$|\Phi\rangle = \alpha|0H\rangle|H\rangle_a + \beta|1V\rangle|V\rangle_a \tag{85}$$

Thus, there is intraparticle entanglement between momentum and polarization of the first particle and interparticle entanglement between the two particles. In particular, for $\alpha = \beta = 1/\sqrt{2}$, $|\Phi\rangle$ is the Greenberger–Horne–Zeilinger (GHZ) state of three qubits.

Suppose Alice sends the first particle to Bob who prepares an ancillary qubit in $|H\rangle_b$. Once received the photon, Bob performs a CNOT on his ancilla controlled by the polarization of the received particle. The resulting 4-qubit state is

$$|\Psi\rangle = \alpha|0H\rangle|H\rangle_a|H\rangle_b + \beta|1V\rangle|V\rangle_a|V\rangle_b \tag{86}$$

where three qubits are physically in Bob's hands and the other one is with Alice. Now Bob acts with a Hadamard gate on the the momentum degree of freedom of the received particle producing the state:

$$\begin{aligned}|\Psi'\rangle = \frac{1}{\sqrt{2}}\big[&|0\rangle \otimes (\alpha|H\rangle|H\rangle_a|H\rangle_b + \beta|V\rangle|V\rangle_a|V\rangle_b)\\ &+|1\rangle \otimes (\alpha|H\rangle|H\rangle_a|H\rangle_b - \beta|V\rangle|V\rangle_a|V\rangle_b)\big]\end{aligned} \tag{87}$$

Beyond the beam-splitter and the phase shifter to implement Hadamard, Bob's apparatus provides a wave-plate to perform R_2 (58) placed in both arms of the interferometer, so the four qubits are processed in

$$\begin{aligned}|\Psi''\rangle = \frac{1}{\sqrt{2}}\Bigg\{&|0\rangle \otimes \Bigg[\frac{1}{\sqrt{2}}|H\rangle(\alpha|H\rangle_a|H\rangle_b - \beta|V\rangle_a|V\rangle_b)\\ &+\frac{1}{\sqrt{2}}|V\rangle(\alpha|H\rangle_a|H\rangle_b + \beta|V\rangle_a|V\rangle_b)\Bigg]\Bigg\}\\ +\frac{1}{\sqrt{2}}\Bigg\{&|1\rangle \otimes \Bigg[\frac{1}{\sqrt{2}}|H\rangle(\alpha|H\rangle_a|H\rangle_b - \beta|V\rangle_a|V\rangle_b)\\ &-\frac{1}{\sqrt{2}}|V\rangle(\alpha|H\rangle_a|H\rangle_b + \beta|V\rangle_a|V\rangle_b)\Bigg]\Bigg\}\end{aligned} \tag{88}$$

Now, if Bob measures momentum and polarization of the first photon (i.e., the received one) the reduced state of the two ancillary qubits (one with Alice, the other one with Bob) collapses into an interparticle entangled state. For example, if Bob obtains outcomes 0 and H, then the reduced 2-qubit state of the ancillary qubits is

$$|\chi_{0H}\rangle = \alpha|H\rangle_a|H\rangle_b - \beta|V\rangle_a|V\rangle_b \tag{89}$$

According to his measurement outcomes, Bob can perform a suitable operation (**Table 2**) in order to share with Alice an

Table 2. Parameter-dependent operations performed by Bob to reconstruct the SPE state prepared by Alice as an entangled state of two distinct particles.

Bob's outcomes (*momentum*, *polarization*)	Bob's operation on his ancilla
(0, H)	σ_z
(0, V)	$\mathbb{I}$
(1, H)	σ_z
(1, V)	$\mathbb{I}$

entangled state that corresponds to the state $|\psi\rangle$ initially prepared by Alice.

The considered entanglement swapping scheme can be applied to transfer single-particle entanglement carried by a photon among its momentum and polarization degrees of freedom to entanglement among two spatially separated spin-$\frac{1}{2}$ particles.

As suggested in ref. [111], single-particle entangled states and their properties discussed in this work could be a resource in duality quantum computing.[113,114] Let us briefly motivate this statement. Duality quantum computing is a paradigm introduced in ref. [113], it is based on a quantum system that carries information to be processed that passes through a double-slit, then quantum operations are separately performed on the sub-wave functions emerging from the slits that are recombined before the readout of the result. Generally speaking, the state of a register in a duality quantum computer is expressed by the tensor product of a path-state and an internal state on which non-unitary transformations can be performed. It is clear that after the double-slit crossing and the action of separated quantum operations, path/position (or momentum) of the system may turn out to be entangled with its internal state. Therefore, the scheme of entanglement swapping can be relevant for this kind of quantum computations.

5.2.2. Quantum Teleportation

The first proposal to use SPE states for quantum teleportation was given in ref. [21], The protocol starts with Alice's preparation of the SPE state $|\Phi\rangle = \frac{1}{\sqrt{2}}(|0V\rangle + |1H\rangle)$ by means of the gate (61) as usual. We call the single-particle initialized in $|\Phi\rangle$ *particle-1*. Alice prepares another particle in $|\psi\rangle_t = \alpha|H\rangle_t + \beta|V\rangle_t$ that is the target state to teleport. Alice processes an ancillary qubit prepared in $|H\rangle_a$ with a CNOT controlled by the polarization state of particle-1. After Alice's operation, the state made by particle-1 and the ancilla is

$$|\Phi'\rangle = \frac{1}{\sqrt{2}}(|0H\rangle \otimes |H\rangle_a + |1V\rangle \otimes |V\rangle_a) \tag{90}$$

Then, Alice applies a CNOT on the target state controlled by the polarization state of particle-1 obtaining the overall state (let us omit the symbol $\otimes$):

$$\begin{aligned}|\Phi''\rangle = \frac{1}{\sqrt{2}}&(\alpha|0H\rangle|H\rangle_t|H\rangle_a + \alpha|1V\rangle|V\rangle_t|V\rangle_a \\ &+ \beta|0H\rangle|V\rangle_t|H\rangle_a + \beta|1V\rangle|H\rangle_t|V\rangle_a)\end{aligned} \tag{91}$$

Let us stress that $|\Phi''\rangle$ is a quantum state of four qubits physically realized by three particles. (105) can be rewritten in the following form:

$$\begin{aligned}|\Phi''\rangle = \frac{1}{2}&[(\alpha|0H\rangle + \beta|1V\rangle)|H\rangle_t|D_+\rangle_a \\ &+ (\alpha|0H\rangle - \beta|1V\rangle)|H\rangle_t|D_-\rangle_a \\ &+ (\alpha|1V\rangle + \beta|0H\rangle)|V\rangle_t|D_+\rangle_a \\ &+ (-\alpha|1V\rangle + \beta|0H\rangle)|V\rangle_t|D_-\rangle_a]\end{aligned} \tag{92}$$

Table 3. Parameter-dependent operations performed by Bob to recover the target state when Alice communicates the outcomes H and D_+ of her polarization measurements.

Bob's outcomes on particle-1 (*momentum*, *polarization*)	Bob's operation on the ancilla
$(0, D_+)$	$\mathbb{I}$
$(0, D_-)$	σ_z
$(1, D_+)$	σ_z
$(1, D_-)$	$\mathbb{I}$

where $\{|D_+\rangle, |D_-\rangle\}$ is the diagonal basis of $\mathcal{H}_p$. Alice sends particle-1, then she measures the target qubit w.r.t the rectilinear basis and the ancillary qubit w.r.t. the diagonal basis and communicates the outcomes to Bob. Now, Bob applies some operations to reconstruct the initial target state. For example, if Alice finds the target particle in $|H\rangle_t$ and the ancilla in $|D_+\rangle$ then after the Alice's measurement the state in Bob's hands is $\alpha|0H\rangle + \beta|1V\rangle$. Bob applies a Hadamard gate to the received state and uses the output to control a CNOT on an ancilla prepared in $|H\rangle_b$. After these operations the system made by particle-1 and Bob's ancilla is

$$\begin{aligned}|\Phi'''\rangle &= \frac{1}{\sqrt{2}}(\alpha|0H\rangle|H\rangle_b + \beta|0V\rangle|V\rangle_b + \alpha|1H\rangle|H\rangle_b - \beta|1V\rangle|V\rangle_b) \\ &= \frac{1}{2}(\alpha|0D_+\rangle|H\rangle_b + \alpha|0D_-\rangle|H\rangle_b + \beta|0D_+\rangle|V\rangle_b - \beta|0D_-\rangle|V\rangle_b \\ &\quad + \alpha|1D_+\rangle|H\rangle_b + \alpha|1D_-\rangle|H\rangle_b - \beta|1D_+\rangle|V\rangle_b + \beta|1D_-\rangle|V\rangle_b)\end{aligned} \tag{93}$$

Then, Bob measures the momentum of particle-1 and its polarization w.r.t. the diagonal basis. If Bob finds particle-1 in the state $|0D_+\rangle$, for example, then his ancilla is in $\alpha|H\rangle_b + \beta|V\rangle_b$ that corresponds to the target state prepared by Alice. If Bob finds particle-1 in the state $|0D_-\rangle$ then his ancilla is in $\alpha|H\rangle_b - \beta|V\rangle_b$, in this case Bob must apply σ_z to obtain the target state. Let us summarize the Bob's operations to obtain the target state prepared by Alice in **Table 3**.

The complete description of Bob's operations when Alice communicates the other three possible outcomes pairs produced by the polarization measurements on the target particle and the ancilla are given in ref. [21]. The remarkable aspect of this teleportation protocol based on SPE is that there is not an initial entanglement sharing and just one particle must be sent from Alice to Bob to teleport an unknown qubit.

Other interesting techniques are bidirectional quantum teleportation by transmitting only one particle in a SPE state and the *simultaneous quantum transmission and teleportation* scheme based on intraparticle and interparticle entanglement.[7,112] Let us outline the procedure of bidirectional transfer of unknown quantum states by the transmission of a single particle: Adopting our usual notation, Alice prepares a *target photon* in the state $|\psi\rangle_t = |1\rangle_t \otimes (\alpha|H\rangle_t + \beta|V\rangle_t)$, where the polarization state is the target of the transmission. Acting with a polarizing beam splitter that transmits a photon with vertical polarization and reflects a photon with horizontal polarization, she obtains the entangled

state:

$$|\psi'\rangle_t = \alpha|0H\rangle_t + \beta|1V\rangle_t \tag{94}$$

Then, Alice performs a CNOT on the polarization degree of freedom controlled by an ancillary qubit initialized in the state $|D_-\rangle_a$, creating the state:

$$\begin{aligned}|\psi\rangle_{Alice} &= \frac{1}{\sqrt{2}}[\alpha(|0H\rangle_t|H\rangle_a - |0V\rangle_t|V\rangle_a) + \beta(|1V\rangle_t|H\rangle_a \\ &\quad - |1H\rangle_t|V\rangle_a)] \\ &= \frac{1}{\sqrt{2}}[(\alpha|0H\rangle_t + \beta|1V\rangle_t)|H\rangle_a - (\alpha|0V\rangle_t + \beta|1H\rangle_t)|V\rangle_a]\end{aligned} \tag{95}$$

Alice sends the target photon to Bob and the ancilla remains on her side. On the received particle, Bob acts with a Hadamard gate on the momentum degree of freedom, with the polarization-flip given by the gate (60) and with a CNOT controlled by an ancilla prepared in $|D_-\rangle_b$. The resulting overall state is the following:

$$\begin{aligned}|\Psi\rangle = \frac{1}{2\sqrt{2}}&[(|0H\rangle_t|H\rangle_a + |0V\rangle_t|V\rangle_a)(\alpha|V\rangle_b + \beta|H\rangle_b) \\ &- (|0H\rangle_t|V\rangle_a - |0V\rangle_t|H\rangle_a)(\alpha|H\rangle_b - \beta|V\rangle_b) \\ &- (|1H\rangle_t|V\rangle_a + |1V\rangle_t|H\rangle_a)(\alpha|V\rangle_b + \beta|H\rangle_b) \\ &+ (|1H\rangle_t|H\rangle_a - |1V\rangle_t|V\rangle_a)(\alpha|H\rangle_b - \beta|V\rangle_b)]\end{aligned} \tag{96}$$

Thus, the amplitudes of Alice's target state appear in the state of the Bob's ancilla particle. In order to teleport the unknown polarization state $|\varphi\rangle_B = \gamma|H\rangle_B + \delta|V\rangle_B$ to Alice, Bob applies gate (60) on the received particle, a CNOT in which the polarization part of the state (110) is the control qubit and the target one is the qubit in $|\varphi\rangle_B$, and, finally, a Hadamard gate on the momentum qubit. In the resulting state the amplitudes γ and δ are transferred to the ancillary qubit in Alice's hands:

$$\begin{aligned}|\psi\rangle_{Bob} = \frac{1}{2\sqrt{2}}&\{|1H\rangle_t(\alpha|V\rangle_b + \beta|H\rangle_b)[|D_-\rangle_B(\gamma|V\rangle_a - \delta|H\rangle_a) \\ &+ |D_+\rangle_B(\gamma|V\rangle_a + \delta|H\rangle_a)] \\ &- |0V\rangle_t(\alpha|H\rangle_b - \beta|V\rangle_b)[|D_-\rangle_B(\gamma|V\rangle_a - \delta|H\rangle_a) \\ &+ |D_+\rangle_B(\gamma|V\rangle_a + \delta|H\rangle_a)] \\ &+ |1V\rangle_t(\alpha|V\rangle_b - \beta|H\rangle_b)[|D_-\rangle_B(\gamma|H\rangle_a - \delta|V\rangle_a) \\ &+ |D_+\rangle_B(\gamma|H\rangle_a + \delta|V\rangle_a)] \\ &+ |0H\rangle_t(\alpha|H\rangle_b + \beta|V\rangle_b)[|D_-\rangle_B(\gamma|H\rangle_a - \delta|V\rangle_a) \\ &+ |D_+\rangle_B(\gamma|H\rangle_a + \delta|V\rangle_a)]\}\end{aligned} \tag{97}$$

In the case Alice prepares the target state $|0\rangle_t \otimes (\alpha|H\rangle_t + \beta|V\rangle_t)$ instead of $|1\rangle_t \otimes (\alpha|H\rangle_t + \beta|V\rangle_t)$, an analogous calculation of $|\psi\rangle_{Alice}$ and $|\psi\rangle_{Bob}$ must be done.[112] On the state $|\psi\rangle_{Bob}$, Bob measures momentum and polarization of the received particle w.r.t. the basis $\{|0H\rangle, |0V\rangle, |1H\rangle, |1V\rangle\}$ and the polarization of particle B w.r.t. the basis $\{|D_+\rangle, |D_-\rangle\}$. Alice communicates the momentum state of $|\psi\rangle_t$ and Bob communicates the outcomes of his measurements, so they act with proper unitary operations which depend on such classical information. For instance, suppose that after Bob's measurement the ancillas of Alice and Bob collapse, respectively, in the states: $\gamma|H\rangle_a + \delta|V\rangle_A$ and $\alpha|H\rangle_b - \beta|V\rangle_b$. Thus, Alice directly recovers the Bob's state $|\varphi\rangle_B$ and Bob acts with a σ_z to recover $|\psi\rangle_t$. All the possible cases are listed in ref. [112]. The outlined protocol based on SPE states performs mutual transfer of two unknown states between two clients, Alice transmits a qubit state to Bob and there is quantum teleportation of another qubit state from Bob to Alice by means of a single-particle transmission.

6. Conclusions

In this review, we have discussed strong quantum correlations between two degrees of freedom of the same particle. This quantum superposition of single particle states is what we mean by single-particle entanglement. Another way to express the same is to consider a quantum correlation of two or more states over which a single excitation (i.e., the particle) is distributed.[115] Both descriptions underline that SPE is local, that is, characteristic of a single particle. Usually, single-particle or two-particles entanglement violations of the Bell inequalities are interpreted as a signature of a non-classical nature of the measured system: contextuality or non-locality, respectively.[92] Non-contextuality is a more stringent demand than locality because it requires mutual independence of the results for commuting observables even if there is no spacelike separation.[116] In more precise wording, non-contextuality requires that the outcome of a measurement of an observable does not depend on the choice of the other compatible observables that one measures together with the target observable. Therefore, SPE may provide a more solid testing ground for the controversial theory of quantum measurements.[60] Interestingly, in SPE coherence and entanglement become mathematically equivalent,[117] and any measure of entanglement is also a measure of coherence.[94]

From an experimental point of view, the use of SPE is advantageous with respect to two-particles entanglement. In fact, to observe a violation of Bell inequalities with two-particles entanglement the knowledge of the joint distribution of the outcomes $N_{ij}^{(\mathbf{a},\mathbf{b})}$ is needed. These data are available only if we are able to recognize when a pair of measurements is referred to a single entangled pair. In other words, a strict control of the pair arrival times is fundamental. This experimentally demanding requirement is not necessary in the case of SPE because, in this case, the numbers $N_{ij}^{(\mathbf{a},\mathbf{b})}$ can be simply obtained by looking at the number of counts in the four different channels of the experimental apparatus. That is why the times of arrival do not play a fundamental role. All the correlations between the different degrees of freedom attain the highest robustness, with minimum dephasing and decoherence.[19] Moreover, since SPE is confined locally within a single particle, it is easier to preserve the entanglement against dissipative effects.[21] This allows using SPE to study quantum decoherence, or the environmentally induced reduction of quantum superpositions into statistical mixtures

and classical behavior.[60] Recently, we have demonstrated that SPE states of single photons can be produced from attenuated sources of light, even classical ones, provided that first-order coherence is maintained between the degrees of freedom involved in the entanglement.[118] Our observation of the violation of the CHSH inequality proves that filtered and attenuated light sources provide a flux of independent single-particle entangled photons that, from a statistical point of view, are indistinguishable from those generated by a single photon source. Therefore, SPE can be generated by cheap, light, compact, and low power hungry photon sources such as laser diodes, light emitting diodes or, even, lamps.

Quantum information processing is largely dependent on the robustness of non-classical correlations. Thus, SPE is a useful resource for quantum technologies, such as quantum communication and QKD.[20,21,119] Moreover, SPE has been proposed for quantum measurements in an interferometer setting,[120] for quantum repeaters,[121] for entanglement purification[121] and for deterministic teleportation.[115] Other applications of SPE can be in the implementation and certification of quantum random number generators.[122] Indeed, the violation of Bell inequalities allows to prove a lower bound for the entropy of the random sequence produced.[123] These applications use SPE since it requires significantly fewer resources than other protocols and is less sensitive to instrument deficiencies.

Acknowledgements

The authors are grateful to the anonymous reviewers for very helpful comments and remarks. This project received funding from Q@TN, the European Union's Horizon 2020 research and innovation programme under grant agreement No. 820405 project QRANGE, and by the India-Trento Programme of Advanced Research ITPAR phase IV project. The work of D.P. was supported by grants from Q@TN and Fondazione Caritro.

Conflict of Interest

The authors declare no conflict of interest.

Keywords

interparticle entanglement, quantum key distribution, quantum teleportation, single-particle entanglement

Received: January 20, 2020
Revised: August 5, 2020
Published online: September 6, 2020

[1] A. Einstein, B. Podolsky, N. Rosen, *Phys. Rev.* **1935**, *47*, 777.
[2] G. Ghirardi, *Sneaking a Look at God's Cards: Unraveling the Mysteries of Quantum Mechanics*, Princeton University Press, Princeton, NJ **2007**.
[3] The Stanford Encyclopedia of Philosophy, http://plato.stanford.edu/ (accessed: June 2020).
[4] A. Shimony, *62 Years of Uncertainty*, Plenum Press, New York **1990**.
[5] A. Zeilinger, *Nat. Phys.* **2018**, *14*, 3.
[6] W. Tittel, *Nature* **2015**, *518*, 491.
[7] J. Heo, C.-H. Hong, J.-I. Lim, H.-J. Yang, *Chin. Phys. B* **2015**, *24*, 050304.
[8] X.-L. Wang, X.-D. Cai, Z.-E. Su, M.-C. Chen, D. Wu, L. Li, N.-L. Liu, C.-Y. Lu, J.-W. Pan, *Nature* **2015**, *518*, 516.
[9] G. W. H. W. T. Jennewein, C. Simon, A. Zeilinger, *Phys. Rev. Lett.* **2000**, *84*, 4729.
[10] A. Ekert, *Phys. Rev. Lett.* **1991**, *67*, 661.
[11] S. Pironio, *Nature* **2018**, *556*, 176.
[12] S. Ashhab, K. Maruyama, C. Brukner, F. Nori, *Phys. Rev. A* **2009**, *80*, 062106.
[13] E. T. Burch, C. Henelsmith, W. Larson, M. Beck, *Phys. Rev. A* **2015**, *92*, 032328.
[14] M. Michler, H. Weinfurter, M. Żukowski, *Phys. Rev. Lett.* **2000**, *84*, 5457.
[15] B. R. Gadway, E. J. Galvez, F. D. Zela, *J. Phys. B: At. Mol. Opt. Phys.* **2009**, *42*, 015503.
[16] Y. Hasegawa, R. Loidl, G. Badurek, M. Baron, H. Rauch, *Nature* **2003**, *425*, 45.
[17] H. Geppert, T. Denkmayr, S. Sponar, H. Lemmel, Y. Hasegawa, *Nucl. Instrum. Methods Phys. Res., Sect. A* **2014**, *763*, 417.
[18] J. Shen, S. J. Kuhn, R. M. Dalgliesh, V. O. de Haan, N. Geerits, A. A. M. Irfan, F. Li, S. Lu, S. R. Parnell, J. Plomp, A. A. van Well, A. Washington, D. V. Baxter, G. Ortiz, W. M. Snow, R. Pynn, *Nat. Commun.* **2020**, *11*, 930.
[19] P. Saha, D. Sarkar, *Quantum Inf. Process.* **2016**, *15*, 791.
[20] S. Adhikari, D. Home, A. Majumdar, A. Pan, A. Shenoy H., R. Srikanth, *Quantum Inf. Process.* **2015**, *14*, 4.
[21] T. Pramanik, D. Home, S. Adhikari, A. Pan, *Phys. Lett. A* **2010**, *374*, 1121.
[22] Y. Hasegawa, K. Durstberger-Rennhofer, S. Sponar, H. Rauch, *Nucl. Instrum. Methods Phys. Res., Sect. A* **2010**, *634*, S21.
[23] E. Schrödinger, *Math. Proc. Cambridge Philos. Soc.* **1935**, *31*, 555.
[24] E. Schrödinger, *Math. Proc. Cambridge Philos. Soc.* **1936**, *32*, 446.
[25] J. Bell, *Physics* **1964**, *1*, 195.
[26] A. Aspect, P. Grangier, G. Roger, *Phys. Rev. Lett.* **1982**, *49*, 91.
[27] V. Moretti, *Spectral Theory and Quantum Mechanics*, Springer, New York **2018**.
[28] J. Garrison, R. Chiao, *Quantum Optics*, Oxford University Press, Oxford **2008**.
[29] D. Bohm, *Quantum Theory*, Dover Publications, Mineola, NY **1989**.
[30] D. Bohm, Y. Aharonov, *Phys. Rev.* **1957**, *108*, 1070.
[31] A more complete model would take into account the fact that the whole state must be anti-symmetric when swapping the electrons, but we disregard these details here.
[32] In fact, as Bell himself pointed out,[35] the non-local phenomena present in the EPR paradox do not allow any exchange of information between S_1 and S_2.
[33] *Quantum [Un]Speakables II. Half a Century of Bell's Theorem* (Eds: R. Bertlmann, A. Zeilinger), Springer, New York **2017**.
[34] Actually the spin values amount to $\hbar A(\mathbf{a}|\lambda)/2$ and $\hbar B(\mathbf{b}|\lambda)/2$ but we henceforth ignore these factors in our discussion.
[35] J. Bell, *The Theory of Local Beables. Speakable and Unspeakable in Quantum Mechanics*, Springer, New York **1974**.
[36] We thank the anonymous referee for clarifying this point.
[37] A. S. J. F. Clauser, M. A. Horne, R. A. Holt, *Phys. Rev. Lett.* **1969**, *23*, 880.
[38] The original Bell's paper[25] presented a slightly different inequality.
[39] B. S. Tsirelson, *Lett. Math. Phys.* **1980**, *4*, 93.
[40] B. Hensen, H. Bernien, A. E. Dréau, A. Reiserer, N. Kalb, M. S. Blok, J. Ruitenberg, R. F. L. Vermeulen, R. N. Schouten, C. Abellán, W. Amaya, V. Pruneri, M. W. Mitchell, M. Markham, D. J. Twitchen, D. Elkouss, S. Wehner, T. H. Taminiau, R. Hanson, *Nature* **2015**, *526*, 682.
[41] K. Landsman, *Foundations of Quantum Theory*, Springer, New York **2017**.
[42] J. Jarrett, *Noûs* **1984**, *18*, 569.

[43] V. Moretti, *Fundamental Mathematical Structures of Quantum Theory*, Springer, New York **2019**.
[44] N. Gisin, *Phys. Lett. A* **1991**, *154*, 201.
[45] R. F. Werner, *Phys. Rev. A* **1989**, *40*, 4277.
[46] M. Horodecki, P. Horodecki, R. Horodecki, *Phys. Lett. A* **1996**, *223*, 1.
[47] R. Horodecki, P. Horodecki, M. Horodecki, *Phys. Lett. A* **1995**, *200*, 340.
[48] R. A. Bertlman, H. Narnhofer, W. Thirring, *Phys. Rev. A* **2002**, *66*, 032319.
[49] G. W. A. Mair, A. Vaziri, A. Zeilinger, *Nature* **2001**, *412*, 313.
[50] J. T. Barreiro, N. K. Langford, N. A. Peters, P. G. Kwiat, *Phys. Rev. Lett.* **2005**, *95*, 260501.
[51] S. Kochen, E. Specker, *J. Math. Mech.* **1967**, *17*, 59.
[52] J. Bell, *Rev. Mod. Phys.* **1966**, *38*, 447.
[53] Y. Huang, C. Li, Y. Zhang, J. Pan, G. Guo, *Phys. Rev. Lett.* **2003**, *90*, 250401.
[54] V. D'Ambrosio, I. Herbauts, E. Amselem, E. Nagali, F. S. M. Bourennane, A. Cabello, *Phys. Rev. X* **2013**, *3*, 011012.
[55] In fact, it is by no means evident how the assignment $A \mapsto v(A) \in \sigma(A)$ should deal with *functional relations* between observables when these relations exist at a quantum level. For instance, if $C = A + B$, we cannot in general assume that $v_\lambda(C) = v(A) + v(B)$, because it is not obvious how to classically interpret $C = A + B$ when the self-adjoint operators A and B*do not commute* so that these observables, within the quantum interpretation, cannot be measured simultaneously. In this case, also the relation between the spectra of A, B, C is generally complicated and unexpected: think of $H = \frac{m\omega^2}{2}X^2 + \frac{1}{2m}P^2$ for a particle on the real line. A discussion of this problem, as well as an explicit formula providing the spectral measure of C given the spectral measures of A and B can be found in ref. [56].
[56] N. Drago, S. Mazzucchi, V. Moretti, *Lett. Math. Phys.* (in press), *arXiv:1904.10974*, **2019**.
[57] Yet, it would remain to explain how "A and B cannot be measured simultaneously" can be interpreted in a hidden-variable theory where, according to the realism postulate, we assume from scratch that every observable is always defined. The Kochen–Specker theorem does not deal with these subtleties and demands only very basic, sensible, and inalienable hypotheses, which should be valid in every complete hidden-variable theory, though producing a powerful no-go statement.
[58] In fact contextuality can be seen as a consequence of Bohr's complementarity, as its proof relies on comparisons (manipulations) of hypothetical (counterfactual) results of unperformed experiment (in partially, or fully complementary bases).
[59] H. W. C. Simon, M. Żukowski, A. Zeilinger, *Phys. Rev. Lett.* **2000**, *85*, 011012.
[60] C. Monroe, D. M. Meekhof, B. E. King, D. J. Wineland, *Science* **1996**, *272*, 1131.
[61] D. J. Wineland, Nobel lecture: Superposition, entanglement, and raising Schroedinger's cat, **2012**, https://www.nobelprize.org/prizes/physics/2012/wineland/lecture/ (accessed: June 2020).
[62] D. Home, S. Sengupta, *Phys. Lett. A* **1984**, *102*, 159.
[63] S. Basu, S. Bandyopadhyay, G. Kar, D. Home, *arXiv:quant-ph/9907030v1*, **1999**.
[64] S. Basu, S. Bandyopadhyay, G. Kar, D. Home, *Phys. Lett. A* **2001**, *279*, 281.
[65] Y. Hasegawa, R. Loidl, G. Badurek, M. Baron, H. Rauch, *Phys. Rev. Lett.* **2006**, *97*, 230401.
[66] H. Bartosik, J. Klepp, C. Schmitzer, S. Sponar, A. Cabello, H. Rauch, Y. Hasegawa, *Phys. Rev. Lett.* **2009**, *103*, 040403.
[67] G. Kirchmair, F. Zähringer, R. Gerritsma, M. Kleinmann, O. Gühne, A. Cabello, R. Blatt, F. Roos, *Nature* **2009**, *460*, 494.
[68] A. Cabello, *arXiv:1904.05306*, **2019**.
[69] L. Chen, W. She, *J. Opt. Soc. Am. B* **2010**, *27*, A7.
[70] E. Karimi, J. Leach, S. Slussarenko, B. Piccirillo, L. Marrucci, L. Chen, W. She, S. Franke-Arnold, M. J. Padgett, E. Santamato, *Phys. Rev. A* **2010**, *82*, 022115.
[71] S. Sponar, J. Klepp, C. Zeiner, G. Badurek, Y. Hasegawa, *Phys. Lett. A* **2010**, *374*, 431.
[72] F. Jeske, T. Stöferle, M. DeKieviet, *Eur. Phys. J. D* **2011**, *82*, 25.
[73] This work does not actually report on a violation of the Bell inequality, since an analysis of the S-parameter is not carried out. However, the presented experimental data would allow to do that. See Section 4.4 for more details.
[74] S. Gröblacher, R. Kaltenbaek, Č. Brukner, M. Żukowski, M. Aspelmeyer, A. Zeilinger, *Nature* **2007**, *446*, 871.
[75] D. A. Meyer, *Phys. Rev. Lett.* **1999**, *83*, 3751.
[76] A. Kent, *Phys. Rev. Lett.* **1999**, *83*, 3755.
[77] J. D. Jackson, *Classical Electrodynamics*, 3rd ed., Wiley, New York **1998**.
[78] D. Meschede, *Optics, Light and Lasers: The Practical Approach to Modern Aspects of Photonics and Laser Physics*, 3rd ed., Wiley, New York **2017**.
[79] L. Allen, M. W. Beijersbergen, R. J. C. Spreeuw, J. P. Woerdman, *Phys. Rev. A* **1992**, *45*, 8185.
[80] L. Marrucci, C. Manzo, D. Paparo, *Appl. Phys. Lett.* **2006**, *88*, 221102.
[81] L. Marrucci, C. Manzo, D. Paparo, *Phys. Rev. Lett.* **2006**, *96*, 163905.
[82] E. Nagali, F. Sciarrino, F. De Martini, L. Marrucci, B. Piccirillo, E. Karimi, E. Santamato, *Phys. Rev. Lett.* **2009**, *103*, 013601.
[83] A. Vallés, V. D'Ambrosio, M. Hendrych, M. Mi čuda, L. Marrucci, F. Sciarrino, J. P. Torres, *Phys. Rev. A* **2014**, *90*, 052326.
[84] T. Stav, A. Faerman, E. Maguid, D. Oren, V. Kleiner, E. Hasman, M. Segev, *Science* **2018**, *361*, 1101.
[85] R. J. C. Spreeuw, *Found. Phys.* **1998**, *28*, 361.
[86] N. Korolkova, G. Leuchs, *Rep. Prog. Phys.* **2019**, *82*, 056001.
[87] S. Berg-Johansen, F. Töppel, B. Stiller, P. Banzer, M. Ornigotti, E. Giacobino, G. Leuchs, A. Aiello, C. Marquardt, *Optica* **2015**, *2*, 864.
[88] A. Aiello, F. Töppel, C. Marquardt, E. Giacobino, G. Leuchs, *New J. Phys.* **2015**, *17*, 043024.
[89] C. Borges, M. Hor-Meyll, J. Huguenin, A. Khoury, *Phys. Rev. A* **2010**, *82*, 033833.
[90] C. Gabriel, A. Aiello, W. Zhong, T. Euser, N. Joly, P. Banzer, M. Förtsch, D. Elser, U. L. Andersen, C. Marquardt, P. S. J. Russell, G. Leuchs, *Phys. Rev. Lett.* **2011**, *106*, 060502.
[91] A. Khrennikov, *arXiv:1909.00267*, **2019**.
[92] M. Markiewicz, D. Kaszlikowski, P. Kurzyński, A. Wójcik, *npj Quantum Inf.* **2019**, *5*, 5.
[93] D. Paneru, E. Cohen, R. Fickler, R. W. Boyd, E. Karimi, *Rep. Prog. Phys.* **2020**, *83*, 064001.
[94] K. H. Kagalwala, G. D. Giuseppe, A. F. Abouraddy, B. E. A. Saleh, *Nat. Photonics* **2013**, *7*, 72.
[95] H. Rauch, S. A. Werner, *Neutron Interferometry*, Oxford University Press, Oxford **2015**.
[96] S. Sponar, J. Klepp, R. Loidl, S. Filipp, K. Durstberger-Rennhofer, R. A. Bertlmann, G. Badurek, H. Rauch, Y. Hasegawa, *Phys. Rev. A* **2010**, *81*, 042113.
[97] http://www.neutroninterferometry.com/research-overview/neptun-vienna (accessed: January 2020).
[98] During the revision of the manuscript, we became aware of ref. [18], where an investigation on the control of entanglement of single-neutron multiple degrees of freedom—spin, path, and energy—is described.
[99] G. B. Roston, M. Casas, A. Plastino, A. R. Plastino, *Eur. J. Phys.* **2005**, *26*, 657.
[100] A. C. de la Torre, *Am. J. Phys.* **1994**, *62*, 808.
[101] N. L. Harshman, *Int. J. Quantum Inf.* **2007**, *05*, 273.

[102] M. DeKieviet, D. Dubbers, C. Schmidt, D. Scholz, U. Spinola, *Phys. Rev. Lett.* **1995**, *75*, 1919.
[103] M. DeKieviet, D. Dubbers, M. Klein, U. Pieles, C. Schmidt, *Rev. Sci. Instrum.* **2000**, *71*, 2015.
[104] C. Cohen-Tannoudji, B. Diu, F. Laloë, *Quantum Mechanics, Volume 1: Basic Concepts, Tools and Applications*, Wiley, New York **2019**.
[105] I. Ali-Khan, C. J. Broadbent, J. C. Howell, *Phys. Rev. Lett.* **2007**, *98*, 060503.
[106] J. Li, N. Li, L.-L. Li, T. Wang, *Sci. Rep.* **2016**, *6*, 28767.
[107] D. Pastorello, *Int. J. Quant. Inf.* **2017**, *15*, 1750040.
[108] C. H. Bennett, G. Brassard, *Theor. Comput. Sci.* **2014**, *560*, 7.
[109] Y. Sun, Q.-Y. Wen, Z. Yuan, *Opt. Commun.* **2011**, *284*, 527.
[110] H. Salih, *Front. Phys.* **2016**, *4*, 59.
[111] S. Adhikari, A. Majumdar, D. Home, A. Pan, *Eur. Phys. Lett.* **2010**, *89*, 10005.
[112] J. Heo, C.-H. Hong, J.-I. Lim, H.-J. Yang, *Int. J. Theor. Phys.* **2015**, *54*, 2261.
[113] L. Gui-Lu, *Commun. Theor. Phys.* **2006**, *45*, 825.
[114] L. Gui-Lu, L. Yang, *Commun. Theor. Phys.* **2008**, *50*, 1303.
[115] G. Björk, A. Laghaout, U. L. Andersen, *Phys. Rev. A* **2012**, *85*, 022316.
[116] C. Simon, M. Żukowski, H. Weinfurter, A. Zeilinger, *Phys. Rev. Lett.* **2000**, *85*, 1783.
[117] R. de J León-Montiel, A. Vallés, H. M. Moya-Cessa, J. P. Torres, *Laser Phys. Lett.* **2005**, *12*, 085204.
[118] M. Pasini, N. Leone, S. Mazzucchi, V. Moretti, D. Pastorello, L. Pavesi, *arXiv:2003.09961*, **2020**.
[119] J.-W. Lee, E. K. Lee, Y. W. Chung, H.-W. Lee, J. Kim, *Phys. Rev. A* **2003**, *68*, 012324.
[120] M. Kolář, T. Opatrný, N. Bar-Gill, N. Erez, G. Kurizki, *New J. Phys.* **2007**, *9*, 129.
[121] D. Salart, O. Landry, N. Sangouard, N. Gisin, H. Herrmann, B. Sanguinetti, C. Simon, W. Sohler, R. T. Thew, A. Thomas, H. Zbinden, *Phys. Rev. Lett.* **2010**, *104*, 180504.
[122] N. Leone, D. Rusca, S. Azzini, G. Fontana, F. Acerbi, A. Gola, A. Tontini, N. Massari, H. Zbinden, L. Pavesi, unpublished.
[123] S. Pironio, A. Acín, S. Massar, A. B. de la Giroday, D. N. Matsukevich, P. Maunz, S. Olmschenk, D. Hayes, L. Luo, T. A. Manning, C. Monroe, *Nature* **2010**, *464*, 1021.

Stefano Azzini, M.Sc. in engineering physics (Milano, Politecnico), Ph.D. in physics (Pavia, 2008), is assistant professor at the Department of Physics of the University of Trento, Italy, in the Nanoscience Laboratory working on nonlinear integrated photonics. He worked on Tamm plasmon structures at the University of Lyon (France), next focusing on the coupling of 2D semiconductors with plasmonic nanostructures at the University of Strasbourg (France). He is an experimental physicist interested in strong light–matter interactions and integrated quantum photonics.

Sonia Mazzucchi obtained M.Sc. in physics (1999) and Ph.D. in mathematics (2003) from Trento University, Italy. In 2007 and 2009 she was a von Humboldt fellow at the Hausdorff Center for Mathematics of Bonn, Germany. In 2007, she was awarded the Francesco Severi fellowship of the Italian National Institute of Higher Mathematics. Since 2018, she is associate professor in probability and mathematical statistics at the University of Trento. Her research interests include stochastic analysis and its applications to quantum physics.

Valter Moretti, M.Sc. in physics (Genova), Ph.D. in theoretical physics (Trento), is full professor of mathematical physics at the Department of Mathematics of the University of Trento (Italy). His research area includes mathematical and foundational aspects of quantum, relativistic and quantum-relativistic theories.

Davide Pastorello, M.Sc. in physics and Ph.D. in mathematics (Trento 2014), was postdoctoral fellow at the Department of Mathematics, University of Trento, from 2015 to 2019 also with a 2-year grant from Fondazione Caritro on quantum technologies. Since 2019, he is assistant professor at the Department of Information Engineering and Computer Science, University of Trento. His research interests focus on mathematical aspects of quantum information theory, quantum computing, and quantum machine learning.

Lorenzo Pavesi is professor of experimental physics at the Department of Physics of the University of Trento. During the last years, he concentrated on silicon-based photonics where he looked for the convergence between photonics and electronics. He is interested in active photonics devices which can be integrated in silicon by using optical nolinearities and modified material properties. His interests encompass also optical sensors or biosensors and solar cells. Recent development is toward integrated quantum photonics and neuromorphic photonics.